PR

MONTHLY WEATHER REVIEW

VOLUME 82 NUMBER 11

NOVEMBER 1954

CONTENTS

	Page
Insolation in Relation to Cloud Amount.....J. Neumann	317
Trajectory Method of Making Short-Range Forecasts of Differential Temperature Advection, Instability, and Moisture.....James F. Appleby	320
The Weather and Circulation of November 1954—Including a Study of Some Major Circulation Changes.....Harry F. Hawkins, Jr.	335
The Tropopause During a Major Change in Circulation Over the Western United States, November 25 to 28, 1954 Grover D. Hughes and Robert L. Foster	343

Charts I–XV

U. S. DEPARTMENT OF COMMERCE • WEATHER BUREAU

PUBLICATIONS OF THE U. S. WEATHER BUREAU

As the national meteorological service for the United States, the Weather Bureau issues several periodicals, serials, and miscellaneous publications on weather, climate, and meteorological science as required to carry out its public service functions. The principal periodicals and serials are described on this page and on the inside of the back cover. A more complete listing of Weather Bureau publications is available upon request to Chief, U. S. Weather Bureau, Washington 25, D. C.

Orders for publications should be addressed to the Superintendent of Documents, Government Printing Office, Washington 25, D. C.

MONTHLY WEATHER REVIEW

First published in 1872, the Monthly Weather Review serves as a medium of publication for technical contributions in the field of meteorology, principally in the branches of synoptic and applied meteorology. In addition each issue contains an article descriptive of the atmospheric circulation during the month over the Northern Hemisphere with particular reference to the effect on weather in the United States. A second article deals with some noteworthy feature of the month's weather. Illustrated. Annual subscription: Domestic, $3.00; Foreign, $4.00; 30¢ per copy. Subscription to the *Review* does not include the *Supplements* which have been issued irregularly and are for sale separately.

CLIMATOLOGICAL DATA—NATIONAL SUMMARY

This monthly publication contains climatological data such as pressure, temperature, winds, rainfall, snowfall, severe storms, floods, etc., for the United States as a whole. A short article describing the weather of the month over the United States, tables of the observational data, and a description of flood conditions are supplemented by 15 charts. An annual issue summarizes weather conditions in the United States for the year. More detailed local data are provided in the Climatological Data (by sections) for 45 sections representing each State or a group of States, and Hawaii, Alaska, and the West Indies. Subscription price for either the National Summary or for a Section: $4.00 per year (including annual issue) domestic, $5.50, foreign; 30¢ per monthly issue; 50¢ for annual issue alone.

(Continued on inside back cover)

The Weather Bureau desires that the *Monthly Weather Review* serve as a medium of publication for original contributions within its field, but the publication of a contribution is not to be construed as official approval of the views expressed.

The issue for each month is published as promptly as monthly data can be assembled for preparation of the review of the weather of the month. In order to maintain the schedule with the Public Printer, no proofs will be sent to authors outside of Washington, D. C.

The printing of this publication has been approved by the Director of the Bureau of the Budget, February 11, 1952

DEPARTMENT OF COMMERCE
SINCLAIR WEEKS, Secretary

WEATHER BUREAU
F. W. REICHELDERFER, Chief

MONTHLY WEATHER REVIEW

Editor, JAMES E. CASKEY, JR.

Volume 82
Number 11

NOVEMBER 1954

Closed January 15, 1955
Issued February 15, 1955

INSOLATION IN RELATION TO CLOUD AMOUNT

J. NEUMANN

Israel Meteorological Service, Hakirya, Tel Aviv, Israel

[Manuscript received May 24, 1954; revision received November 1, 1954]

ABSTRACT

Assuming a simple pyrheliometric station model, an equation is derived relating the amount of insolation Q from a sky whose fraction C is covered by clouds, to the insolation Q_0 arriving at the same surface from a cloudless sky. The equation is of the form

$$Q/Q_0=1-(A-a)(1+a)C,$$

where A is the sum of cloud albedo and absorptivity expressed as fraction of the radiation incident on cloud tops and the symbol a represents the depletion coefficient of insolation in cloudless air in the layer between cloud top and cloud base levels.

The theoretical equation resembles the empirical equation $Q/Q_0=1-kC$ where k is supposed to be a constant. The theoretical equation shows the dependence of k on relevant physical variables.

It is shown that the theoretical equation combined with results of pyrheliometric observations, from which a value of k has been deduced, leads to a value of A which is in close accord with its value obtained by independent methods. On the other hand, if we assume reasonable values for A and a, the resulting value for k is in good agreement with the best value found from pyrheliometric observations.

INTRODUCTION

In the literature on empirical calculations of insolation, an equation of the type

$$Q=Q_0\,(1-kC) \qquad (1)$$

is often cited as a useful means for computing, in an approximate manner, the amount of insolation reaching a horizontal surface from a cloudy sky under average conditions. In the equation the symbols have the following meaning:

Q=amount of insolation incident on a horizontal surface from a cloudy sky,
Q_0=as Q but from a cloudless sky,
C=cloud amount on the scale of, say, 0.0 to 1.0,
k=a suitable constant.

For simplicity, k is considered a constant in spite of the fact that k is known to vary with cloud type and depth, height of cloud base, etc. It would be desirable to have quantitative information on the dependence of k on the various cloud characteristics and the purpose of the present paper is to investigate the problem in a simple manner. Such an investigation is all the more timely as the "best" values reported for k differ in some cases fairly considerably.

DERIVATION OF AN EQUATION

We will assume a simplified station model. In this model: (a) all clouds have their bases and tops at respectively uniform levels, (b) the optical properties, i. e., albedo and absorptivity, of clouds are uniform with respect to insolation, (c) transmission conditions of insolation in the cloud-free spaces of a partly cloudy sky are similar to those of the corresponding layer under conditions of a cloudless sky, and (d) the station is situated in a level terrain whose surface is uniform from an optical point of

view. At any level in the atmosphere, the insolation has a downward component and an upward component. The upward component is produced by reflections of insolation from the air, clouds, and terrain. In the present paper, the downward component alone is considered.

Let Q_0'' and Q' be the insolation incident on a horizontal surface at the cloud-top and cloud-base levels, respectively. For a sky partly covered by clouds, Q' should be thought of as *a weighted average* for the cloudy and cloudless areas on the constant-height surface corresponding to cloud-base level. Let $(1-a)$ be the transmission coefficient (a is the depletion coefficient) of insolation *in cloudless air* between the levels of cloud tops and cloud bases. Further, let A be the sum of figures representing cloud albedo and absorptivity expressed as fractions of the radiation incident on the cloud tops. On the one hand, for the cloud-free spaces, the insolation arriving at cloud base level will be proportional to $Q_0''(1-a)$. On the other hand, the insolation arriving at the bases of clouds will be proportional to $Q_0''(1-A)$. Hence Q', the weighted areal average of insolation reaching cloud-base level, will be

$$\begin{aligned} Q' &= Q_0''(1-a)(1-C)+Q_0''(1-A)C, \\ &= Q_0''[(1-a)-(A-a)C], \end{aligned} \tag{2}$$

where, as before, C is the cloud amount expressed as fraction of the sky covered by clouds. For a cloudless sky, $C=0$ and $a=0$, by definition.

Let a' and a'' be transmission coefficients of insolation: a' for air between cloud-base level and ground, and a'' for *cloudless* air between cloud-top level and ground. Then, if Q and Q_0 have the same meaning as in (1),

$$Q=a'Q' \tag{3}$$

and

$$Q_0=a''Q_0'' \tag{4}$$

The latter is based on our assumption (c) according to which transmission conditions in the cloudless spaces of a partly cloudy sky are similar to those of a cloudless sky. Inserting (3) and (4) in (2) yields

$$Q=Q_0\frac{a'}{a''}[(1-a)-(A-a)C]. \tag{5}$$

As a'' is the transmission coefficient in cloudless air between cloud-top level and ground whereas a' is the transmission coefficient for the layer between cloud-base level and ground, a'' will be smaller than a' by a factor representing the transmission coefficient for the layer of cloudless air between cloud-top and cloud-base levels. The latter coefficient has been denoted earlier by the symbol $(1-a)$. Hence,

$$\frac{a'}{a''}=\frac{1}{1-a} \tag{6}$$

If (6) is inserted in (5), we find that

$$Q=Q_0\left[1-\frac{A-a}{1-a}C\right] \tag{7}$$

If cloud depth is not too great, $a<<1$, and then, to a good approximation,

$$\frac{1}{1-a}=1+a \tag{8}$$

With the aid of (8), (7) now takes the form

$$Q=Q_0[1-(A-a)(1+a)C] \tag{9}$$

This is the equation we have intended to derive.

DISCUSSION

Equation (9) is the general form of the relationship between Q, Q_0, and C under the simplified model adopted. This equation shows the dependence of the coefficient of cloudiness (which in the empirical equation (1) is considered a constant) on the appropriate physical variables such as cloud albedo and absorptivity and transmission conditions in cloudless air for insolation. As both A and a are subject to temporal and spatial variations, a loss of accuracy will be incurred if the coefficient $(A-a)(1+a)$ of (9) is replaced by a constant as is done in (1). Equation (9) enables us to assess the error in replacing $(A-a)(1+a)$ by a constant provided, of course, that A and a can be estimated in a satisfactory manner.

Equation (6) shows that a is a function of the transmission coefficients a' and a''. For a given solar zenith distance, the transmission coefficients tend to vary with altitude as the logarithm of altitude. Klein [1] has reviewed this subject and compiled two diagrams (his figures 2 and 3, p. 125), one for summer conditions and the second for winter conditions, indicating the variation of transmission coefficients with altitude as a function of solar zenith distance, *for direct solar radiation*. In the absence of more complete data, we shall be compelled in the next section, where a numerical application is given, to use Klein's figures as if they were applicable for total insolation, direct and diffuse. The influence of this error is reduced by the fact that the value of the factor $(A-a)(1+a)$ is determined primarily by the value of A. This follows from the observation that an error in the value of a is compensated through a appearing with opposite signs in the two factors $(A-a)$ and $(1+a)$. This fact is of some usefulness in applications of equation (9) as it will often be difficult to estimate a to a sufficient accuracy.

APPLICATION: CLOUD ALBEDO AND ABSORPTIVITY FOR SOLAR RADIATION

Two immediate applications of equation (9) suggest themselves. In the first application, the factor $(A-a)$

$(1+a)$ is considered a constant and it is assumed that its "best" value is known. By assuming also that a is known, we can proceed to calculate the value of A, the sum of fractions representing cloud albedo and absorptivity for solar radiation, and compare the value of A so obtained with values derived by independent methods. The second application is the converse of the first one. By assuming that representative values of A and a are given, the value of the cloudiness coefficient $(A-a)\ (1+a)$ can be computed and then checked for reasonable agreement with the value of k (equation (1)) determined empirically on the basis of pyrheliometric observations.

First application.—In equation (9) it will be assumed that $(A-a)\ (1+a)=k$, k=constant, in which case (9) reduces to (1). Some writers (e. g., Sverdrup [2], p. 51), give the "best" value of k as 0.71. Dr. S. Fritz of the U. S. Weather Bureau has, however, pointed out, in a private communication, that if average monthly periods are considered, the value of k is more likely near 0.6 or even near 0.5. These estimates of k are based on pyrheliometric observations. On the basis of this, we shall adopt tentatively $k=0.55$.

With regard to a, we note from equation (6) that

$$a=\frac{a'-a''}{a'} \tag{10}$$

To obtain a value for a, we shall estimate a' and a'' from Klein's ([1], p. 125) diagrams. By assuming a cloud base at 1, 2, and 3 km., and a cloud depth of 1, 2, and 3 km., it is found that a varies between ca. 0.1 and 0.2. We shall adopt for a the average of the two figures, i. e. we assume $a=0.15$. As was pointed out in the preceding section, errors in estimates of a are partly balanced by the manner in which the a enters the cloudiness coefficient.

From $(A-a)(1+a)=0.55$ and $a=0.15$, $A=0.63$, that is, the sum of cloud albedo and absorptivity works out to be 0.63. This value is in close agreement with values obtained recently by independent methods. Both Fritz (private communication) and Houghton [3] give the average value of cloud albedo as 0.55. Fritz's estimate was presented in 1951 at the Brussels General Assembly of the International Union of Geodesy and Geophysics. The estimate falls in the interval 0.47 and 0.60 given earlier by Fritz [4] for the worldwide average for cloud albedo. As to cloud absorptivity, Houghton [3] presents a table, based on the work of various authors, indicating an absorptivity of 0.01 for high clouds, at the one extreme, and 0.1 for cumuliform clouds, at the other extreme. It is probably a reasonable conjecture that the worldwide average is nearer the value for cumuliform clouds, say, it is 0.07. If the latter is combined with the figure 0.55 for albedo, it results that $A=0.62$, in close agreement with the value 0.63 deduced above.

Second application.—As was stated earlier, the second application is the converse of the first one. Setting out from a cloud albedo of 0.55, an absorptivity of, say, 0.07 and a value of $a=0.15$, equation (9) becomes

$$Q=Q_0(1-0.54\ C)$$

i. e., k of (1) is 0.54, in good accord with Fritz's estimated value of k based on pyrheliometric observations.

ACKNOWLEDGMENT

The writer is pleased to record his indebtedness to Dr. S. Fritz, U. S. Weather Bureau, for his valuable comments and criticisms.

REFERENCES

1. W. H. Klein, "Calculation of Solar Radiation and the Solar Heat Load on Man," *Journal of Meteorology*, vol. 5, No. 4, Aug. 1948, pp. 119–129.
2. H. U. Sverdrup, *Oceanography for Meteorologists*, Allen & Unwin, London, 1945, 246 pp.
3. H. G. Houghton, "On the Annual Heat Balance of the Northern Hemisphere," *Journal of Meteorology*, vol. 11, No. 1, Feb. 1954, pp. 1–9.
4. S. Fritz, "The Albedo of the Planet Earth and Clouds," *Journal of Meteorology*, vol. 6, No. 4, Aug. 1949, pp. 277–282.

TRAJECTORY METHOD OF MAKING SHORT-RANGE FORECASTS OF DIFFERENTIAL TEMPERATURE ADVECTION, INSTABILITY, AND MOISTURE

JAMES F. APPLEBY

Hydrometeorological Section, U. S. Weather Bureau, Washington, D. C.

[Manuscript received March 22, 1954; revised August 16, 1954]

ABSTRACT

A method is presented of forecasting indices of the strength of horizontal differential temperature advection, instability, and moisture—factors which have been found useful in locating areas of moderate to heavy rainfall. Carefully analyzed data from charts currently used in most forecast programs are used. Examples of the techniques and several cases giving the forecast of parameters and the corresponding observed rainfall are shown. Also included is a comparison of forecast areas of horizontal differential advection and tornado occurrence.

INTRODUCTION

The Hydrometeorological Section of the Weather Bureau has been conducting a study of the feasibility of making short-range forecasts of areas of heavy precipitation (1 inch or more per 6 hours). A trajectory method of forecasting the areas and magnitude of differential temperature advection,[1] instability, and moisture has produced some encouraging results when compared with observed rainfall. The purpose of this paper is to describe the procedure and the reasoning which led to its adoption and to present the results of several studies of heavy rainfall cases prepared under the direction of George A. Lott. A comparison of the parameters determined from forecast trajectories and from trajectories as computed from observed winds is made from results of a case study by Lillian K. Rubin. Finally, the association of severe storms with areas of warm differential temperature advection is illustrated with results from a case study by Morton H. Bailey.

Experience of the Hydrometeorological Section in the study of major rainstorms in the United States has indicated that the analysis of observed data by present day techniques does not always offer a satisfactory solution of the mechanisms involved. In the past we have frequently attributed heavy rainfall to: (1) frontal lifting, (2) increased cyclonic turning of the isobars, and (3) convergence in convectively unstable tropical air. However, very similar conditions, as far as they can be observed or inferred from the data, occur on occasions when little or no rain falls. Present theories of storm mechanisms seem to work well in some cases, but not in others. Therefore, it seems that these mechanisms, although contributing, do not fully explain the rainfall—at least insofar as they are observable.

One major difficulty in deriving a satisfactory explanation of many heavy rainfall situations may be the extreme mobility of the atmosphere. As unstable conditions develop, reactions begin immediately to return the atmosphere to equilibrium. Thus the observed data cannot help being affected by these stabilizing influences. It is an observed fact that temperature and moisture do not move horizontally with the winds. This is because the action of the wind field on the existing temperature field creates unstable situations,[2] and vertical motions result, causing additional changes in the temperature field. However, advecting the physical properties of the air forward should give some indication of where vertical motion should occur and some indication of its strength if indices are chosen to describe adequately conditions accompanying heavy rainfall.

SELECTION OF INDICES

The main sources of energy available for lifting of the air are those of potential energy of temperature contrast and thermodynamic instability. Indices relating to the air temperature (density) horizontally and vertically along with moisture were considered.

Gilman [1] has hypothesized that horizontal differential temperature advection is a cause of vertical motion. He believes it is brought about by the relative rise of the constant pressure surfaces in a layer where the curvature of the advection profile is like that where warm differential advection is at a maximum. This causes divergence aloft and consequently a pressure fall at the surface and convergence in the lower portion of the layer. Erickson [2]

[1] Differential advection is here defined as the finite difference equivalent of the horizontal Laplacian of temperature advection.

[2] By an unstable situation is meant one in which air of different densities is brought together in such manner as to cause vertical motion either by overturning, or realization of the potential energy of temperature contrast.

in a study of 11 extremely heavy rainfalls has found this to be verifiable in 9 of the 11 cases at 5,000 ft. and in 7 of the 11 at 10,000 ft. So differential temperature advection was one parameter selected. Instability has long been recognized by meteorologists as a source of energy and this was chosen as the second parameter. The importance of available moisture for precipitation, the third parameter, is obvious.

It is postulated that areas showing marked differential warm air advection depict areas where the part of potential energy of temperature contrast is most likely to be expended in lifting the air and that in areas showing convective instability there is a possibility of energy being added after vertical motion starts. Then if sufficient moisture is present heavy rainfall results.

The first problem then was to develop a method of obtaining future trajectories of the air to test the validity of the selected parameters. Undoubtedly, the nature of the approach limits the length of time it can be projected into the future. However, since the total strong vertical motion compared to horizontal motion in the atmosphere is small, the trajectory approach should be applicable up to 18–24 hours.

CONSTRUCTION OF TRAJECTORIES

Since a forecast tool was the ultimate aim, a reasonable balance between time expended, accuracy, and area applicability had to be reached. For some purposes, the trajectory methods described in the literature (c. f. [3] and [4]) are adequate, but for forecasting purposes these have several shortcomings. One is the time required to construct the trajectories. Another is the requirement of a series of prognostic charts which are not routinely available. The chief objection is the departure of the observed winds from the geostrophic. Some very large departures from the geostrophic are observed in many of the major storms in the United States, and probably are an important factor in the heavy rainfall mechanism.

Trajectories computed from observed wind data are accurate for short intervals, but translation and changes in shape of the pressure systems, with time, limit their applicability. Since Gustafson [5] has shown that there is some reason to believe ageostrophic winds occur in the same location relative to a moving system, allowances for the movement, changes in shape, and intensity of the systems must be made to avoid discarding the ageostrophic flow. With these allowances fairly accurate trajectories can be drawn from the information on the observed chart by the use of acetate overlays, shifted to allow for movement and changes in shape of the systems. Trajectories for the 850-mb. level drawn by this method approximate those computed by the accepted methods and can be drawn over the eastern United States in a relatively short time. No attempt was made to draw trajectories over the Plateau Region for the 850-mb. level for the obvious reason that this level is below the surface there.

The most accurate trajectory would be one made by selecting very short time intervals and drawing vectors from the winds, making allowance for the movement of the pressure systems. The decision to use an average trajectory for periods of up to 9-hour intervals was made after balancing the time required for preparation against the accuracy of the two methods.

To explain the details of the adopted procedure, an example of preparing the trajectories from the observed 0300 GMT 850-mb. chart, October 26, 1953, to 1200 GMT and 1800 GMT the same day, is discussed. Since the advection of temperature and the advection of moisture are the end results, they have been included.

Step 1. Analysis.—The 850-mb. chart (supplied by the WBAN Analysis Center) is prepared by drawing isotherms at intervals of 2° C.—carefully drawing for every temperature unless it is obviously in error. Dewpoint isotherms are drawn for intervals of 4° C., except in areas with dewpoints above 8° C. where the analysis is made for every 2° C. On completing this analysis, future positions of the pressure systems (Highs, Lows, ridges, and troughs) at 0730 GMT and 1500 GMT [3] are sketched in. These are the locations of the systems at the midpoints of the periods for which trajectories are needed. These future positions are based on extrapolation, the WBAN Analysis Center 30-hour prognostic charts, and the analyst's judgment when the two former disagree radically. If the pressure systems differ significantly in their rates of movement the region influenced by each is outlined. Any intensification or filling of the pressure systems is converted into its effect on the winds and noted on the chart as a percentage increase or decrease of the wind speed. In the work done to date, anticipated changes in wind direction relative to the moving system have not been considered.

Step 2. Trajectories.—A sheet of clear acetate is superimposed on the analyzed chart and check marks placed on convenient latitude and longitude intersections for later reference. The future positions of the pressure systems are traced lightly on the acetate and points are selected for starting points of the trajectories. (See fig. 1.) The spacing and number of points necessary to determine the changing isotherm field varies with the situation, but with experience it can be determined quite closely. Points between the present and the first future position of the pressure feature should not be trajected since shifting of the acetate would put the points to the rear of the feature. In most cases this area is not large and by examination of the wind field, isotherms from this area can be drawn. In rare cases where the area is large, shorter time intervals can be used, for example, two 4½-hour periods instead of one 9-hour period can be selected to draw several trajectories in this area.

[3] Since radiosonde and precipitation observations begin shortly after the hour, the time interval between the 0300 and 1230 GMT observations is considered as 9 hours, that between 1230 and 1830 GMT as 6 hours.

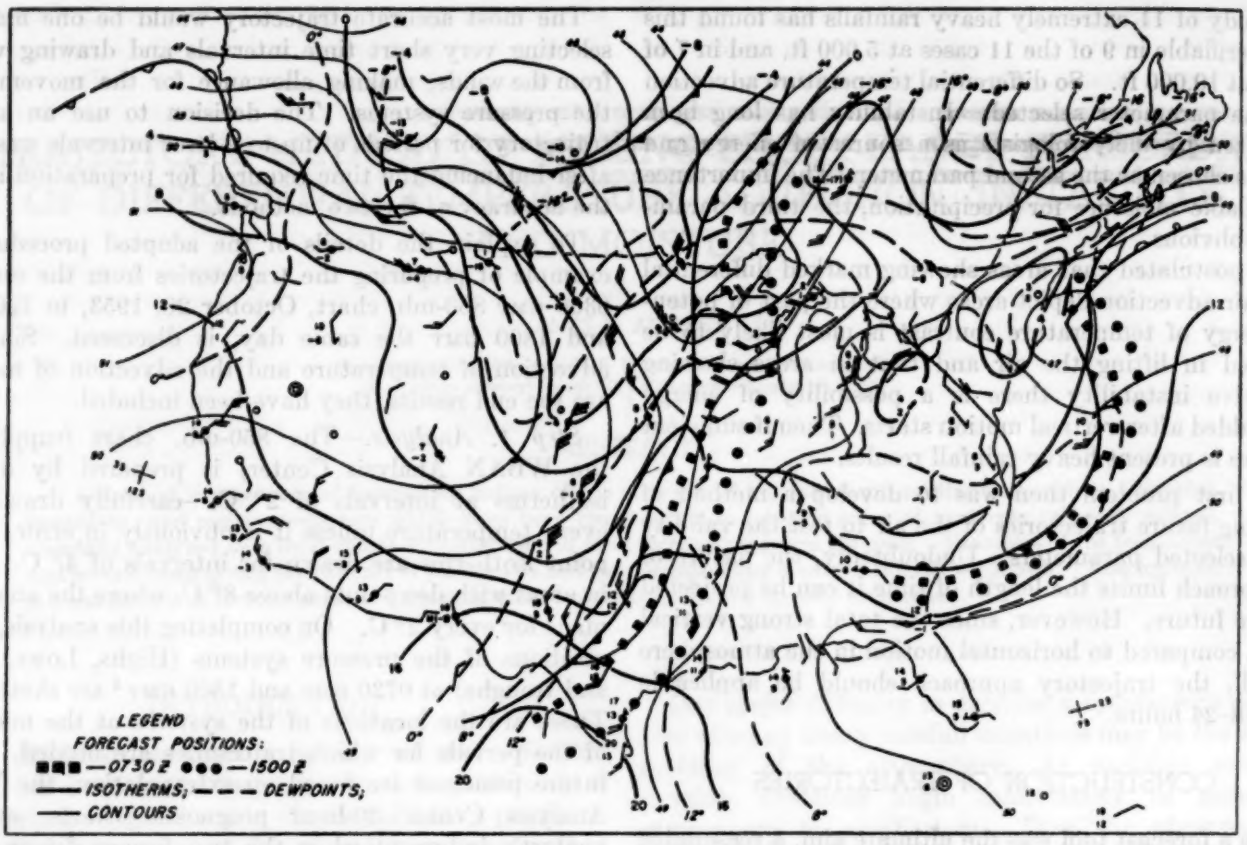

FIGURE 1.—850-mb. chart for 0300 GMT, October 26, 1953 with forecast trough positions at the midpoints in the time periods for which trajectories will be computed as a first step in the forecast of areas of heavy rain. See following figures for successive steps in the procedure.

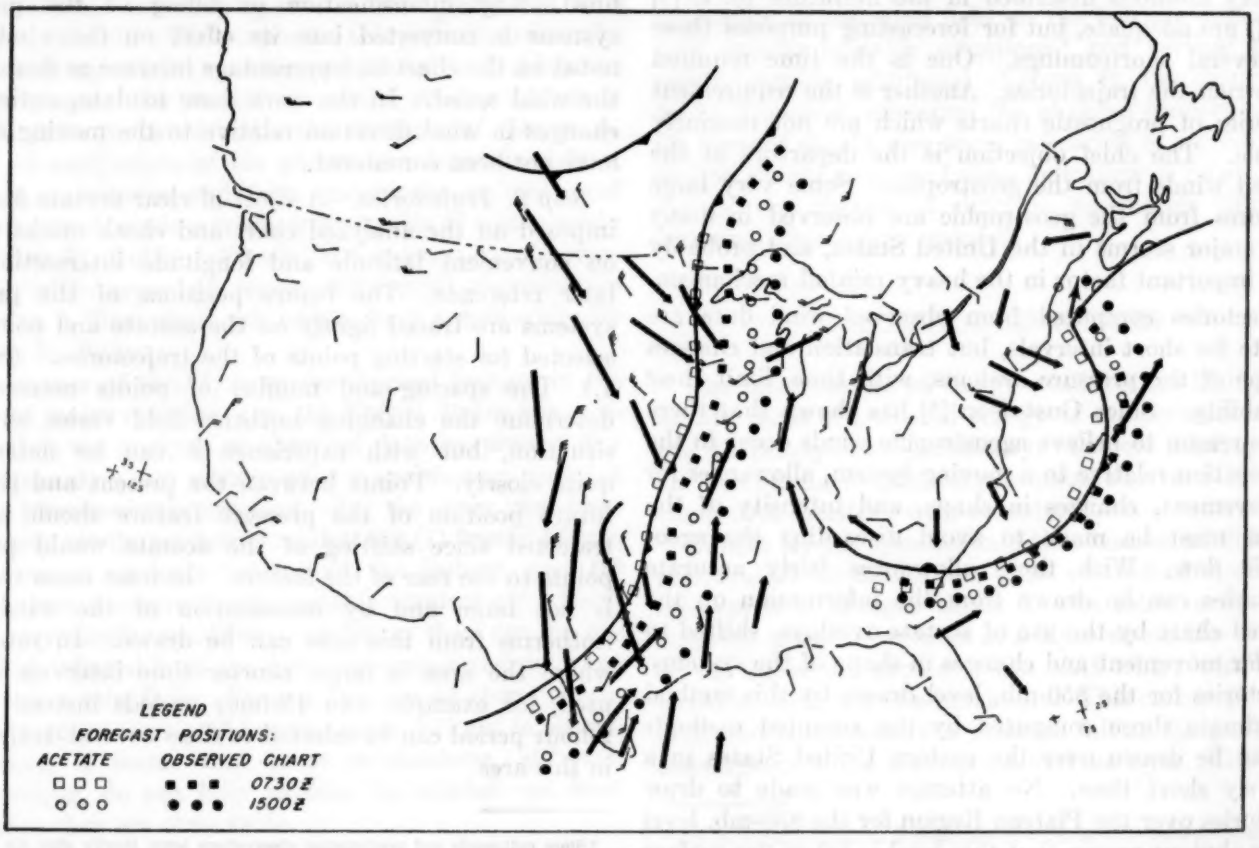

FIGURE 2.—Forecast trajectories for the period 0300–1200 GMT, October 26, 1953 showing position of the acetate overlay on the observed map (0300 GMT, October 26, 1953) when these trajectories were computed.

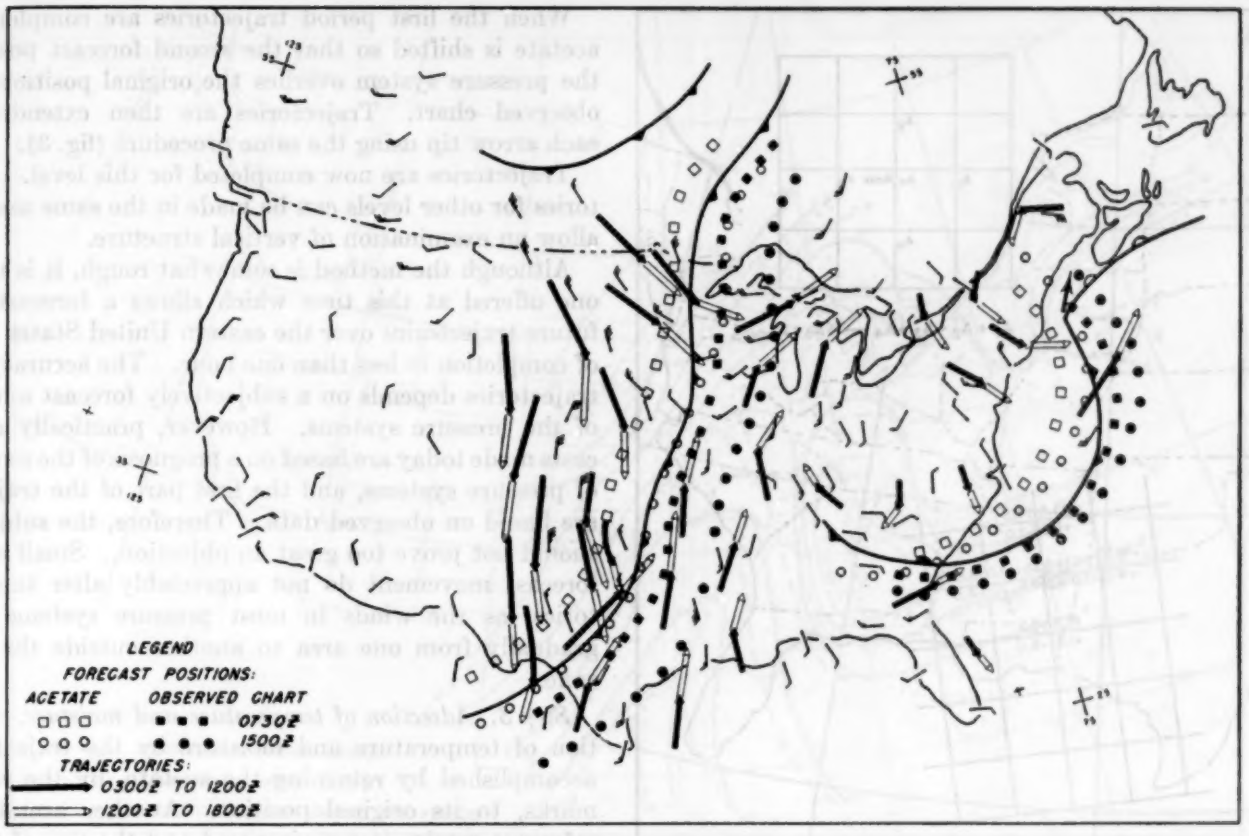

FIGURE 3.—Forecast trajectories for the periods 0300–1200 GMT (solid arrows) and 1200–1800 GMT (open arrows) October 26, 1953 showing position of acetate overlay on observed map (0300 GMT, October 26, 1953) when 1200–1800 GMT trajectories were computed.

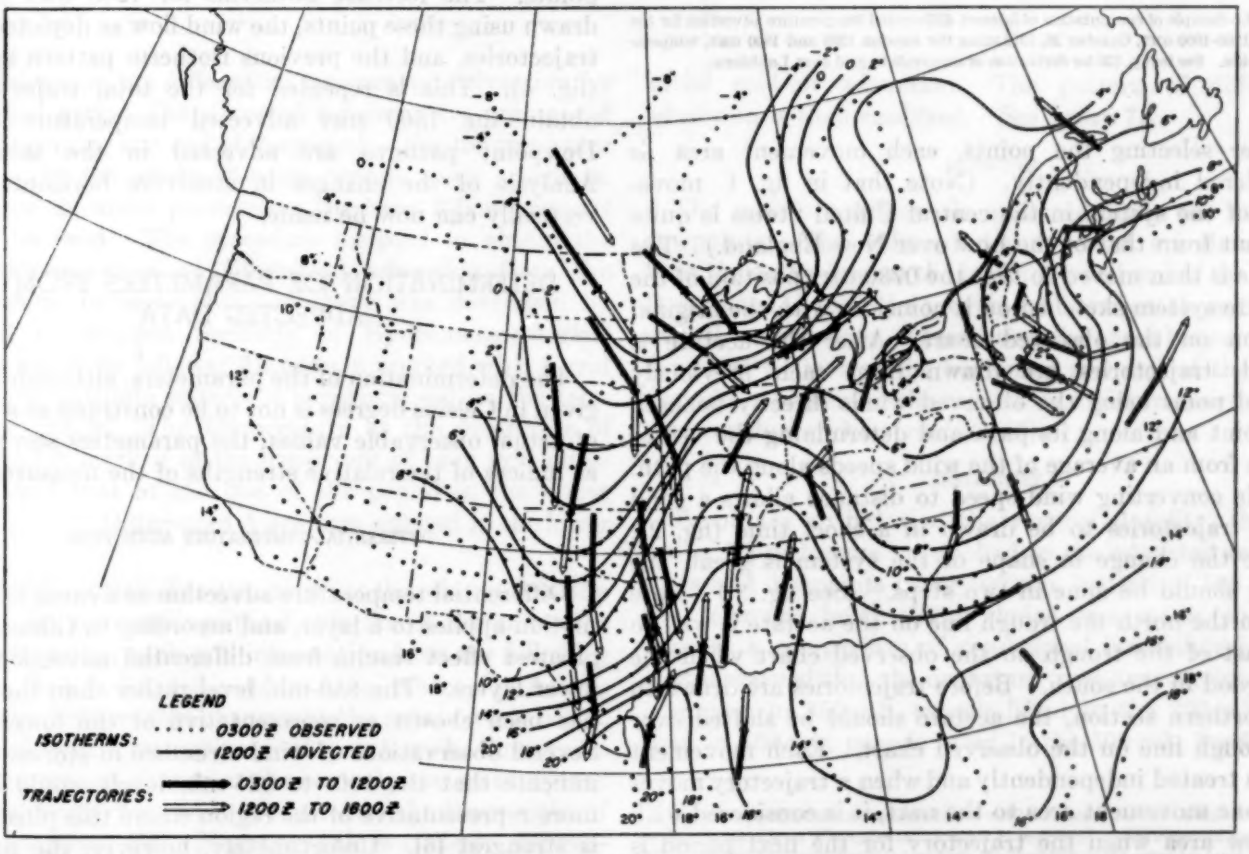

FIGURE 4. Forecast 850-mb. temperature field for 1200 GMT, October 26, 1953 (solid lines) obtained by advecting the 850-mb. temperature observed at 0300 GMT (dotted lines) from the beginning point to the tip of each solid arrow. The forecast of the 1800 GMT temperature field (needed in the next step but not shown here) is obtained by advecting the 0300 GMT temperature to the tip of the open arrow.

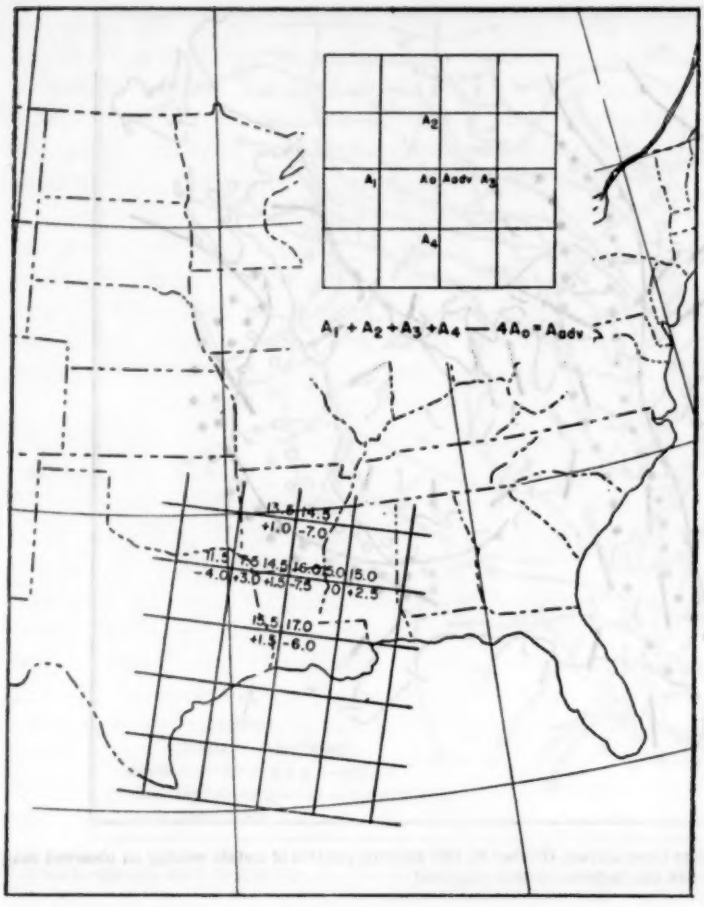

FIGURE 5.—Sample of computation of forecast differential temperature advection for the period 1200–1800 GMT, October 26, 1953 using the forecast 1200 and 1800 GMT, temperature fields. See text p. 325 for derivation of numerals in grid over Louisiana.

After selecting the points, each movement area is considered independently. (Note that in fig. 1 movement of the system in the central United States is quite different from that of the Low over New England.) The acetate is then moved so that the 0730 GMT position of the pressure system sketched on it coincides with the original position on the observed chart. After the acetate is shifted, trajectories are drawn from each previously located point using the observed winds directly beneath the point and along its path and determining the vector length from an average of the wind speeds along the path. A scale converting wind speed to distance allows a good many trajectories to be drawn in a short time (fig. 2). Where the change in shape of the system is great, the fitting should be done in two steps. (See fig. 3.) Note that in the north the trough line on the acetate is well to the east of the trough on the observed chart when the fit is good in the south. Before trajectories are drawn in the northern section, the acetate should be shifted over the trough line on the observed chart. Each movement area is treated independently and when a trajectory moves from one movement area to the next, it is considered with the new area when the trajectory for the next period is drawn.

When the first period trajectories are completed, the acetate is shifted so that the second forecast position of the pressure system overlies the original position on the observed chart. Trajectories are then extended from each arrow tip using the same procedure (fig. 3).

Trajectories are now completed for this level. Trajectories for other levels can be made in the same manner to allow an examination of vertical structure.

Although the method is somewhat rough, it is the only one offered at this time which allows a forecast of the future trajectories over the eastern United States capable of completion in less than one hour. The accuracy of the trajectories depends on a subjectively forecast movement of the pressure systems. However, practically all forecasts made today are based on a prognosis of the movement of pressure systems, and the first part of the trajectories are based on observed data. Therefore, the subjectivity should not prove too great an objection. Small errors in forecast movement do not appreciably alter the trajectories, as the winds in most pressure systems change gradually from one area to another outside the frontal zone.

Step 3. Advection of temperature and moisture.—Advection of temperature and moisture by the trajectories is accomplished by returning the acetate, by the reference marks, to its original position. Another acetate, with reference marks, is superimposed and the tips of the first trajectories labeled with the temperatures at the beginning points. The forecast isotherms for 1200 GMT are then drawn using these points, the wind flow as depicted by the trajectories, and the previous isotherm pattern as guides (fig. 4). This is repeated for the total trajectories to obtain the 1800 GMT advected temperature pattern. Dewpoint patterns are advected in the same way. Analysis of the changes in structure horizontally and vertically can now be made.

DETERMINATION OF PARAMETERS FROM THE ADVECTED DATA

The determination of the parameters, although they are given in Celsius degrees is not to be construed as a forecast of actual observable values; the parameters serve merely as indices of the relative strengths of the measured items.

DIFFERENTIAL TEMPERATURE ADVECTION

Differential temperature advection as a cause of vertical motion applies to a layer, and according to Gilman [1], its greatest effect results from differential advection in the lower layers. The 850-mb. level rather than the surface has been chosen as representative of the lower layers. Several observations of wind structure in storms seem to indicate that the 900- to 925-mb. levels would be even more representative of the region where this phenomenon is strongest [6]. Unfortunately, however, the necessary data are not available for those levels.

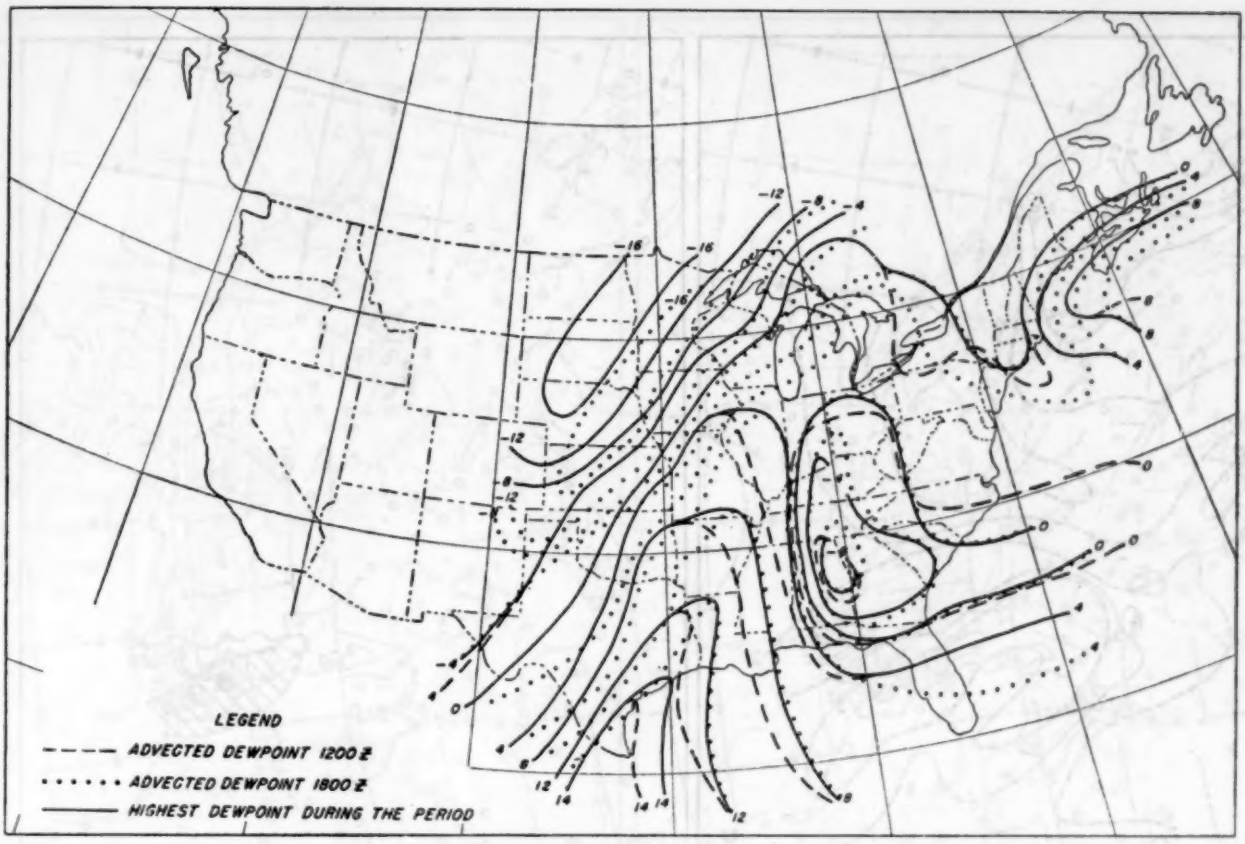

FIGURE 6.—Forecast moisture fields for 1200 and 1800 GMT, October 26, 1953 obtained by advecting the observed dewpoints along the trajectories in the same way the temperature was advected. Also shown is the field of the highest dewpoint forecast for the interval 1200–1800 GMT.

To determine the differential temperature advection for a specified period, the advected temperatures are needed at the beginning and end of the period. For the particular purposes of the study, 6-hour periods seem adequate. For short duration phenomena, perhaps 3-hour periods should be used. The procedure adopted to obtain the quantitative values of differential advection from the temperature patterns obtained above was developed by Richard C. Bourret formerly of Hydrometeorological Section and is as follows: An acetate marked with a grid of 2-degree latitude squares is superimposed on the temperature charts. The temperature at the beginning of the period is marked in the upper left of each grid intersection and that at the end of the period in the upper right (fig. 5). Differences A are then entered in the lower left.

Since differential advection involves the relationship of a point to its surroundings the Laplacian of the advection A_{ADV} is found for each grid intersection from the following formula $A_1+A_2+A_3+A_4-4A_0=A_{ADV}$, where A_1, A_2, A_3, A_4 are the temperature changes at the points west, north, east, and south respectively of point with change A_0. This temperature change at the central point as compared with the change around it is plotted in the lower right of the grid intersection. Negative values indicate differential warm-air advection; positive values indicate differential cold-air advection. The pattern of differential advection is then analyzed. See figure 7A.

MOISTURE

The moisture pattern is analyzed from the advected dewpoints. The values for the period are determined from those obtained at the beginning and end of the period. It is assumed that the movement between these two is a smooth progression. Connecting the areas between equal dewpoint isolines at the beginning and end of the period provides a picture of the maximum moisture existing over the area during the period (fig. 6).

INSTABILITY

To obtain an index of the vertical stability, the Showalter [7] technique [4] is applied to the advected temperatures and dewpoints using 700 mb. instead of 500 mb. as the reference level. This choice was made, in part, because a comparison of conditional instability in large storms showed that the departure rom average conditions is greater in 850-mb. parcels lifted to the 700-mb. level than in 850-mb. parcels lifted to the 500-mb. level. The

[4] The parcel is lifted along the dry adiabat until saturated, then along the moist adiabat to the reference level where the temperature is compared to the observed temperature. When the lifted temperature is colder than the observed at the reference level, the departure is noted as positive, and vice versa.

326683—55——2

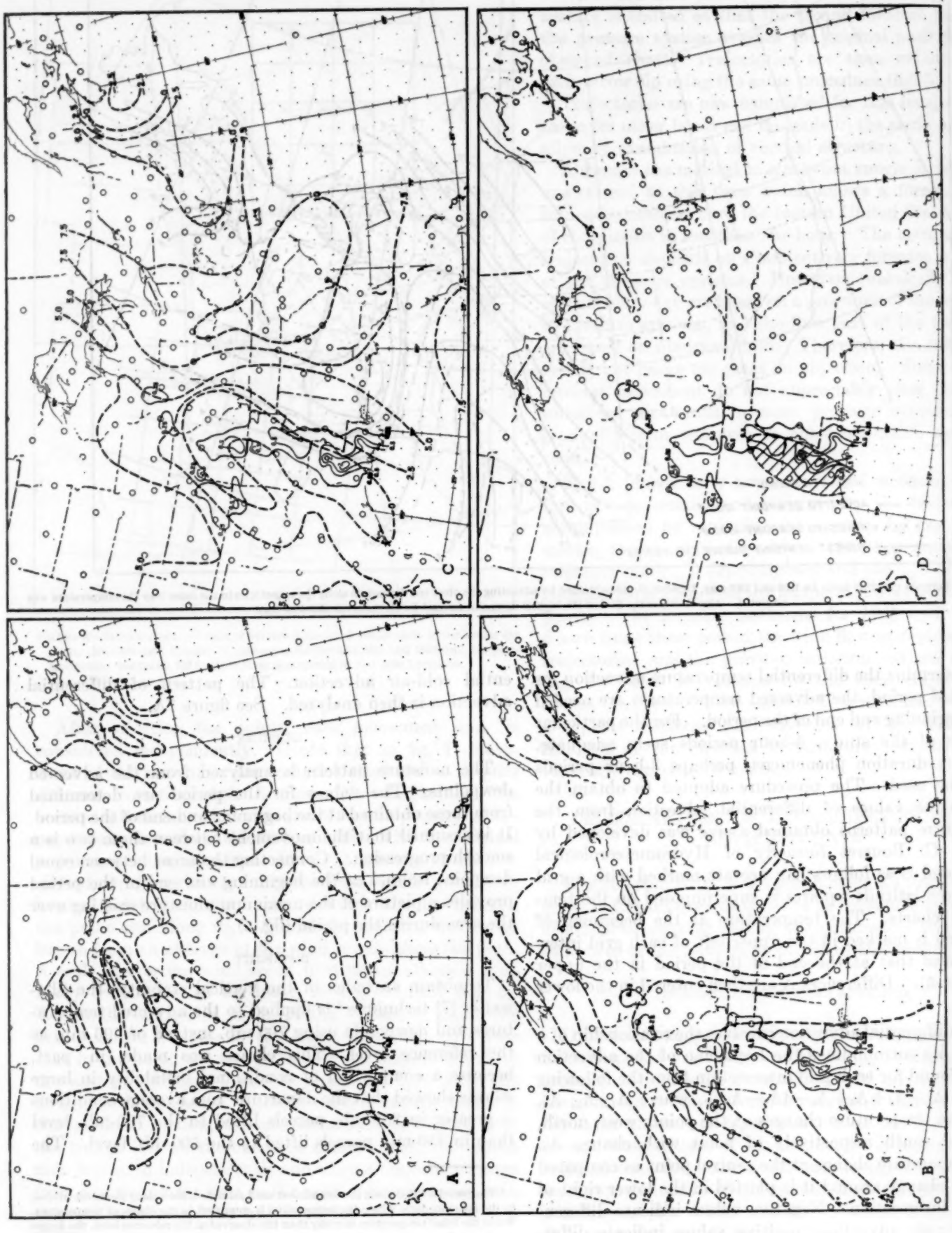

FIGURE 7.—Forecast parameters and forecast heavy rain area each superimposed on isohyets of observed precipitation (thin solid lines) for period 1200–1800 GMT, October 26, 1953. (A) Forecast differential temperature advection field resulting from operations shown in figures 1–5. (B) Forecast dewpoint for the period. (C) Forecast stability computed by the Showalter technique using the advected temperatures and dew points and the 700-mb. rather than the 500-mb. level as the reference level. (D) Forecast heavy precipitation area (hatched) based on coincidence of centers of intensity of the parameters shown in parts A, B, C. Note correspondence with area of observed rain.

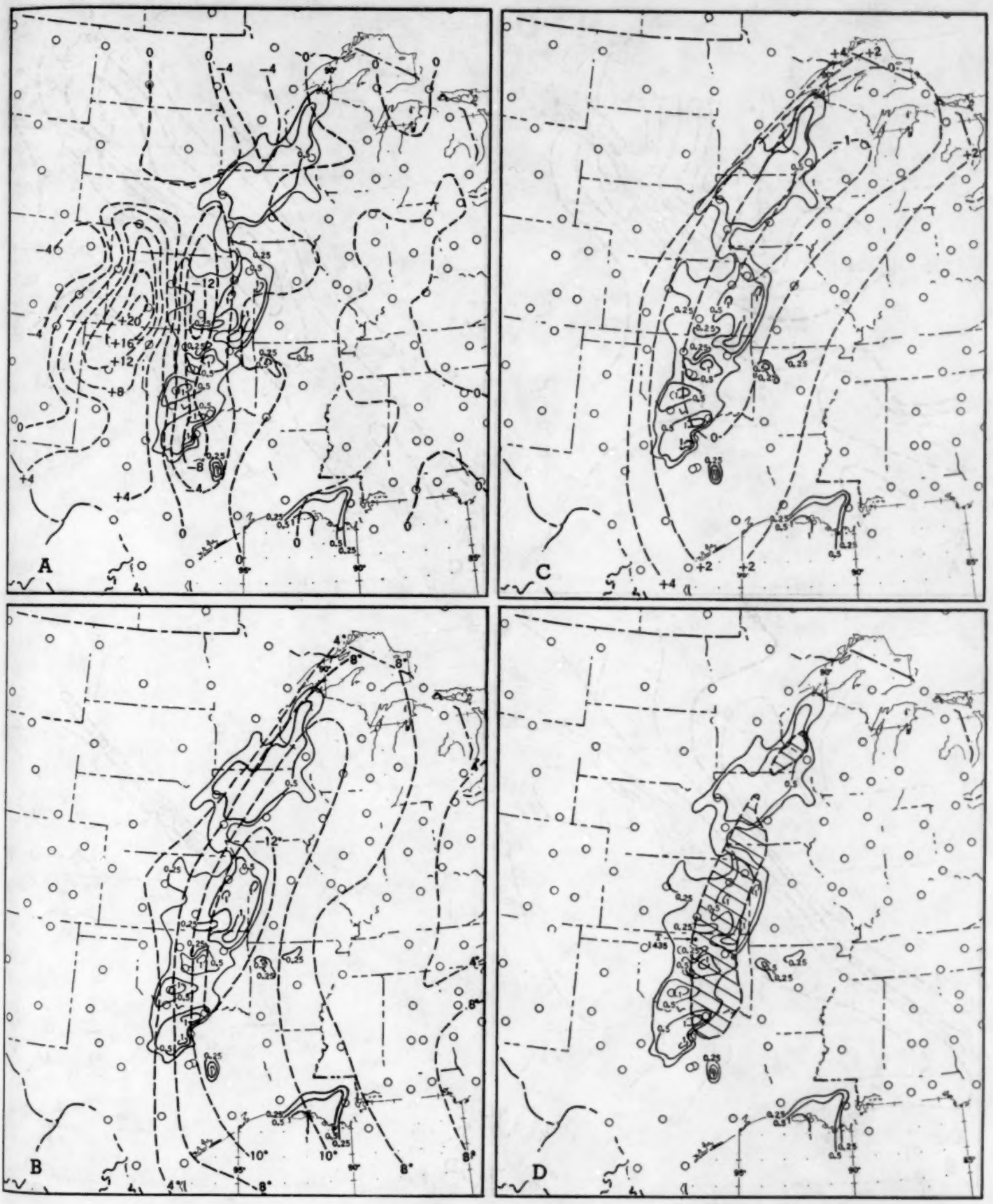

FIGURE 8.—Forecast parameters (A—differential temperature advection, B—dewpoint, C—stability) and (D) forecast heavy rainfall area each superimposed on isohyets of observed precipitation (thin solid lines), 1200–1800 GMT, November 19, 1953.

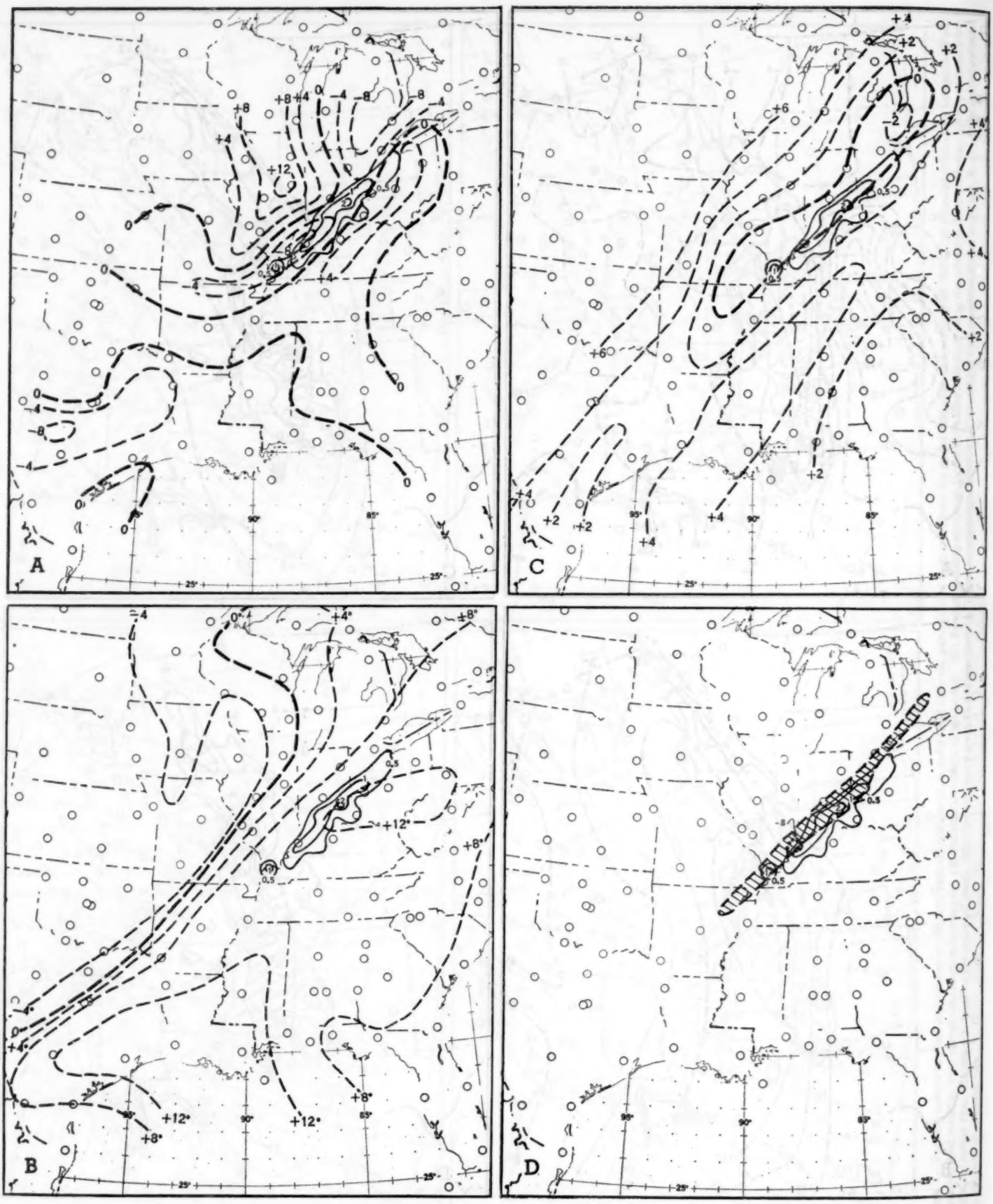

FIGURE 9.—Forecast parameters (A—differential temperature advection, B—dewpoint, C—stability) and (D) forecast heavy rainfall area each superimposed on isohyets of observed precipitation (thin solid lines), 0300-0900 GMT, December 7, 1953. In (D) center of warm differential advection is again shown (dotted).

difficulty in handling the high winds at the 500-mb. level on the small-scale chart on which it is now plotted also influenced the choice.

The conditional instability is computed for both periods and combined by the same method used for the dewpoints. See figure 7C.

TESTS OF METHOD AND PARAMETERS

Comparison of the patterns and intensities of these parameters with rainfall areas observed during the periods permits a test of both the trajectory method and the chosen parameters. Both have to be reasonably correct to obtain any correspondence between the areas indicated by parameters and the areas of observed rain. Slight displacements in areas of heavy rainfall and the areas indicated by the parameters suggest the parameters are probably correct but the trajectories are inaccurate. If no correspondence in areas is obtained it indicates either the reasoning behind the trajectory method, the method itself, the parameters chosen, or all three are incorrect.

FORECAST PARAMETERS vs. RAINFALL

To test the trajectory method and the parameters, daily forecasts of the parameters for the period from 1200 GMT to 1800 GMT have been made from 0300 GMT data for October and November 1953. The example used to explain the procedure for determining trajectories (fig. 7) is one of these. George A. Lott and Lillian K. Rubin have made special forecasts of the parameters in several heavy rainfall cases without previous knowledge of the exact location of the heavy rain. A few of these will be shown along with the corresponding rainfall.

In figure 7 the forecast values of the parameters from the previously discussed example are superimposed on the isohyets of observed rainfall during the period. Note in figure 7A that the areas with rainfall are usually where warm differential advection has been forecast. The exception in northern Illinois is displaced, probably due to the formation of a Low in southeastern Kansas which was not forecast. The Low would cause warm air to flow more toward the northwest than forecast, shifting the differential advection in that direction. To explain the lack of rainfall in areas of strong warm differential advection and the variation in rainfall amounts, one must take the forecast moisture (fig. 7B), and stability (fig. 7C), patterns into consideration. The small rainfall center in southeastern Kansas and northeastern Oklahoma is associated with an area of instability, high differential warm-air advection, and a dewpoint of 4° C. The light rainfall between this center and the north-south band occurred in an area of greater moisture, the same instability, but a high value of differential cold-air advection. The heavy rainfall in Louisiana corresponds closely to high values of all three parameters.

Again in figure 8 the parameters fit the rainfall pattern fairly well; however, in the south where we are dependent on data over the Gulf, the high moisture and low stability values cut off before heavy rainfall. There could be several reasons for this. One may be lack of data over the Gulf, another, the effect of the change from over-water to over-land flow.

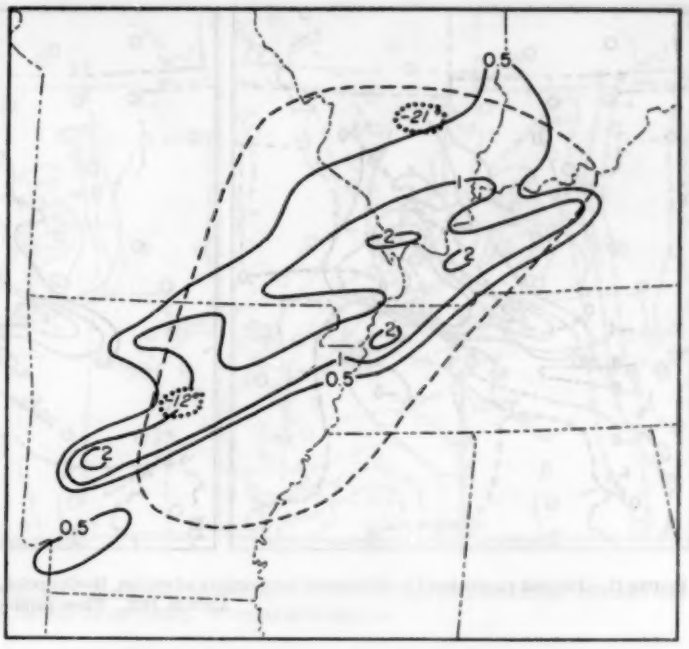

FIGURE 10.—Forecast heavy rainfall area (based on same parameters as shown in figs. 7, 8, and 9) superimposed on isohyets of observed precipitation (thin solid lines) 1500 GMT, March 21 to 0300 GMT, March 22, 1952. The magnitude and position of the centers of areas of warm differential temperature advection are shown by dotted lines.

Experience indicates that the areas of heavy rainfall (approximately 1 inch per 6 hrs.) usually coincide with the areas where differential temperature advection of −2° C. or greater (negatively), dewpoints of 10° C. or higher, and stability of less than 0° C. are forecast to coincide during the 6-hour period. Figures 7D and 8D show these forecast areas as compared to the rainfall for the two previous examples. Figure 9 shows the results of one of the heavy rainfall situations analyzed by Rubin and Lott. Figure 10 shows a comparison of a 12-hour forecast of heavy rain areas with the observed rainfall. The 12-hour forecast is made by combining the forecast areas from two consecutive 6-hour forecasts.

The correspondence of the areas is fairly good considering the inaccuracies in the trajectories and the limitations in determining the original temperature and moisture fields. Forecasts shown in figures 7D and 8D were made using 850- and 700-mb. charts plotted on a scale of 1:12,500,000. A large-scale map increases the precision with which the trajectories can be drawn which in turn might improve the correspondence between the forecast and observed rainfall. Figure 9 was made using charts with a ratio of 1:5,000,000. This perhaps accounts for the better correspondence. (All maps are reproduced here on the same scale.)

A more definite quantitative forecast cannot be made until the effects of the gradient of the differential temperature advection parameter, and the relative importance of

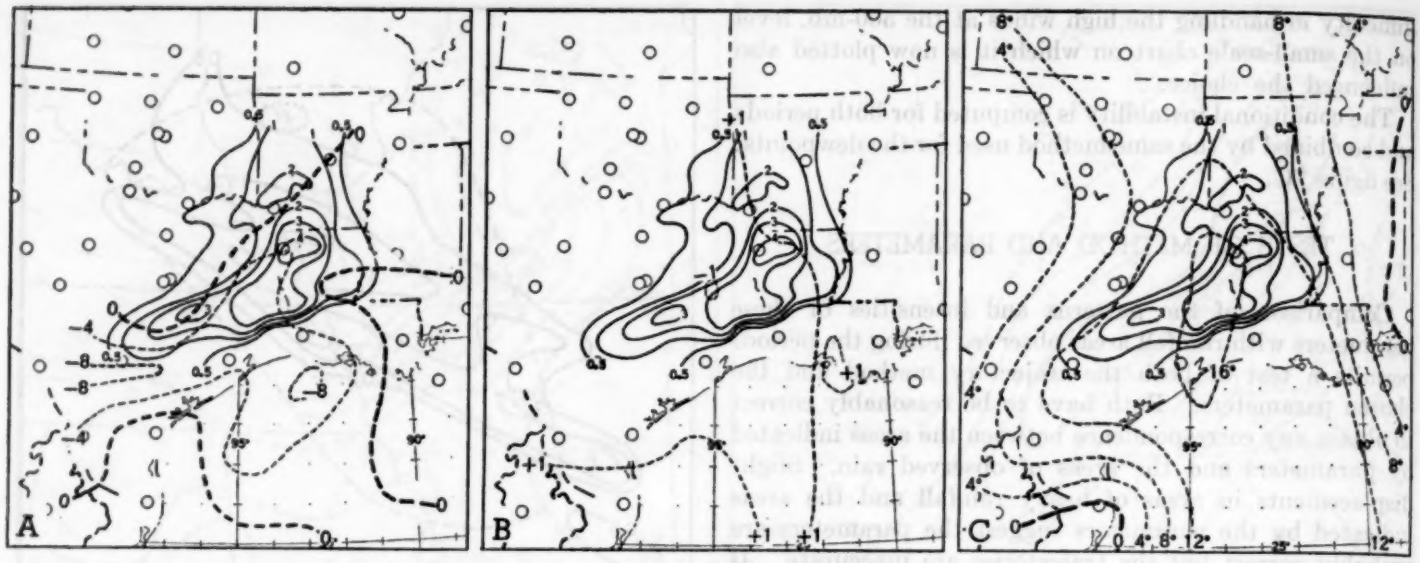

FIGURE 11.—Forecast parameters (A—differential temperature advection, B—dewpoint, C—stability) superimposed on isohyets of observed rainfall (thin solid lines), 0300-0900 GMT, April 29, 1953. These parameters based on forecast trajectories.

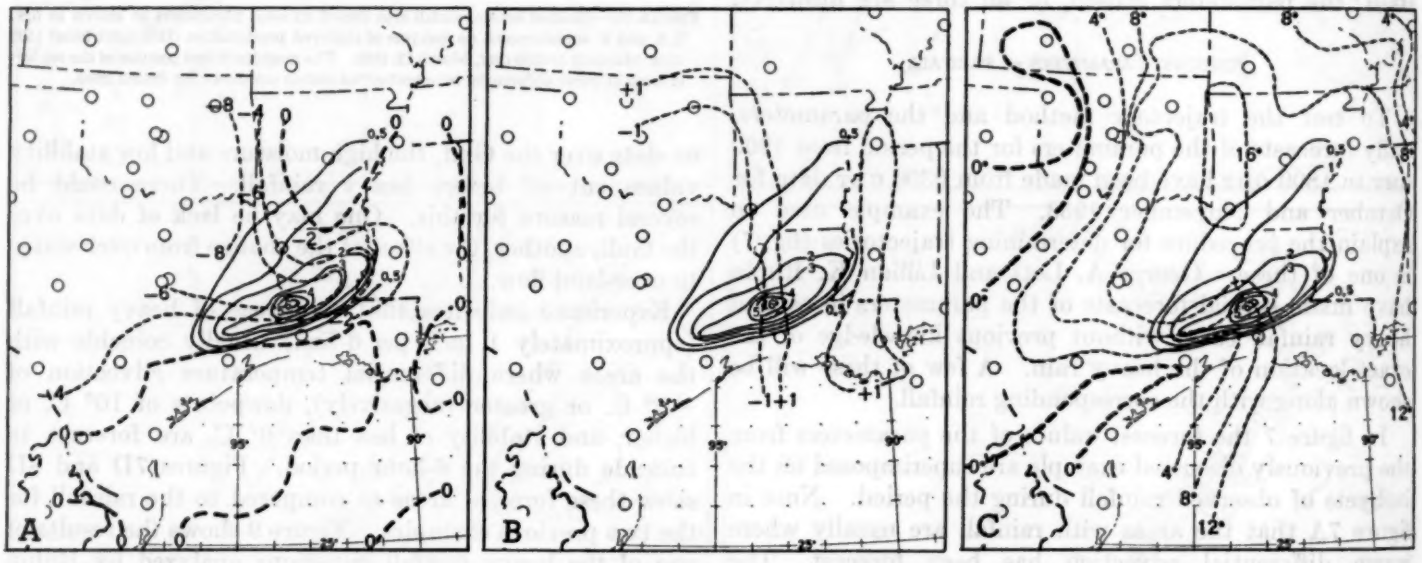

FIGURE 12.—Forecast parameters (A—differential temperature advection, B—dewpoint, C—stability) superimposed on isohyets of observed rainfall (thin solid lines), 0900-1500 GMT, April 29, 1953. These parameters based on forecast trajectories.

the other two parameters, are determined. However, it seems the forecasting of the approximate areas of heavy precipitation would be useful to some interests.

COMPARISON OF THE PARAMETERS DETERMINED FROM FORECAST TRAJECTORIES AND FROM OBSERVED TRAJECTORIES

A comparison of the parameters forecast from the trajectory method and those computed from observed streamlines and their relation to the rainfall pattern has been made by Rubin [8]. The results that follow in this subsection were extracted from her paper.

Exceedingly heavy rain fell over the northern two-thirds of Louisiana, eastern Texas, and southwestern Mississippi on April 28–29, 1953, Many of the values reported were new 24-hr. records, 12.77 inches at Pollock in central Louisiana on the 29th, 12.54 inches at Camp Polk on the same date. In Mississippi, Vicksburg reported the heaviest 12-hour rainfall of record, 8.73 inches, between 3:10 a. m. and 3:00 p. m. on the 29th. High winds accompanied the heavy rainfall, and a tornado was reported in northern Louisiana just after midnight of the 28th. This situation was used to test the trajectory method for the short-period forecast of heavy rains.

The axis of the differential temperature advection pattern (fig. 11) at 850-mb. for the first 6-hour forecast period of the April 28–29 storm was coincident with the axis of the northeastern part of the precipitation area for the same time. Westward, however, the axis of the differential advection pattern became increasingly east-west. Nevertheless, almost the entire precipitation area lay within the area of warm differential temperature advection. A flaw in the pattern was the center of warm

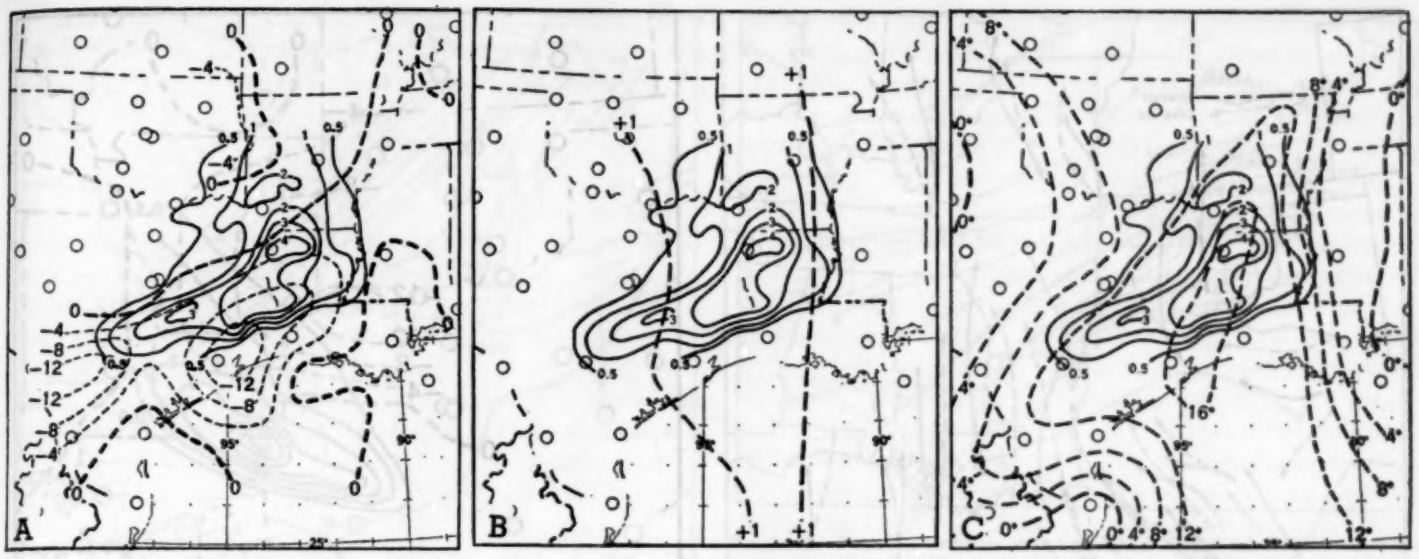

FIGURE 13.—Forecast parameters (A—differential temperature advection, B—dewpoint, C—stability) superimposed on isohyets of observed rainfall (thin solid lines), 0300-0900 GMT, April 29, 1953. These parameters based on observed trajectories for the period. Compare with figure 11.

differential advection in the Gulf, south of the edge of the rain area. Although the greatest part of the precipitation area lay within the +1 limit of the stability parameter, a part of the area was cut off. The moisture pattern (dewpoint parameter) forecast for the first period agreed well with the precipitation pattern.

For the second 6-hour forecast period, the axis of the differential temperature advection (fig. 12) was coincident with that of the eastern half of the precipitation pattern. Although the axis of the western part of the differential advection pattern turned slightly north of west while the axis of the precipitation was slightly south of west, the entire precipitation area for this period was within the area of warm differential temperature advection. The agreement was closer than in the first period. The area of strong warm differential advection northwest of the rain area caused no concern, for it has been observed in previous cases that when one center of warm differential advection lies upstream from another, the rain will occur with the upstream center. The vitiation of the downstream center is probably due to a distortion of the upstream temperatures as a result of the rainfall there. The +1 limit of stability bisected the precipitation area for this forecast period. Although the moisture pattern for the second period indicated a drying-out over part of the precipitation area, there was probably an upwelling from below the 850-mb. level.

The differential temperature advection was also computed for the 700-mb. level for both 6-hour periods. In the first period there was some warm differential advection over the northeastern third of the heavy rain area, while there was cold differential advection over the rest of the precipitation area. In the second period there was cold differential advection over the entire precipitation area.

If the basis for the trajectory method is sound, use of the actual wind flow for the forecast period should improve the verification. As a test, observed trajectories were constructed for the period from 0300 to 0900 GMT based on streamlines at 0300 GMT and at 0900 GMT, and for the period from 0900 to 1500 GMT, based on streamlines for these two times. The observed trajectories for the first 6-hour period at the 850-mb. level were then used to advect the temperature and dewpoint fields as they existed at that level at 0300 GMT, and those for 700 mb. were used to advect the temperature field at that level. The usual procedure was then applied to the advected data to determine the 850-mb. differential temperature advection, dewpoint, and stability parameters (fig. 13).

The most significant improvement in the resulting pattern of differential temperature advection was that the center of warm differential advection that appeared over the Gulf in the original forecast chart was now situated on land, partially overlapping the heavy rain area. Orientation of the moisture parameter pattern with relation to the precipitation pattern was also somewhat improved. The errors in the original forecast chart appeared to be due primarily to an increase in the speed of the winds that was not forecast. Figure 14 shows a comparison of forecast and observed trajectories. The network actually used in projecting temperatures and dewpoints was far more dense. The lack of a more perfect pattern on the forecast chart based on observed trajectories may be due in part to the sparse wind data available. Stronger winds than those reported may have occurred between stations.

The observed trajectories for the second period were applied to the 850-mb. temperature field as it was forecast for 0900 GMT, and the differential temperature advection for the second period was computed. Surprisingly, the resulting pattern of warm differential advection, figure 15, was very much worse than that originally forecast. There was no apparent reason for this.

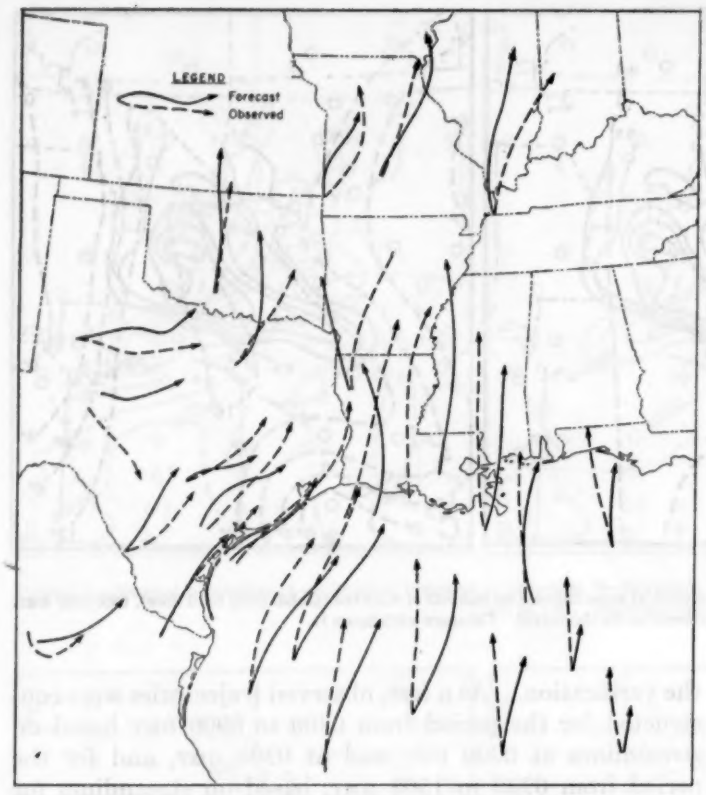

FIGURE 14.—Comparison of forecast and observed trajectories, 0300-0900 GMT, April 29, 1953.

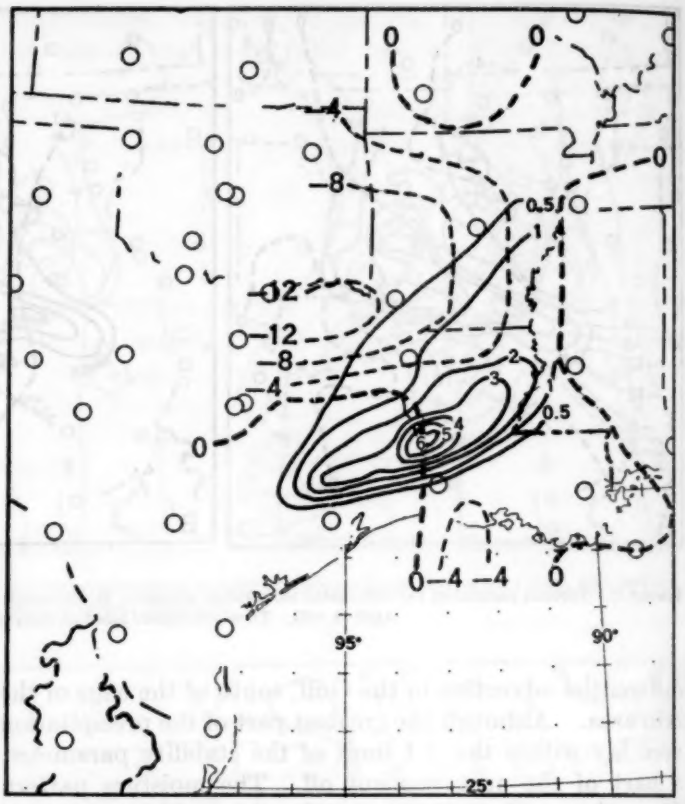

FIGURE 15. Forecast differential temperature advection superimposed on isohyets of observed rain (thin solid lines), 0900-1500 GMT, April 29, 1953. This forecast, based on observed trajectories. Compare with figure 12.

FORECAST OF DIFFERENTIAL TEMPERATURE ADVECTION AND TORNADO OCCURRENCE

During the course of the study it was noted that reported tornado occurrences were associated with forecast areas of warm differential temperature advection. As a step toward determining the value of forecasts of differential advection as an aid in tornado forecasting, the tornado situation of June 7–9, 1953, was selected for study by Bailey [9]. The results presented in this section were extracted from his report.

The differential advection for the approximate time of occurrence of the tornadoes of June 7, 8, and 9, 1953, was computed by the method already outlined. Difficulty was experienced in constructing an accurate 850-mb. chart far enough westward into the mountainous terrain to forecast the differential temperature advection for eastern Nebraska on June 7. It was decided to use the 700-mb. chart for 1500 GMT, June 7, and to carry out the process exactly as is ordinarily done on the 850-mb. chart. The resulting forecast for the 6-hour period centered at 2200 GMT, June 7 (fig. 16), shows good agreement with the tornado locations.

The use of the 700-mb. chart in this example raises the question of the generality of results for the Rocky mountain areas and other localities. Some other cases have since been studied by the Hydrometeorological Section using the 700-mb. chart when the area of interest was

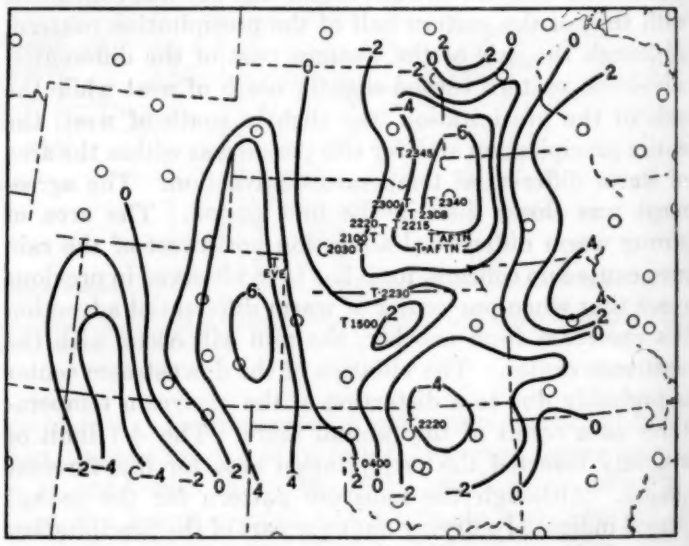

FIGURE 16.—Tornado occurrences plotted on field of forecast differential temperature advection at 700 mb., 1900 GMT, June 7, to 0100 GMT, June 8, 1953. Forecast made from chart for 1500 GMT, June 7.

west of about 95° W. longitude. Results from these cases show better correspondence with areas of rainfall than use of the 850-mb. charts for the same dates. This indicates that the 700-mb. chart should be used in areas where the 850-mb. chart is near or below the surface. However, since low level differential advection is desired, the 850-mb. chart is still recommended for areas where it is near the gradient wind level or above.

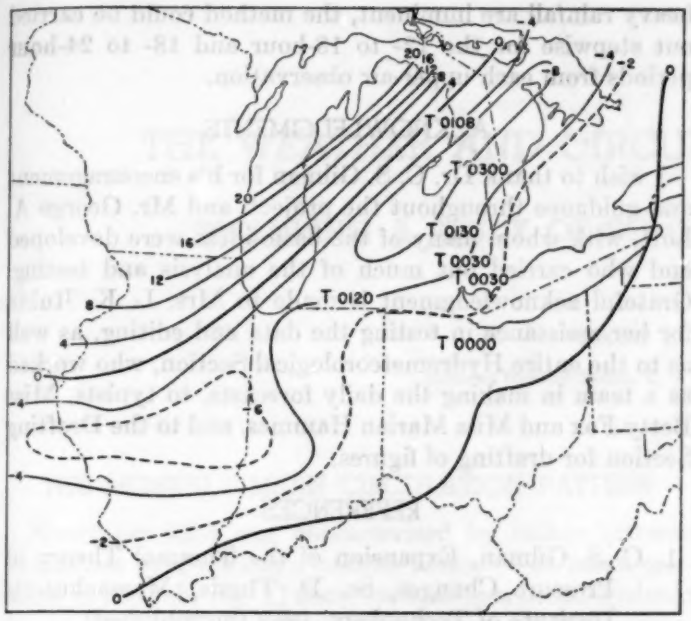

FIGURE 17.—Tornado occurrences plotted on field of forecast differential temperature advection at 850 mb., 0000–0600 GMT, June 9, 1953. Forecast made from chart for 1500 GMT, June 8.

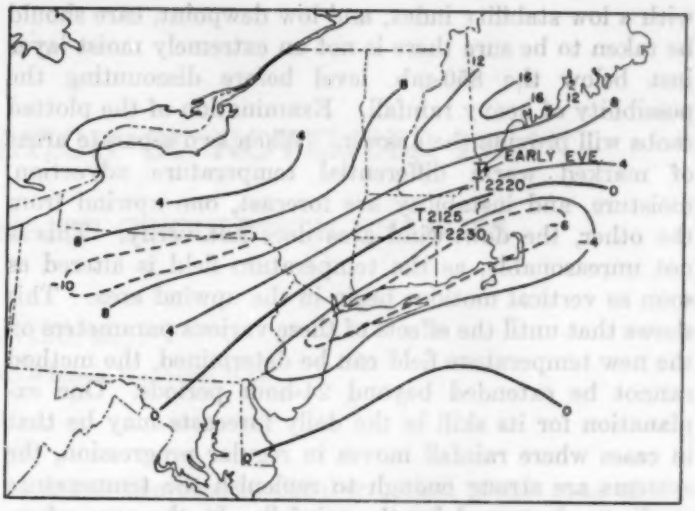

FIGURE 18.—Tornado occurrences plotted on field of forecast differential temperature advection at 850 mb., 1900 GMT, June 9 to 0100 GMT, June 10, 1953. Forecast made from chart for 1500 GMT, June 9.

The differential temperature advection was computed from the 850-mb. chart 12 hours in advance for the approximate time of occurrence of the highly destructive tornadoes at Flint, Mich., and nearby areas on June 8, 1953, and is shown in figure 17. The tornadoes occurred within the area of largest values of warm differential advection. Even though very small values, which might be considered within the error of calculation, are neglected, there was an area of rather large warm differential advection extending to the south of the area in which the tornadoes occurred.

The forecast of differential advection for the approximate time of the tornadoes at Worcester, Mass., and nearby areas on June 9, 1953 (fig. 18), shows the largest negative values to the southeast of the area of tornado occurrence but very nearby. This forecast was made from the 850-mb. chart for 1500 GMT June 9. This case and others in which the computed maximum of future warm differential advection occurs near the area of severe weather indicates that the method used is not always accurate in forecasting the exact location of future storm areas.

Computations of the 850-mb. divergence fields from the actual maps for the times of occurrence of the tornadoes at Flint, Mich., and Worcester, Mass., have been presented by Cressman [10]. His computations showed a line of maximum convergence associated with the tornado development which agrees approximately with the areas of negative differential advection computed above for the same times. Therefore, convergence in the lower levels is confirmed in this case and is consistent with Gilman's [1] hypothesis for the physical processes involved.

The results of these three tornado cases are not sufficient for drawing definite conclusions. However the Hydrometeorological Section has made these forecasts on a daily basis during much of the 1954 tornado season and most cases showed areas of maximum warm differential advection within or near the areas in which tornadoes occurred. Moreover, other cases, such as that in figure 9A as well as several which the Severe Local Storm Center worked up while experimenting with this technique, show similar results.

In general the results indicate that the computed differential temperature advection usually has the largest negative values within the areas of most severe weather. It seems that the local maximum of warm differential advection is associated with tornado development. However it is obvious that this is not the only requirement. The absence of latent instability in the atmosphere may account for the failure of the warm differential advection to act as a trigger mechanism in some cases. The use of a 6-hour period for computing the differential advection involved a definite timing problem. However, it is doubtful that shortening the period would alleviate this problem because of the limitations of the temperature field analysis with respect to the size of a tornado. At best the method would suggest probable areas of tornado occurrence when combined with other parameters.

LIMITATIONS OF THE METHOD

It should be pointed out that the differential temperature advection parameter as defined and used in this paper is an average over a period and only where the values are large or continue over most of the period will they show up as definite centers. Because the moisture and stability indices are maxima for the period, occasionally the three parameters are not coincident in time and the forecast area of heavy rain is larger than the observed.

There are several points where caution should be used in interpreting the significance of the forecast parameters. Where warm differential temperature advection is high,

with a low stability index, and low dewpoint, care should be taken to be sure there is not an extremely moist layer just below the 850-mb. level before discounting the possibility of heavy rainfall. Examination of the plotted raobs will provide the answer. When two separate areas of marked warm differential temperature advection, moisture, and instability are forecast, one upwind from the other, the downwind area does not verify. This is not unreasonable, as the temperature field is altered as soon as vertical motions begin in the upwind area. This shows that until the effects of these various parameters on the new temperature field can be determined, the method cannot be extended beyond 24-hour periods. One explanation for its skill in the daily forecasts may be that in cases where rainfall moves in regular progression, the systems are strong enough to replenish the temperature gradients destroyed by the rainfall. In the case where progression is irregular, little vertical motion occurs upstream to destroy the contrasts.

The objection may be raised that only the lower levels of the atmosphere are being considered. Undoubtedly, the inclusion of the surface and the 500-mb. levels would be helpful. However, the greatest moisture transport is above the gradient level [11] (about 925 mb.) and approximately one-half the earth's atmosphere is below the 500-mb. level. Since time is always an important factor in a forecast method, the search is always for the best results with the least expenditure of time.

CONCLUSIONS

From the relations shown in the figures, the basic reasoning of the trajectory method appears to be sound and the method of preparing the trajectories fairly accurate. The indices of the differential temperature advection, stability, and moisture seem to be related to the rainfall mechanism although they are not necessarily the only influences. An attempt is being made to apply statistical methods to determine the relative importance of each factor or combination of factors in the production of heavy rainfall. When this is completed it should be possible to forecast areas of heavy rainfall 12 to 18 hours in advance, with a more definite indication of intensity.

The trajectory method lends itself well to a centralized forecast unit. Although there is a considerable amount of labor involved, it should be pointed out that on many days the possibilities of heavy rainfall can be discounted for a large part of the United States, by examination of the observations. In these cases, trajectories and the parameters need be computed for only a small area. As each parameter is computed it reduces the area for which the other parameters are necessary. When possibilities of heavy rainfall are imminent, the method could be carried out stepwise for the 12- to 18-hour and 18- to 24-hour periods from each upper-air observation.

ACKNOWLEDGMENTS

I wish to thank Dr. C. S. Gilman for his encouragement and guidance throughout the project, and Mr. George A. Lott, with whom many of the basic ideas were developed and who carried out much of the analysis and testing. Grateful acknowledgment is made to Mrs. L. K. Rubin for her assistance in testing the data and editing, as well as to the entire Hydrometeorological Section, who worked as a team in making the daily forecasts, to typists, Miss Betty Fox and Miss Marian Hammer, and to the Drafting Section for drafting of figures.

REFERENCES

1. C. S. Gilman, Expansion of the Thermal Theory of Pressure Changes, Sc. D. Thesis, Massachusetts Institute of Technology, 1949 (unpublished).
2. C. E. Erickson, Synoptic Characteristics of Extreme Rainfalls, Hydrometeorological Section, U. S. Weather Bureau, Washington, D. C., 1945 (unpublished).
3. H. R. Byers, *General Meteorology*, 1st ed. McGraw-Hill Book Co., Inc., New York, 1944.
4. S. Petterssen *Weather Analysis and Forecasting*, 1st ed. McGraw-Hill Book Co., Inc., New York, 1940.
5. A. F. Gustafson, "On Anomalous Winds in the Free Atmosphere," *Bulletin of the American Meteorological Society*, vol. 34, No. 5, May 1953, pp. 196–201.
6. G. A. Lott, "The Unparalleled Thrall, Texas Rainstorm," *Monthly Weather Review*, vol. 81, No. 7, July 1953, pp. 195–203.
7. A. K. Showalter, "A Stability Index for Thunderstorm Forecasting," *Bulletin of the American Meteorological Society*, vol. 34, No. 6, June 1953, pp. 250–252.
8. Lillian K. Rubin, Trajectory Method Applied to the Louisiana Storm of April 28–29, 1953, Hydrometeorological Section, U. S. Weather Bureau, Washington, D. C., April 1954 (unpublished).
9. M. H. Bailey, Forecast of Differential Advection and Tornado Occurrence, Hydrometeorological Section, U. S. Weather Bureau, Washington, D. C., May 1954 (unpublished).
10. G. P. Cressman, "An Approximate Method of Divergence Measurement," *Journal of Meteorology*, vol. 11, No. 2, April 1954, pp. 83–90.
11. G. S. Benton, M. A. Estoque, and J. Dominitz, "An Evaluation of the Water Vapor Balance of the North American Continent," *Scientific Report* No. 1, Dept. of Civil Engineering. The Johns Hopkins University, July 1953, 101 pp.

THE WEATHER AND CIRCULATION OF NOVEMBER 1954[1]

INCLUDING A STUDY OF SOME MAJOR CIRCULATION CHANGES

HARRY F. HAWKINS, JR.

Extended Forecast Section, U. S. Weather Bureau, Washington, D. C.

THE MONTHLY MEAN CIRCULATION PATTERN

November 1954 was characterized by rather extreme storminess over northern oceanic areas. The mean contours at 700 mb. (fig. 1) show essentially a broad cyclonic sweep of westerlies from eastern Asia to the eastern Pacific. This current was stronger and farther south than normal with heights as much as 280 ft. below normal in the northeast Pacific. A similar circulation pattern prevailed at 200 mb. (fig. 2) accompanied by a belt of westerly winds with average speeds of 50 to 55 m. p. s. extending from Korea to the mid-Pacific. Cyclones which were both numerous and intense, showed a marked tendency to rendezvous in the western Gulf of Alaska (see Chart X), where sea-level pressures averaged some 8 to 11 mb. below normal in a 992-mb. mean Low (Chart XI and inset).

After traversing the eastern Pacific, the westerlies turned quite sharply in anticyclonic fashion over western North America where a stronger-than-normal ridge was located. (Fig. 1 shows heights 180 ft. above normal in Idaho.) Despite the proximity of this ridge, a weak trough maintained off the southern California coast (somewhat similar to the pattern of the preceding month [1]). Downstream a well-marked trough dominated eastern North America, although heights remained above normal through mid-latitude sections of the trough. At 200 mb. the mean westerly maximum split over central North America, with one branch going eastward through James Bay to Newfoundland, and the other going southeastward from the Dakotas to Florida and thence northeastward along the east coast to Newfoundland. The principal storm track was either through central Canada or along the Canadian-United States border (Chart X). However, a number of secondaries occurred at lower latitudes in the United States and contributed to the sharp trough over the Southeastern States.

Anticyclonic circulation prevailed over the central Atlantic (a definite change from the mid-latitude trough of October) with a well-marked mean "jet" at higher latitudes. The mean Low at sea level between southern Greenland and Iceland (Chart XI) was both intense (11 mb. below normal) and persistent throughout November, as it had also been in October. East of this zone of concentrated westerlies the contours (fig. 1) diverged markedly to the weak trough in the eastern Atlantic and a deeper trough over the central Mediterranean.

At very high latitudes the polar vortex continued stronger than average with heights some 200 ft. below normal in Baffin Bay. Below normal heights in the Arctic Basin have been a prominent feature of quite a few monthly mean maps this year [2]. It remains to be seen whether or not the current persistence of above average polar westerlies (at 700 mb.) represents a real secular trend, a temporary abnormality, or an error in the normals at high latitudes due to the scarcity of data in early years.

SOME WORLD WEATHER NOTES

The prolonged spells of stormy weather which had affected the British Isles and, to some extent, central and southern Europe (see previous articles in this series) were temporarily interrupted in November. The area of difluence over the eastern Atlantic was accompanied by some interludes of more clement conditions. On November 18 this reversal was accompanied by a heavy fog over southern areas of the British Isles which reduced visibility in some places to only 5 yards. However, a return to strong cyclonic circulation due to migratory perturbations associated with the North Atlantic westerly maximum was soon experienced. On November 26, winds of 60 m. p. h. and over delayed sailings and caused coastal flooding in southwestern counties. This was the onset of a stormy period which continued into early December and resulted in the sinking of several ships. The combination of heavy rains and wind-driven flooding furnished a fitting wet-harvest climax to a disastrous summer.

The typhoon season of 1954 was notably late in getting under way but, since its onset, typhoon activity has been both frequent and strong. While typhoons in November are far from unknown, November 1954 had more than the usual two. Indications of these occurrences may be seen in figure 1, where a 700-mb. mean Low prevailed over the northern Philippines.

Of additional interest was the first strong "Kona"

[1] See Charts I-XV following p. 353 for analyzed climatological data for the month.

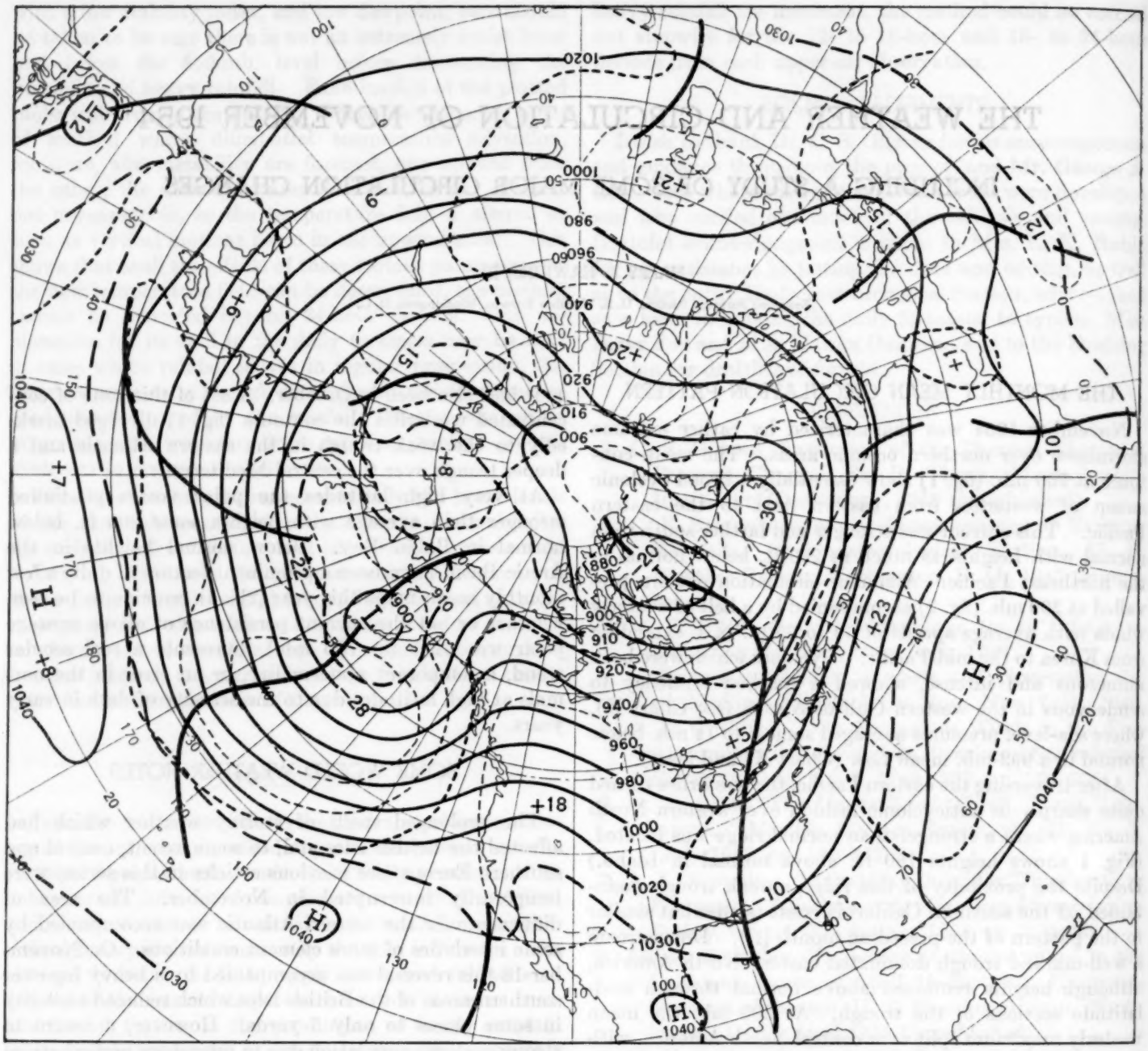

FIGURE 1.—Mean 700-mb. contours and height departures from normal (both in tens of feet) for October 30 to November 28, 1954. Strong cyclonic circulations and fast westerlies were conspicuous over the northern Atlantic and Pacific. Prevalence of ridge conditions over western and well-marked trough over eastern North America were significant features of the local circulation.

storm in the Hawaiian Islands since 1951. This disturbance gave 13.80 inches of rain at Hilo, Hawaii, from November 27 through December 1 and was associated with a major change in Pacific circulation at the end of November. The sequence of events leading to this development is discussed in more detail in the latter portion of this article.

WEATHER AND ANOMALIES OVER THE UNITED STATES

With the exceptions of central California and the southeastern United States (from central Texas through Pennsylvania and New Jersey) the country was unseasonably warm during November (Chart I–B). The center of undue warmth was located over the Northern Plains with temperatures as much as 12° F. above normal in eastern Montana. This mild regime may be attributed to the strong southwesterly flow of marine air which entered the continent between northern California and northern British Columbia. Monthly mean thicknesses (1000–700 mb.) were above normal over the whole continent except the southeastern United States and northeastern Canada (chart not shown). In general these characteristics were not atypical of the regime usually associated with a Great

Basin High and stronger-than-normal westerlies to its north.

In such cases above normal temperatures frequently extend to the New England coast. And, as in this month, cold cP outbreaks are rather infrequent and most apt to affect only eastern United States areas. The surges of maritime air and resulting Basin Highs are indicated on Chart IX, as are the glancing cP Highs (exception, the early period outbreak over the Plains). As might be anticipated this modified maritime air usually produces below normal temperatures only in lower latitudes at this season. Thus the southeastern United States, under the upper-level trough, was quite consistently the coldest area in the Nation relative to normal.

Basin High patterns frequently show near to below normal temperatures in or near the high pressure centers. These result from an excess of outgoing radiation, accompanied by low minima and, with high albedo when snow cover is extensive, depressed maxima. Occasionally a similar effect is observed when a radiation fog is slow to burn off and sharply reduces the maxima although the minima may remain above normal. The characteristic "radiation pocket" has been rather uncommon in recent years, and the anomaly of this November, showing below normal temperatures in California, appears to be associated with this latter type of mechanism. Below normal temperatures did not occur in the mean High center (in Idaho) but rather in the protected terrain of the Central Valley of California where air movement was quite slow. Fogs were frequent and slow in burning off. Once the air was chilled, lack of air movement permitted the regime to be almost self-propagating. When destroyed, the situation returned again as the preferred pattern again became effective. In a local extension of this stagnant regime during November fog, smog, and haze were particularly offensive in the southern California coastal region from the 24th to the 28th. Most of some 2,000 traffic accidents reported during this 5-day period were attributed to the poor visibility.

Despite the ridge aloft over the Great Basin, precipitation was adequate over the Far West. In the north, the west-southwesterly flow of marine air gave the coastal States moderate to heavy amounts. Precipitation of note also occurred in California, Nevada, and Colorado due to cyclonic activity associated with the California coastal trough. However, in widespread areas east of the ridge, where the dry northwesterly flow was also subject to foehn influence, precipitation was significantly less than normal.

From Arizona east-northeastward across the Panhandle through Indiana precipitation was less than half of normal. Statewide averages showed these percentages: Arizona, 13; New Mexico, 15; Oklahoma, 14; Kansas, 1; Nebraska, 14; Iowa, 15; Missouri, 34; Arkansas, 37; Illinois and Indiana, each 49. Thus the drought (see previous articles) continued unbroken in the Central Plains.

In the East, on the other hand, additional recovery from summer rainfall deficiencies was made. Under and east of the trough aloft precipitation ranged from about 75 percent of normal to 150 percent of the normal amounts over and east of the Appalachians. In addition Alabama and Mississippi received respectively, 75 and 86 percent of their normal November precipitation. As an oddity, Key West, Fla., received 18.33 inches of precipitation in 24 hours on the 13th, due apparently to easterly wave instability in combination with a weak frontal discontinuity.

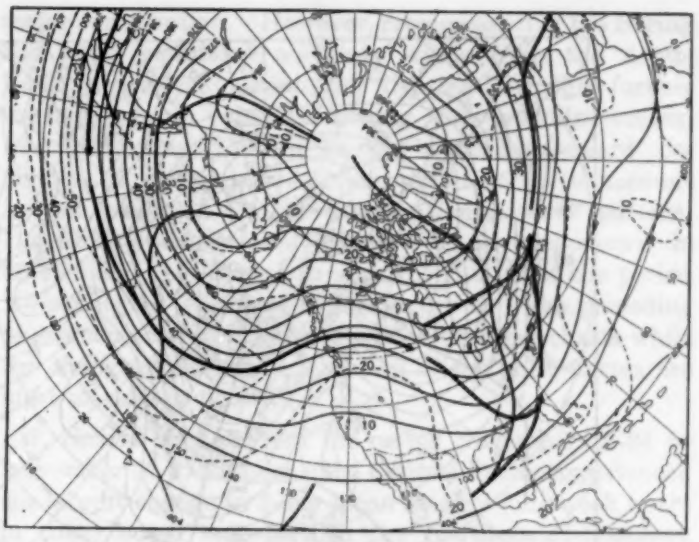

FIGURE 2.—Mean 200-mb. contours (in hundreds of feet) and isotachs (dashed, in meters per second) for October 30 to November 28, 1954. Solid arrows indicate axes of monthly "mean jet stream". Well-marked Pacific maximum speeds and the split jet over central North America are interesting features although the pattern is essentially similar to figure 1.

In general, the anomalies of temperature and precipitation over the United States showed a marked tendency to reverse from those observed in October. This has been a frequent phenomenon in recent years [3] but in this case the reversal was accompanied by changes in the hemispheric wave patterns mainly at middle and not at high latitudes. Nevertheless there were a series of changes which took place in the latter half of November and early December which were noteworthy in themselves as well as in other contexts [4]. The last part of this article is concerned with these changes and an adjacent article by Hughes and Foster discusses in detail some of these changes as they related to tropopause behavior over western United States and Canada.

CIRCULATION CHANGES OF LATTER NOVEMBER THROUGH EARLY DECEMBER—INCLUDING SOME CONCURRENT SOLAR DATA

Between the periods November 13–17 and December 4–8 there occurred a series of marked changes in the hemispheric circulation pattern involving sharp reversals in the phase and/or the amplitude of the wave pattern. In one case the change in height at 700 mb. was of a magnitude unequaled in the available record. While the transitions appear to be to some extent explainable with existing

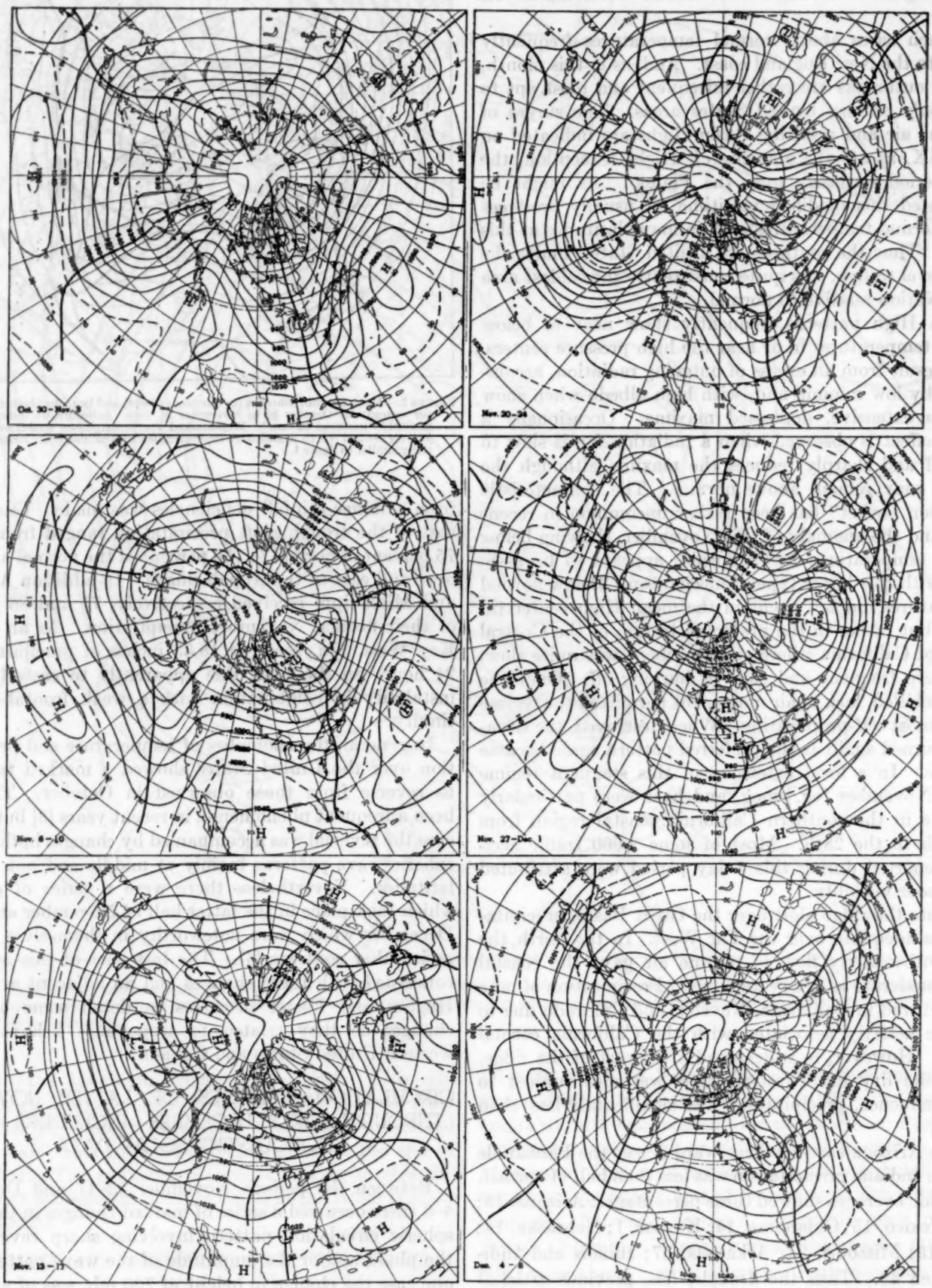

FIGURE 3.—Five-day mean contours at 700 mb. (in tens of feet) for periods one week apart, October 30–December 8, 1954. Note changes which appeared near Novaya Zemlya (Nov. 20–24), over the Central Pacific (Nov. 27–Dec. 1), and over the Atlantic (Dec. 4–8).

knowledge of synoptic meteorology, the rationalization is far from simple and satisfactory. Apparently a barotropic mechanism alone is insufficient to explain the evolutions, and application of more complex systems without high speed computors is not practicable at present. In view of recent attempts to relate solar influences to meteorological events, an inspection of the variations in a few of the contemporary solar indices has been made. While some appreciable solar variations are discernible, their influence on the meteorological events which transpired is highly questionable.

The following discussion of the problem is divided into three parts: A. Description of early November circulation and its evolution, B. Description of the circulation changes with an attempted rationalization, and C. Solar variations. The basic data showing the changes of interest are given in figures 3 and 4, the 5-day mean contour patterns at 700 mb. and their departure from normal, one week apart, (no overlapping data) from October 30 through December 8.

A. EARLY NOVEMBER CIRCULATION AND EVOLUTION

The following transitions may be pointed out:

1. A fast, small-amplitude westerly pattern over the Pacific gradually intensified with the westerlies sharply peaked and south of their normal position by November 13–17. The mean departure from normal clearly indicates the abnormality inherent in this pattern.

2. Over North America there occurred a gradual relaxation of the large-amplitude ridge-trough conditions of Oct. 30–Nov. 3, as the westerlies of the Pacific gradually spread their influence downstream and lower latitude elements of the wave pattern moved eastward.

3. A somewhat similar relaxation and eastward displacement of the ridge-trough system was noted over the Atlantic during the same time (Oct. 30–Nov. 10).

4. Asia was the site of moderate westerly flow (50°–60° N.) with the development of a deep vortex near Novaya Zemlya, following ridge intensification in the eastern Atlantic (Nov. 6–10). In addition, there occurred a slow retrogression and marked buildup of a warm blocking High north of the Bering Straits. Initially this could hardly be classified as a blocking phenomenon. The marked intensification of the High, which strengthened quite steadily from the 8th through the 13th, resulted in a significant block and contributed to the suppression of the Pacific westerlies noted above.

B. MAJOR CIRCULATION CHANGES OF LATE NOVEMBER-EARLY DECEMBER

In the course of the succeeding three weeks (following Nov. 13–17) some very pronounced changes in the hemispheric pattern took place.

1. First week.—During November 20–24 blocking was centered south of Novaya Zemlya, a marked reversal in circulation from the preceding week. This block appeared to be a merger of the Bering Sea High and the Atlantic ridge, with the latter apparently making the major contribution. However, retrogression of the Bering Sea High permitted northerly winds from the Arctic Basin to pour cold air into the Aleutian Low, thus further intensifying an already strong mid-latitude vortex. From this area (Central Pacific) a straightforward dispersion of energy downstream would seem to account for the amplified United States-Atlantic wave pattern. Height anomalies for November 20–24 are shown in figure 4 and the changes in mean heights from the period November 13–17 are shown in figure 5. The preceding phenomena can be readily identified on these charts while the changes involved in initiation of the polar vortex are most marked in figure 5.

2. Second week.—From the period November 20-24 to November 27–December 1 the Central Pacific experienced the largest change in 5-day mean heights (one week apart in time) noted anywhere in the Northern Hemisphere since records became available in December 1947. The reversal from an 8,600-ft. Low (Nov. 20–24) to the 10,500-ft. High (Nov. 27–Dec. 1) was a complete change in phase of the wave pattern and involved height changes of over 1,860 ft. (in 5-day mean)! These were some 300 ft. larger than any previous changes of record. Rationalization of this event might follow these lines: The strong block of western Asia certainly favored trough activity well to the west of the existing central Pacific vortex. As the trough developed along the northeastern Asiatic coast, a strong High moved eastward off the coast and, supported by the new, more favorable vorticity flux from upstream, split the strong westerlies of the mid-Pacific. Cool air at low latitudes developed into an intense Kona storm which inundated parts of the Hawaiian Islands. This low-latitude disturbance in turn furnished warm air and dynamic support for the ridge to its north.

As might be anticipated, this "about face" in the Pacific was accompanied by immediate adjustments downstream. In the course of one week the warm stable ridge along the west coast of North America which had persisted for many weeks (see adjacent article) was replaced by a much colder northwesterly flow, much of it cyclonic in character. The upstream changes in the Pacific seem to answer, but to remove by one step only, the more immediate reasons for the changes over western North America.

From mid-United States through the eastern Atlantic this period (Nov. 27–Dec. 1) was marked by a flattening of the wave pattern, in part due to the cessation of any supporting vorticity flux from upstream for the previous standing-wave pattern. The result was a strong band of mid-latitude westerlies, supported by confluence over eastern North America, but perilously long and flat in terms of a subjective evaluation of their inherent stability of flow.

In figure 4, the height departure from normal for November 27–December 1 highlights the further intensification of the polar Low, the anticyclonic wedge which replaced the Pacific vortex of the previous week, and circulation abnormalities from mid-United States through the

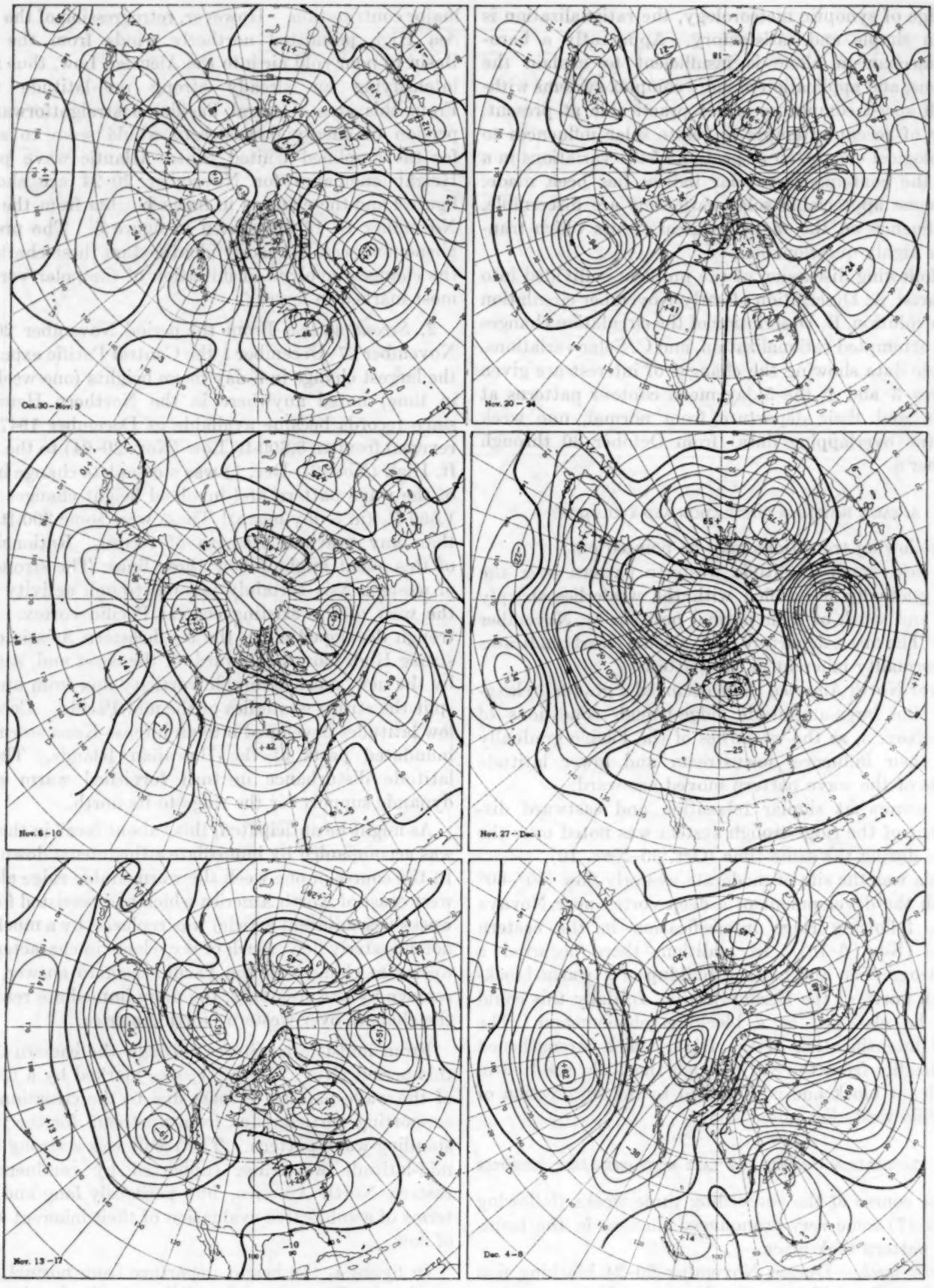

FIGURE 4.—Height departures from normal (in tens of feet) accompanying patterns shown in figure 3. From November 13 through Dec. 8 the polar vortex intensified and the westerlies were displaced northward as circulation reversals proceeded progressively from Novaya Zemlya (Nov. 20–24) through the central Pacific (Nov. 27–Dec. 1) to the Atlantic (Dec. 4–8).

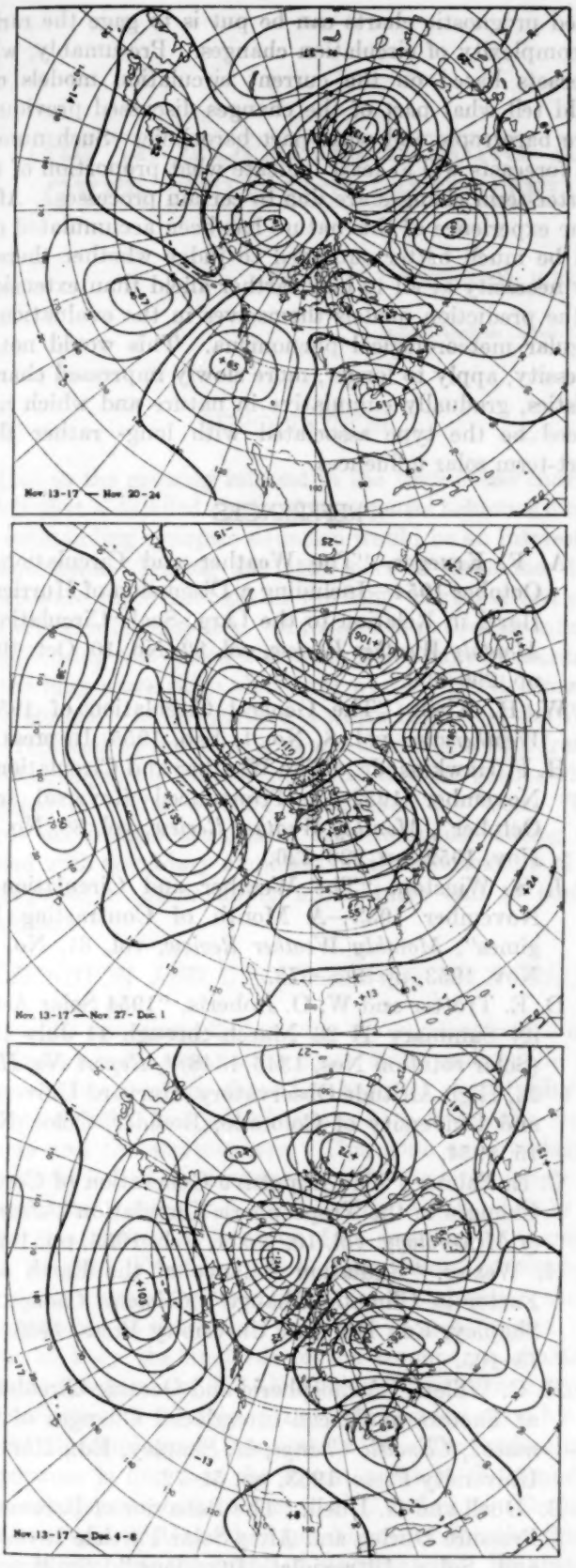

FIGURE 5.—Total height changes (in tens of feet) from the period November 13-17 to the periods November 20-24, November 27-December 1, and December 4-8, showing the progression of the major pattern readjustments and the total changes accompanying the sequence.

Atlantic which were opposite to those of the period Nov. 13–17. In figure 5 the height change between the November 13–17 and November 27–December 1 5-day means are shown on the middle map and reflect most of the features already discussed.

3. Third week.—The period December 4–8 is the final stage considered in this series. The most significant development was a sudden buckling of the Atlantic westerlies (one week height changes of over 1,200 ft.) and the partial relaxation of blocking conditions northeast of the Caspian Sea. Other features of interest include: (1) Further intensification of the Asiastic coastal trough, (2) Development of a strong trough off the west coast of North America in phase with Pacific vorticity flux, (3) Increasingly anticyclonic circulation over west-central North America as upstream features extended their influence downstream, (4) Trough intensification along the eastern coast of the United States, (5) Strong trough from southern Scandinavia southeastward, and (6) Perpetuation of the strong polar vortex. Comparison of these features with the normal state is shown in figure 4 and the changes from November 13–17 are given in figure 5.

In summation.—The block which became established over northwestern Russia during November 20–24 appears to have been out of phase with a vigorous Pacific circulation. Reactions in the Pacific were both rapid and unusually intense, with implications that more than barotropic influences were instrumental in subsequent evolution. Both North America and (even more markedly) the Atlantic underwent greater than normal fluctuations as readjustment proceeded downstream. The net change (fig. 5) was a marked intensification and contraction of the circumpolar vortex, with the major westerlies shifting northward and with cutoff or semi-cutoff vortices becoming established at middle and lower latitudes.

C. SOLAR VARIATIONS

It is expected that solar activity probably reached what will be regarded as the intercycle minimum some time between May and July 1954 [5]. In consequence, spottedness was rare, at relatively high solar latitudes, and accompanied by no sudden ionospheric disturbances. In table 1 are listed the relative sunspot numbers, the daily sums of the Cheltenham 3-hr K indices of geomagnetic disturbance, and the Mt. Wilson K_2 index (apparent area of K_2 flocculi) [6] which correlate quite highly with relative sunspot numbers. The geomagnetic character figures from Cheltenham failed to reveal any storms with 3-hour intensity greater than 5 (storms of intensity 5 occurred on the 2d and 30th). For November they appear inversely arrayed when compared to sunspot numbers.

The usual relation of K_2 index to sunspot number is apparent in this array. However, the variations in sunspot number are probably the most striking aspect of the data. The obvious question is whether such short term variations in spottedness could possibly effect, in miniature, responses similar to those longer term effects indicated by studies in this field [7, 8, 9]. Also, with what time lag might the responses be expected?

TABLE 1.—*Indices of solar activity, October 24 to December 8, 1954*

Date	Zurich provisional relative sunspot numbers	Daily sums of Cheltenham 3-hr. index of geomagnetic disturbance	Mt. Wilson K_3 index (in 1/10,000 of solar hemisphere)
1954			
Oct. 24	8	33	31
25	8	23	11
26	7	18	15
27	0	21	15
28	0	12	12
29	0	9	0
30	0	21	2
31	0	19	0
Nov. 1	0	30	10
2	0	25	14
3	0	22	14
4	0	13	20
5	0	15	20
6	7	13	25
7	8	9	19
8	7	7	
9	24	12	30
10	36	5	
11	44	12	
12	38	15	29
13	37	13	71
14	23	11	72
15	9	2	
16	7	0	31
17	7	8	36
18	7	13	30
19	7	17	33
20	0	20	27
21	0	17	27
22	0	16	0
23	0	20	0
24	0	12	0
25	0	15	14
26	0	13	5
27	0	14	9
28	0	12	8
29	0	16	9
30	0	20	10
Dec. 1	0	12	5
2	0	14	10
3	0	11	
4	0	7	14
5	0	9	14
6	0	11	
7	0	16	20
8	0	9	20

In general, no compelling correspondence was found with either the January sunspot maximum minus sunspot minimum maps of Wexler [7] or with Willett's description of general behavior expected at analogous phases in the cycle [8]. The latter may be due to the fact that this small-term cycle may have no direct counterpart in Willett's description of the long-term cycle. It is pertinent to note that a somewhat similar cycle in spottedness was also noted in October 1954 but with a less pronounced maximum (24 on Oct. 16).

This brief recital hardly exhausts the list of solar criteria, nor can the lack of similarity in reaction to those responses cited by others be taken as indicative of either the reality or unreality of atmospheric response to solar stimuli. One can only point out that, following some interesting evidences of increasing solar activity, a major block was set up in northwestern Asia. In the gross sense this type of activity was the sort of response which is expected to accompany these solar changes. However, many details of the patterns showed little or only fleeting resemblance to the more "typical" changes.

A recent paper by Namias [10] investigates an analogous problem, i. e., evaluating weather pattern evolution relative to solar activity (flares). In his case more obvious mechanisms to account for atmospheric changes were available. This comes to a very timely point. It seems to the writer that one use to which the numerically computed prognostic charts can be put is to gage the rarity or complexity of circulation changes. Presumably, with forecasts based on the current circulation models one could tell what part of the changes discussed previously were barotropic and what part baroclinic. Such numerical forecasts will at least indicate what proportion of the shorter-term changes are due to certain processes. After some experience of this nature has been accumulated one will be much better equipped to judge whether there is any necessity at all to look farther afield than extensions of the prediction models themselves in the evaluation of singular meteorological phenomena. This would not of necessity, apply to longer, more slowly impressed characteristics, gradually cumulative in nature and which may indeed be the type associated with long- rather than short-term solar influences.

REFERENCES

1. A. F. Krueger, "The Weather and Circulation of October 1954—Including a Discussion of Hurricane Hazel in Relation to the Large-Scale Circulation", *Monthly Weather Review*, vol. 82, No. 10, Oct. 1954, pp. 296–300.
2. W. H. Klein, "The General Circulation of 1954", *Weatherwise*, vol. 8, No. 1, Feb. 1955, In press.
3. H. F. Hawkins, Jr., "The Weather and Circulation of November 1952—A Pronounced Reversal from October", *Monthly Weather Review*, vol. 80, No. 11, Nov. 1952, pp. 220–226.
4. J. S. Winston, "The Weather and Circulation of November 1953—A Month of Contrasting Regimes", *Monthly Weather Review*, vol. 81, No. 11, Nov. 1953, pp. 368–373.
5. D. E. Trotter and W. O. Roberts, "1954 Solar Activity Summary II 23 March through 11 July 1954 (Solar rotation Nos. 1345–1348)", *Report No. HAO 24*, High Altitude Observatory, Harvard University and University of Colorado, Boulder, Colo., Nov. 15, 1954.
6. C. E. Palmer, "The Impulsive Generation of Certain Changes in the Tropospheric Circulation", *Journal of Meteorology*, vol. 10, No. 1, Feb. 1953, pp. 1–9.
7. H. Wexler, "Radiation Balance of the Earth as a Factor in Climatic Change", *Climatic Change*, H. Shapley, Ed., Harvard University Press, 1953, pp. 73–105.
8. H. C. Willett, "Atmospheric and Oceanic Circulation as Factors in Glacial-Interglacial Changes of Climate", *Climatic Change*, H. Shapley, Ed., Harvard University Press, 1953, pp. 51–72.
9. B. Duell and G. Duell, "The Behavior of Barometric Pressure During and After Solar Particle Invasions and Solar Ultraviolet Invasions," *Smithsonian Miscellaneous Collection*, vol. 110. No. 8, 1949.
10. J. Namias, A Major Change in General Circulation During August 1953 and Its Possible Relationship to Solar Flare Activity, U. S. Weather Bureau, 1954 (Unpublished).

THE TROPOPAUSE DURING A MAJOR CHANGE IN CIRCULATION OVER THE WESTERN UNITED STATES, NOVEMBER 25 TO 28, 1954

GROVER D. HUGHES AND ROBERT I. FOSTER

WBAN Analysis Center, U. S. Weather Bureau, Washington, D. C.

INTRODUCTION

Due to the growing interest in the tropopause chart, it is felt that a detailed study of tropopause behavior during an outstanding synoptic situation would be an interesting contribution. During the latter part of November 1954 there were rapid changes in the long wave pattern over the Western Hemisphere. A feature of particular interest noted during this period was the rapid (3-day) replacement of the long wave ridge aloft over western North America by a trough. At the surface, a warm High over the West was replaced by moving Lows and cold Highs with frontal systems migrating southward to the Mexican border which resulted in colder weather throughout the West. This paper emphasizes changes in the tropopause during this period with secondary emphasis on the relationship of the tropopause to other upper air features and to surface conditions.

DEFINITION AND DISCUSSION OF TROPOPAUSE

Due to numerous flights into the stratosphere during the last decade, and to the more dense radiosonde and rawinsonde networks, there has been an opportunity for a more detailed analysis of that zone between the troposphere and the stratosphere. This zone or boundary is commonly called the tropopause. In the troposphere the temperature generally decreases with height, while in the lower stratosphere it is quite often constant or increases with height. Frequently the change from tropospheric lapse rate to stratospheric lapse rate is so gradual that it is impossible to determine the point of stabilization. In order to keep the analyses of the tropopause charts as objective as possible, WBAN Analysis Center has adopted the definition of the tropopause point agreed upon by the World Meteorological Organization [1]. The predominant tropopause is found at the lowest point in the sounding where the lapse rate decreases to 2° C. or less per kilometer and averages 2° C. or less per kilometer for the first 2 kilometers above the point of stabilization. Frequently several such stabilization points are found on a sounding, in which case the lower point is considered the predominant tropopause. Points which do not meet the definition of a tropopause, but show stabilization as well as satisfying the requirement that the lapse rate be 3° C. per kilometer less than the layer immediately below are called significant points. Strict compliance to these definitions is not always practical and deviations for the sake of continuity are often necessary.

The potential temperature along a tropopause surface is conservative with respect to time, and generally conservative (15°–20° C.) with respect to space. Many authors have typed or named tropopauses with respect to their potential temperatures. Such titles as Arctic, polar, extratropical, and tropical have been suggested. The tropical tropopause with a potential temperature near 400° A. seems to be the only one for which there is uniform agreement.

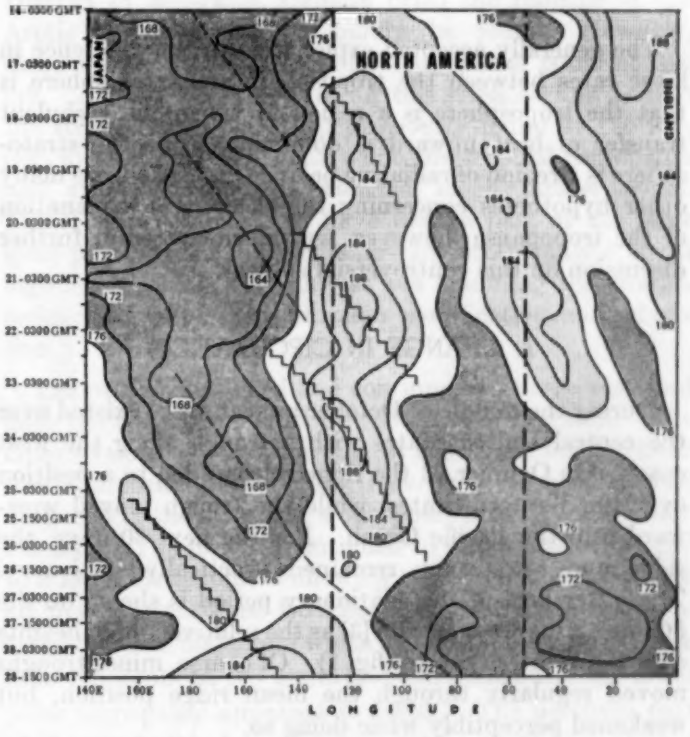

FIGURE 1.—500-mb. time cross section [3] at 50° N. latitude for November 16–28, 1954. Contours in hundreds of feet. The two heavy dashed vertical lines represent the coast lines of North America at 50° N. latitude, the left border Japan, and the right border England. Heavy shading indicates areas of low heights and dashed lines indicate movement of minor troughs. Light shading indicates areas of high heights and zig-zag lines the movement of minor ridges. Note rather stationary major ridge over western North America until the 26th with minor ridges moving from the Pacific and reaching maximum intensity in this favorable area. A good Pacific trough moved across the west coast on the 27th and in the Eastern Pacific a major ridge replaced a trough that had been in that position for 30 days (only 7 of these days show on chart).

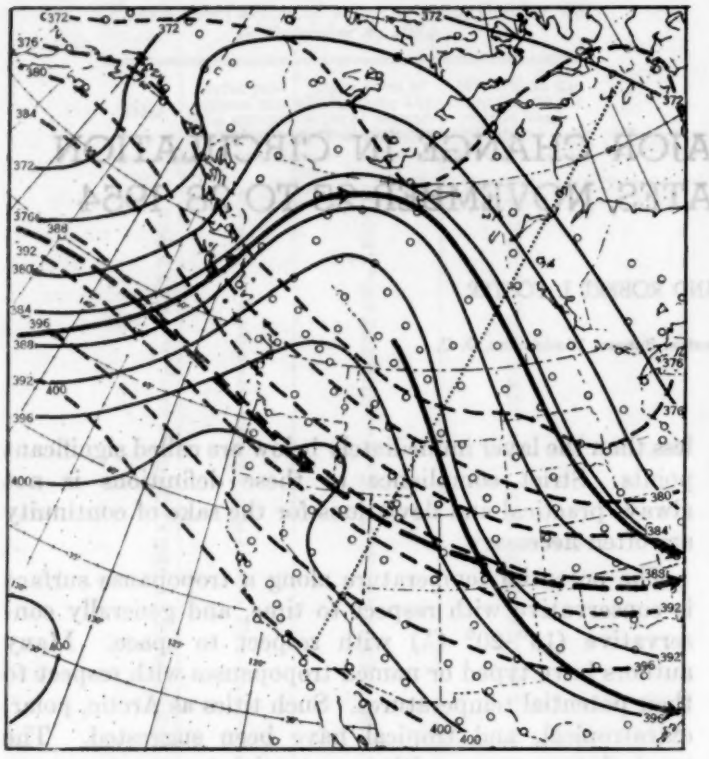

FIGURE 2.—200-mb. contours in hundreds of feet and jet streams (heavy lines), for 0300 GMT, November 25 (solid) and 0300 GMT, November 28, 1954 (dashed). Dotted line represents position of cross sections.

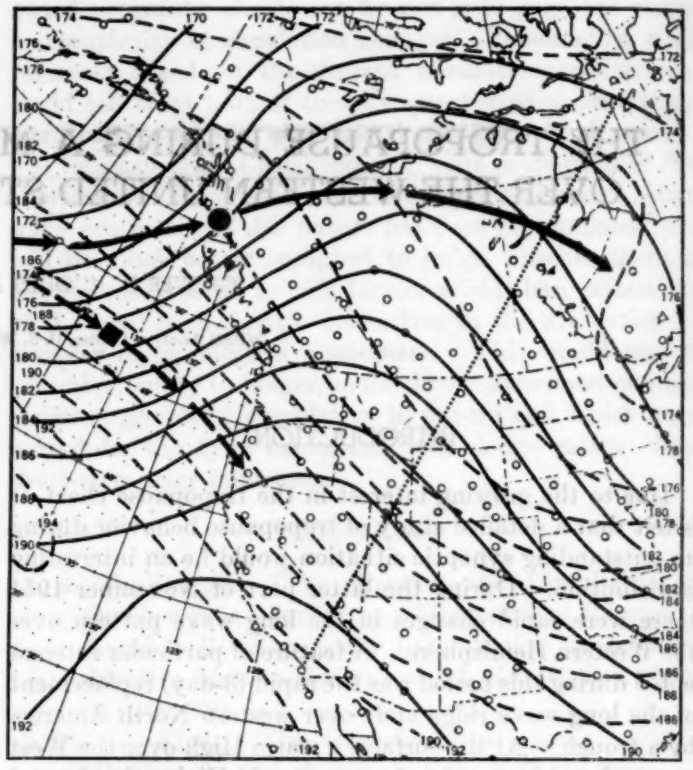

FIGURE 3.—500-mb. space mean contours [5, 6] in hundreds of feet and trajectory of relative cyclonic vorticity centers (heavy arrows). Solid lines, both contours and trajectories, for 0300 GMT November 25 and dashed lines for 0300 GMT, November 28, 1954. The dot and square are positions of a cyclonic vorticity center at map time while arrow heads show past and succeeding 12-hour positions.

The generally accepted explanation of the difference in lapse rates between the troposphere and stratosphere is that the troposphere is a region in which the turbulent transfer of heat upward is dominant, while the stratosphere is a region of radiative balance [2]. There are many other hypotheses concerning the theoretical explanation of the tropopause; however, we will not attempt further discussion on this controversial subject.

A CHANGE IN CIRCULATION

During the middle of October a mean ridge existed over the central United States with a trough along the west coast. On October 23 the ridge retrograded to a position over the Western States, while the trough moved westward into the Pacific Ocean. For the next 30 days, the ridge and the trough remained practically stationary. The latter part of this stationary period is shown on the 500-mb. time cross section [3] as the relatively high heights over the Western States (fig. 1). Of course, minor troughs moved regularly through the mean ridge position, but weakened perceptibly while doing so.

From November 23 to 28, there occurred a very rapid retrogression of the western ridge. During this interval the mean ridge actually replaced the mean trough that had previously existed over the Pacific. The events that led to this major change were the successive intensification and weakening of the rapidly moving minor troughs and ridges. First, the ridge over the West moved eastward and weakened. Simultaneously, a trough from the Pacific moved across the west coast with considerably more intensity than any during the previous 30-day period. This trough intensified and reached a maximum depth over the central United States. Previous troughs had reached their maximum intensity over the east coast. The first step in the retrogression process was the rapid intensification of a minor Pacific ridge reaching its maximum intensity in the eastern Pacific. Thus, during this brief period, the Pacific trough was replaced by a ridge, and the ridge over the western United States was replaced by cyclonic flow (figs. 2 and 3). For a more complete study of the major circulation see preceding article by Hawkins [4].

CHANGES IN THE TROPOPAUSE

Vertical cross sections are the most convenient tool in a tropopause analysis. For convenience in cross section analysis it is important that the wind field be perpendicular to the cross section in order to avoid the task of computing perpendicular components of these vectors. A selected cross section from San Diego, Calif. to Churchill, Manitoba, Canada, met this requirement very well. Figures 2 and 3 indicate how the flow changed from anticyclonic to cyclonic but remained essentially perpendicular to this cross section.

At 0300 GMT November 25, a warm ridge aloft (figs.

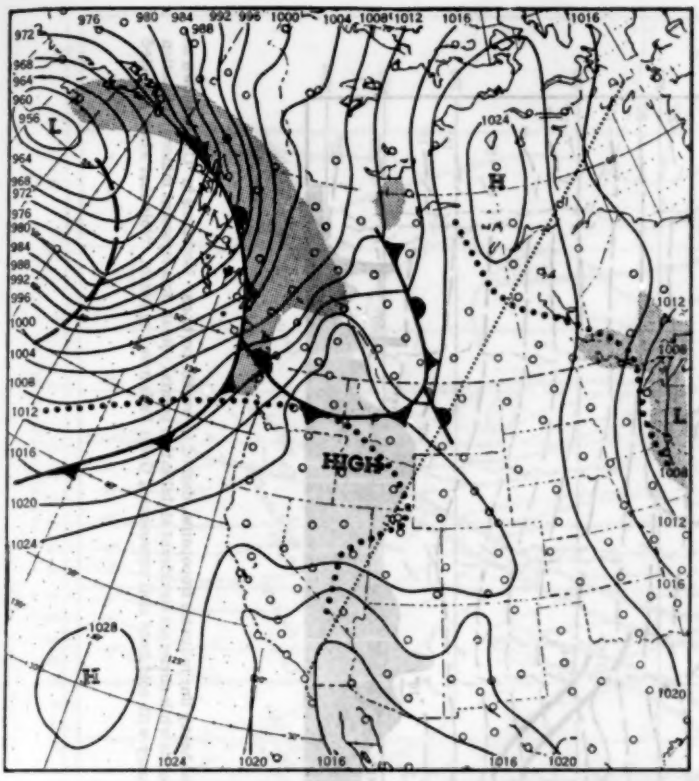

FIGURE 4.—Surface chart for 0030 GMT and tropopause break line (dotted) for 0300 GMT, November 25, 1954. Shading indicates areas of active precipitation.

2 and 3) covered western North America. At the surface (fig. 4) pressures were also high with a warm cell over the Plateau, a cool maritime Pacific ridge over southwestern Canada and a polar High over central Canada. A dissipating warm type occlusion separated the mP ridge from the cP High. The remains of the upper cold front associated with the dissipating occlusion appeared on the cross section over Glasgow, Mont. (fig. 5). The Arctic tropopause with a potential temperature from 310° to 325° A. existed near 300 mb. and extended as far south as The Pas, Manitoba, Canada, where its relationship with the upper front became diffuse. Above the southern edge of the Arctic tropopause there was a weak jet core. This jet corresponds to the tropopause break-line in figure 4. Just above the jet core near 200 mb. were found the first of two polar tropopause leaves (fig. 5). The lower polar leaf with a potential temperature near 335° A. appeared to lie directly through a strong jet core over Great Falls, Mont., and extended southward to Salt Lake City, Utah, where there was another tropopause break-line (fig. 4). The upper polar leaf near 150 mb. with a potential temperature of 344° to 370° A. extended southward to off the California coast and showed considerable overlap (fig. 5). The tropical tropopause near 100 mb. with a potential temperature of about 400° A. extended from Great Falls southward. The cross section does not extend far enough south to show the southern limits of the upper polar leaf. Continuity from previous upper air charts indicates that there was a high level jet over Baja California at the supposed break-line between the polar and tropical tropopauses.

The cross section for 1500 GMT, November 25 (fig. 6) shows the remains of the quasi-stationary front reaching the ground near Havre, Mont. This front, located in the lee-of-the-mountains trough, also shows up on figure 5. The upper cold front that was approaching Great Falls moved eastward out of the cross section; however the frontal zone still existed aloft over Canada. An approaching minor upper level trough caused the upper level winds over Canada to shift from northwest to west. At the same time, the minor jet in the vicinity of The Pas, the northern edge of the polar tropopause, and the southern limit of the Arctic tropopause all moved northward. The northern limits of the upper polar and tropical tropopauses also moved northward. The main jet located over Montana moved slightly southward. The polar leaf still appeared to lie through the jet core and extended rather weakly all the way to California.

By 0030 GMT on the 26th (fig. 12) a new surge of mP air moved into the northern Rockies accompanied by a deepening minor trough aloft. Figure 7 shows the deepening cold air from Ely, Nev., to Glasgow and the warm type occlusion over The Pas. An old upper cold front lay parallel to and east of the cross section over the Northern Plains (not shown on surface chart.) Over Coral Harbour, District of Keewatin, Canada (915) the remains of the Arctic tropopause could barely be found. However, there was a well-defined polar tropopause point at 300 mb. A remarkable feature on this cross section is that the strong upper polar leaf previously found at 150 mb. (fig. 6) was now very weak while the tropical tropopause had strengthened and extended much farther north. These changes appear to have been a part of the large scale process whereby old polar-Low stratospheric air at high levels over the Southwest was assuming the characteristics of tropical air through modification and advection.

The mP air deepened and continued to move eastward onto the Northern Plains by 1500 GMT of the 26th. The cross section for this time (fig. 8) shows the surface front was approaching Las Vegas, Nev. and the cold air had deepened to the top of the troposphere over Saskatchewan, Canada. The jet core continued to move southward and to a lower elevation. Following the deepening of the cold air over the northern Rockies, the jet strengthened considerably with maximum winds increasing in 12 hours from near 130 knots to 160 knots and simultaneously the lower polar tropopause appeared to break. The northern part of this leaf sloped to lower elevation to the south and merged with the lower boundary of the cold front. The southern half of the polar tropopause had intensified and extended to California.

By 0030 GMT, November 27 (fig. 13) an mP High had broken off from the Pacific High and was located over the

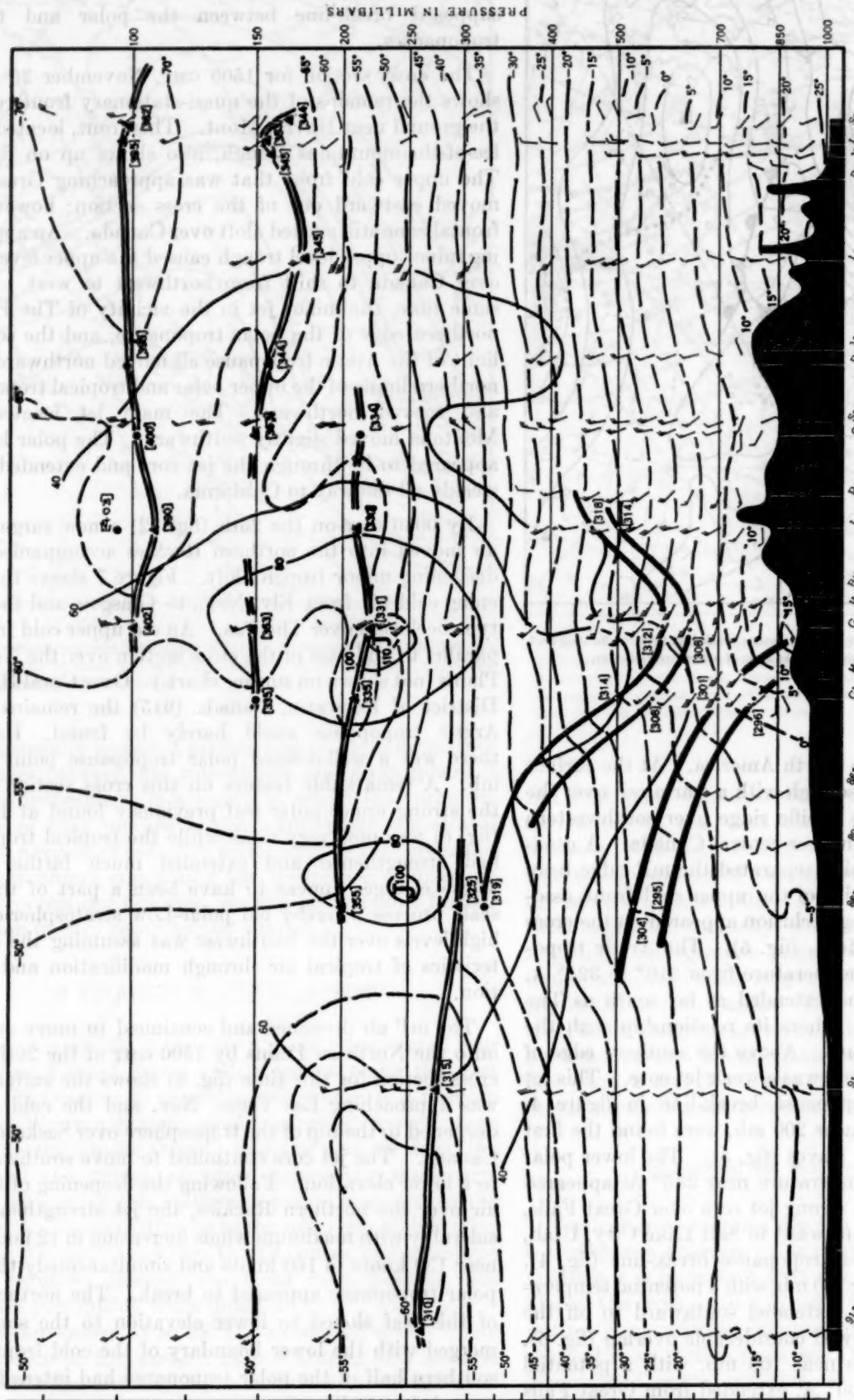

FIGURE 5.—Cross section at 0300 GMT, November 25, 1954. Heavy lines indicate fronts, dashed for weaker portions. Horizontal heavy line indicates tropopause, dashed in weaker portions. Isotherms in °C. are shown as dashed lines. Isotachs (thin solid lines) are in knots. Large "J" shows position of jet core. Large triangles are tropopause points while circles are significant stabilization points. Small dots represent minor stabilization and frontal points. Numbers in brackets are potential temperatures. Front reaching ground near Glasgow is quasi-stationary with cold front aloft approaching Great Falls from the north. Note that when projected to the cross section, Yuma happens to fall on the wrong side of the coastal mountains.

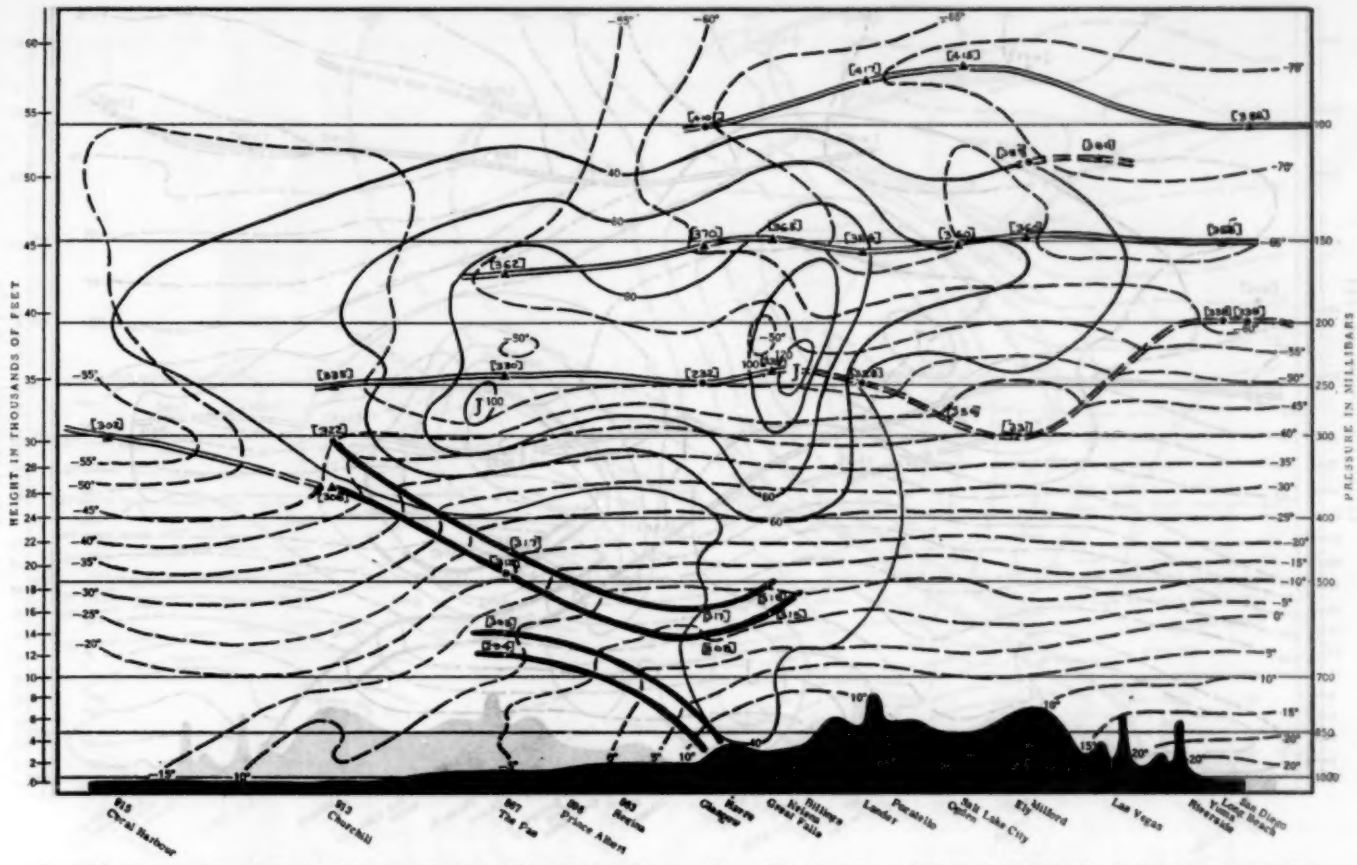

FIGURE 6.—Cross section at 1500 GMT, November 25, 1954. Warm front reaches ground near Glasgow. Upper front is remains of system to the east of cross section.

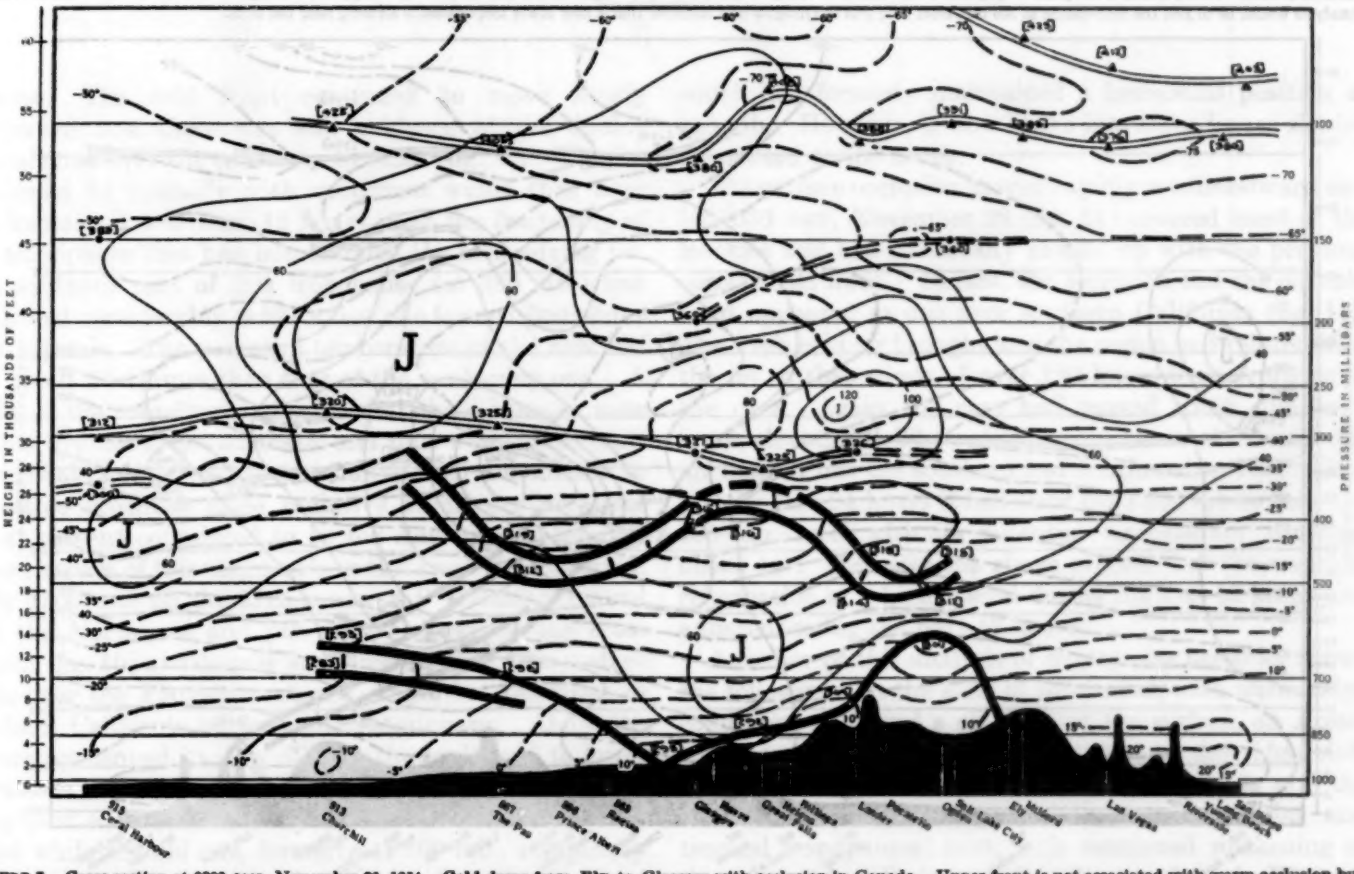

FIGURE 7.—Cross section at 0300 GMT, November 26, 1954. Cold dome from Ely to Glasgow with occlusion in Canada. Upper front is not associated with warm occlusion but is the remains of systems farther east. Note that the analysis neglects the 250-mb. wind at Great Falls. The angle of elevation was so small that the sounding was incomplete for the next 10,000 feet and since a high velocity would be completely incompatible with the thermal field disregard of the report is believed to be justified.

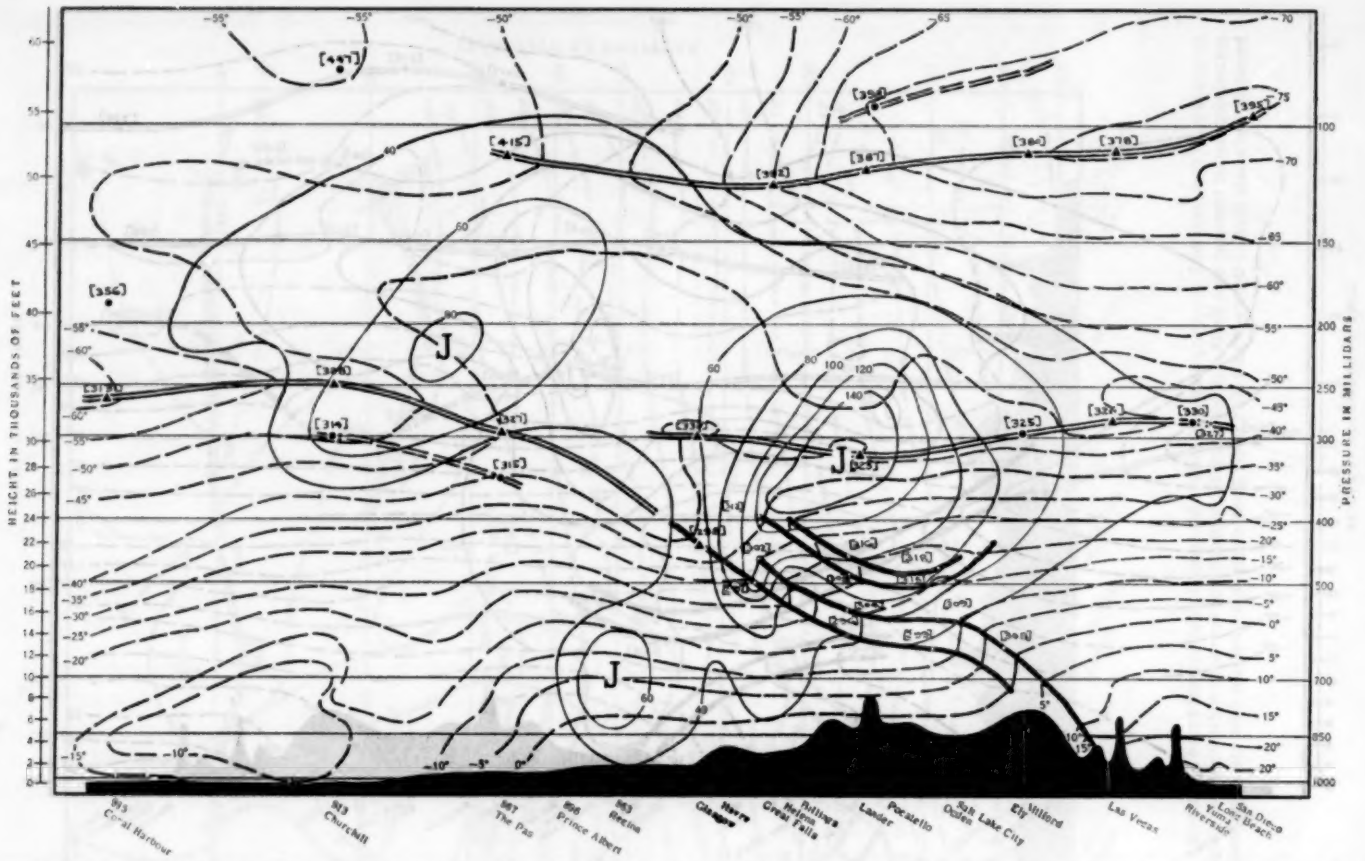

FIGURE 8.—Cross section at 1500 GMT, November 26, 1954. Note that cold air over Wyoming and Montana is now quite deep and polar tropopause is starting to split near the Canadian border. That portion of the polar tropopause from Lander to Glasgow lying through the jet core is untenable and disappears during the next 12 hours. An alternate analysis would be to join the tropopause at 300 mb. from The Pas to Glasgow and consider that a new lower tropopause is forming near the front.

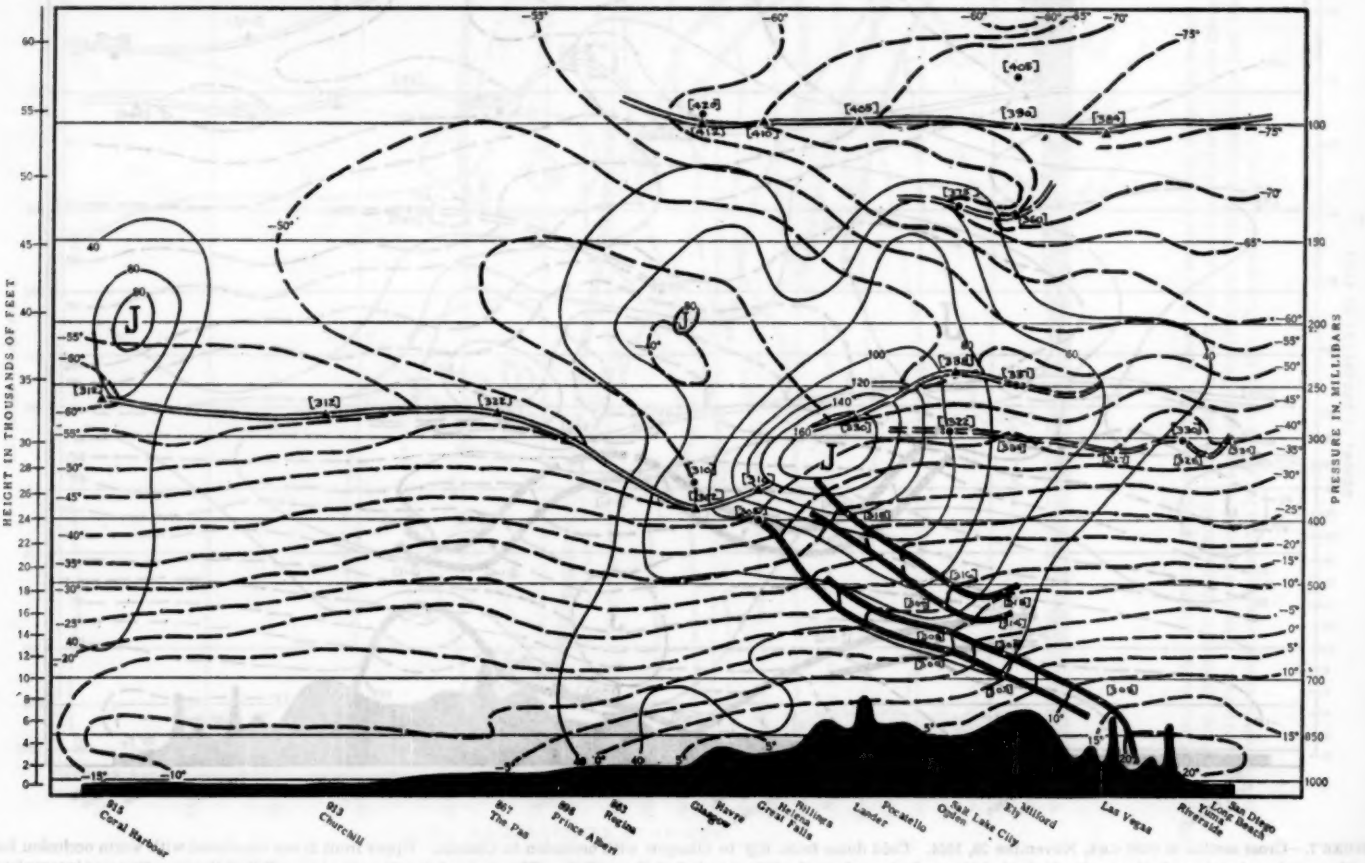

FIGURE 9.—Cross section at 0300 GMT, November 27, 1954. Now all of the troposphere north of the cold front has cooled and the fracture of the tropopause continues in the vicinity of the jet core. To the south of the jet core a new tropopause is forming near the 250-mb. level while the old one at 300 mb. weakens.

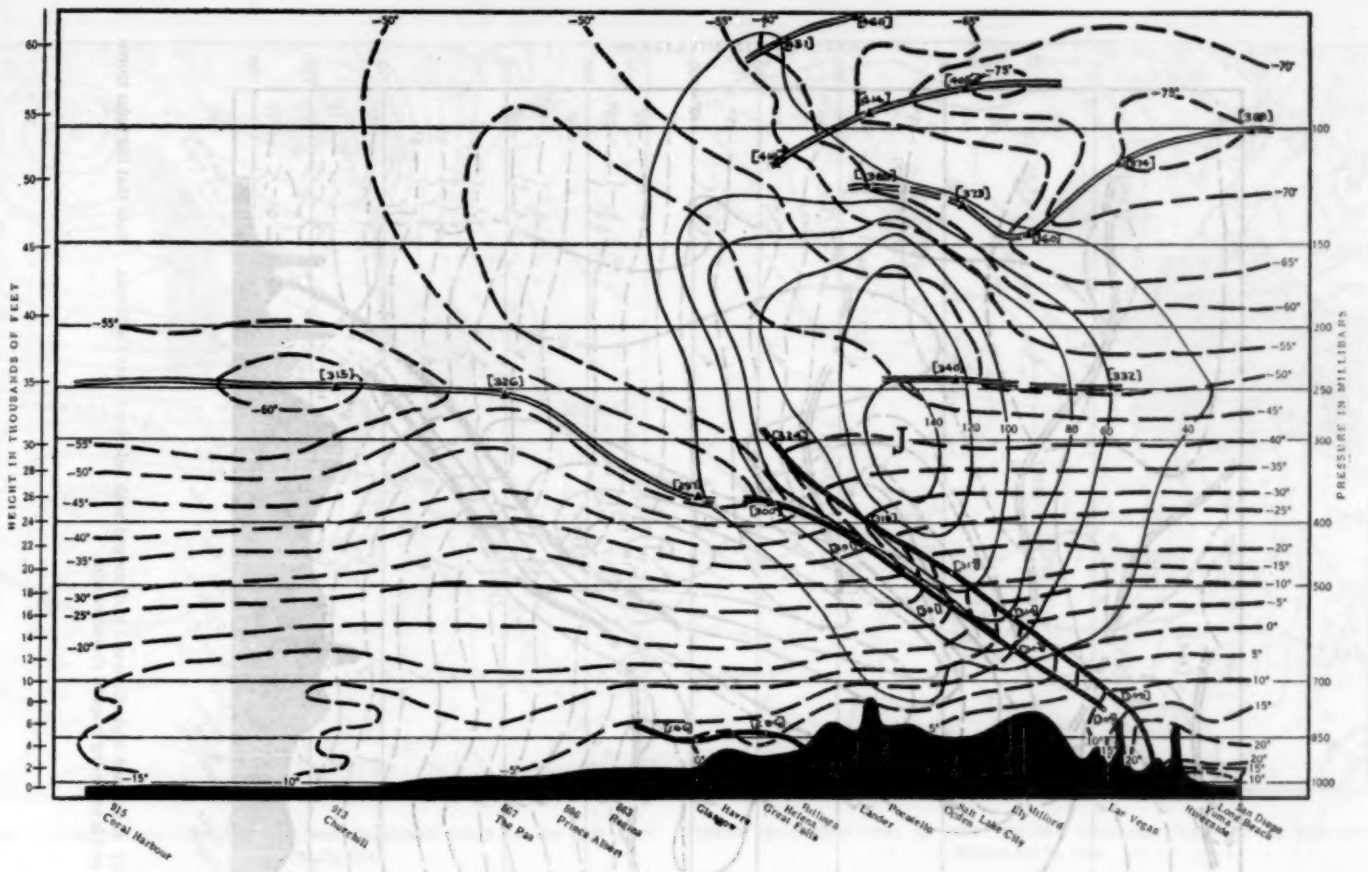

FIGURE 10.—Cross section at 1500 GMT, November 27, 1954. New fast moving occlusion just enters cross section near Great Falls. Old tropopause over the Southwest at 300 mb. has disappeared.

Plateau. The cold front continued to move slowly southward and there was still evidence of the double frontal zone over the northern Rockies (fig. 9). The jet continued to intensify with maximum winds then near 180 knots. It was then 12 hours after the fracturing of the tropopause that had lain through the intensifying jet. The southern part of this tropopause (at 300 mb.) had weakened considerably, while a new one formed just above it at 250 mb. The potential temperature of the new leaf was about 5° warmer than that of the weakening one. A study of the soundings indicates that these changes were neither dry nor moist adiabatic and thus were not a result of vertical motions and so must have been due mainly to advective processes since radiative modifying processes are at present considered to be too slow to give temperature changes of this magnitude in this small time interval.

By 1500 GMT on the 27th a new mP occlusion moved into the Northwest and just barely shows on the cross section (fig. 10) at Glasgow and Great Falls. The surface High over the Plateau weakened while the cold front in southern California became quasi-stationary. Aloft, the jet core continued its slow drift to the south and to lower elevations. The split in the Polar tropopause was now completed with the southerly leaf at 250 mb. well established while the old one, formerly at 300 mb., completely disappeared. For the first time in two days there seemed to be changes taking place in the tropical tropopause which had formerly maintained a horizontal position at 100 mb. However, it now broke into three leaves sloping downward to the north.

The surface occlusion moved rapidly southeastward and by 0030 GMT, November 28 (fig. 14) covered most of the Rockies and had practically caught up with the previous surface cold front. In fact, the occlusion and the old cold front appeared as one over southern California (fig. 11). The fresh cold air brought into the region had reintensified the jet so that winds of over 180 knots were probable in the core. Again the core had moved south and to a lower elevation. The polar tropopause to the north was unchanged but the southern leaf continued to rise. During the last 24 hours it had risen from 300 mb to near the 200–mb. level with its potential temperature warming about 10°. Actually the above process was the result of reformation at a higher level during the first 12 hours and apparent rising the next 12 hours.

A review of this analysis of tropopause behavior shows the following: At the start of the period, with warm ridge conditions aloft and a cP High at the surface, an Arctic tropopause existed over Canada; then as the ridge aloft weakened, mP air replaced cP air over Canada and the Arctic tropopause disappeared leaving only polar and tropical tropopauses; next, with continued weakening of the ridge aloft, mP air moved farther south in the Western States; and finally, when trough conditions aloft did exist

326683—55——3

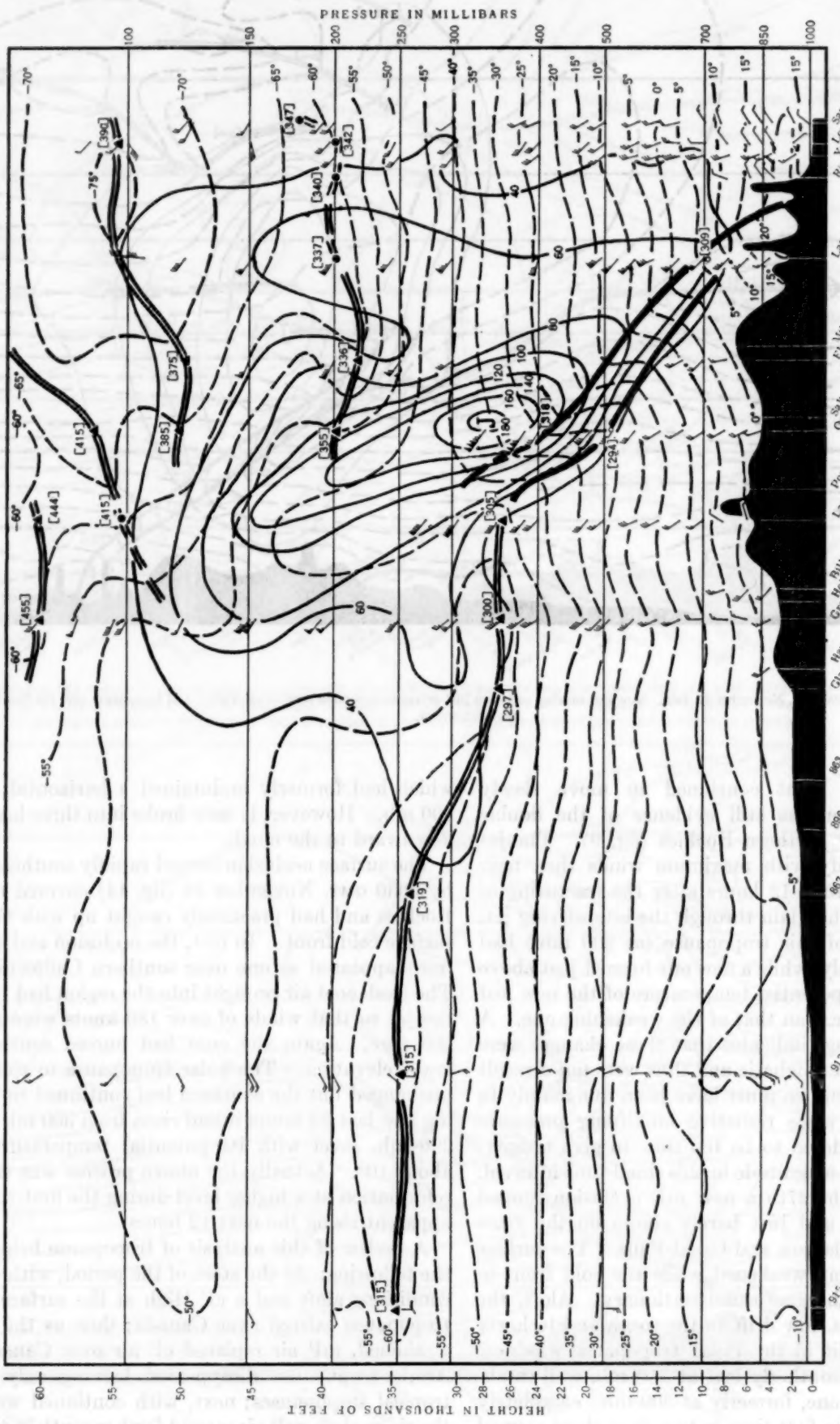

FIGURE 11.—Cross section at 0300 GMT, 22, November 1954. During last 12 hours new occlusion has moved rapidly southward and reinforced and merged with cold front over California. Note that the polar tropopause over the Southwest continues to lift and is assuming tropical characteristics.

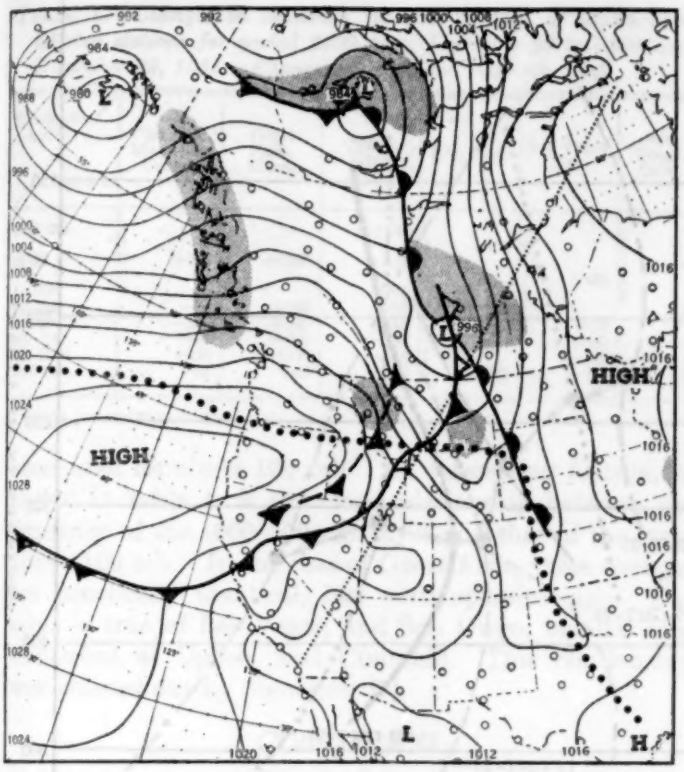

FIGURE 12.—Surface chart for 0030 GMT and tropopause break-line for 0300 GMT, November 26, 1954.

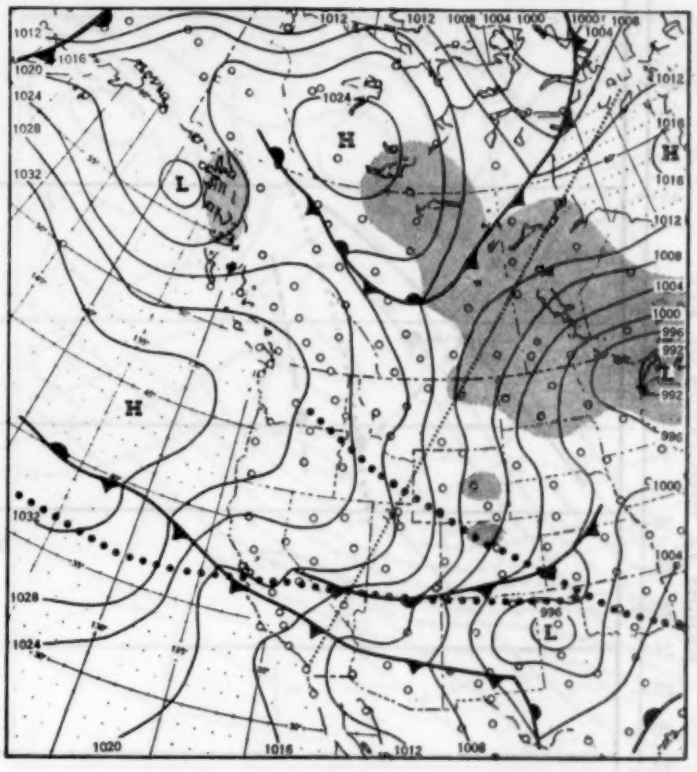

FIGURE 14.—Surface chart for 0030 GMT and tropopause break-line for 0300 GMT, November 28, 1954.

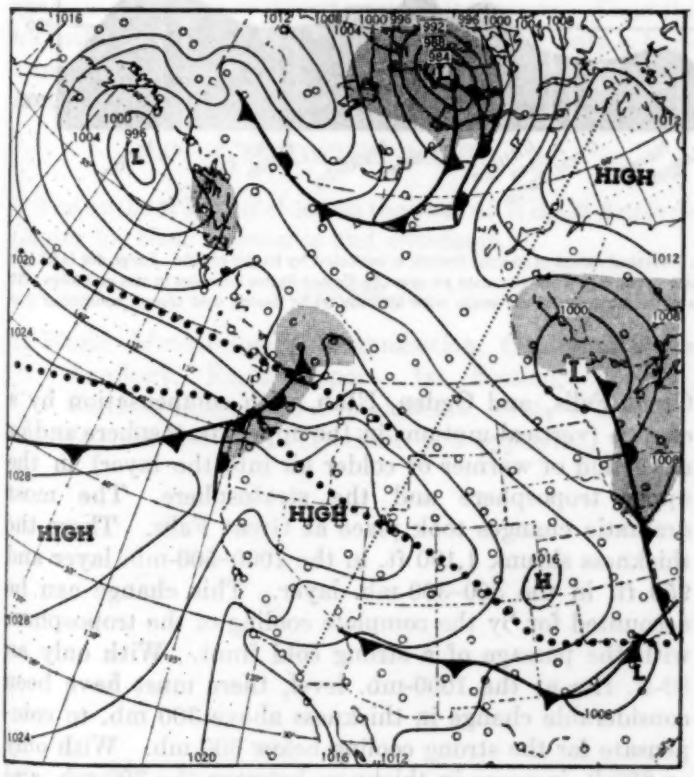

FIGURE 13.—Surface chart for 0030 GMT and tropopause break-line for 0300 GMT, November 27, 1954.

over the West, the mP air deepened throughout the troposphere, the jet stream associated with the mP air strengthened, and the polar tropopause split with its southern leaf gradually rising and taking on more tropical characteristics.

OTHER RELATIONSHIPS

In the WBAN Analysis Center relative vorticity at the 500-mb. level is computed graphically by the Fjørtoft technique [5,6]. In figure 3 the movement of cyclonic vorticity centers in relation to the mean flow is illustrated both for the beginning and ending of the 3-day interval. With the warm ridge over western North America the cyclonic vorticity moved east-northeastward into western Canada. At this time the Arctic tropopause was the dominant feature in Canada. By the 28th, with cyclonic flow over the West, the cyclonic relative vorticity centers (of moving systems but not of major troughs) were moving east-southeastward toward the Plateau region. At this time an intensifying jet was located near Salt Lake City and the polar tropopause had split.

The change in the position of the jet stream at the 200-mb. level can readily be seen from figure 2. This is representative of the approximate position of the jet stream at other levels, but the slope with altitude varies as shown in figure 15. Under warm-ridge conditions the vertical axis of the jet sloped to the south with altitude. With the breakdown of the warm ridge and the influx of

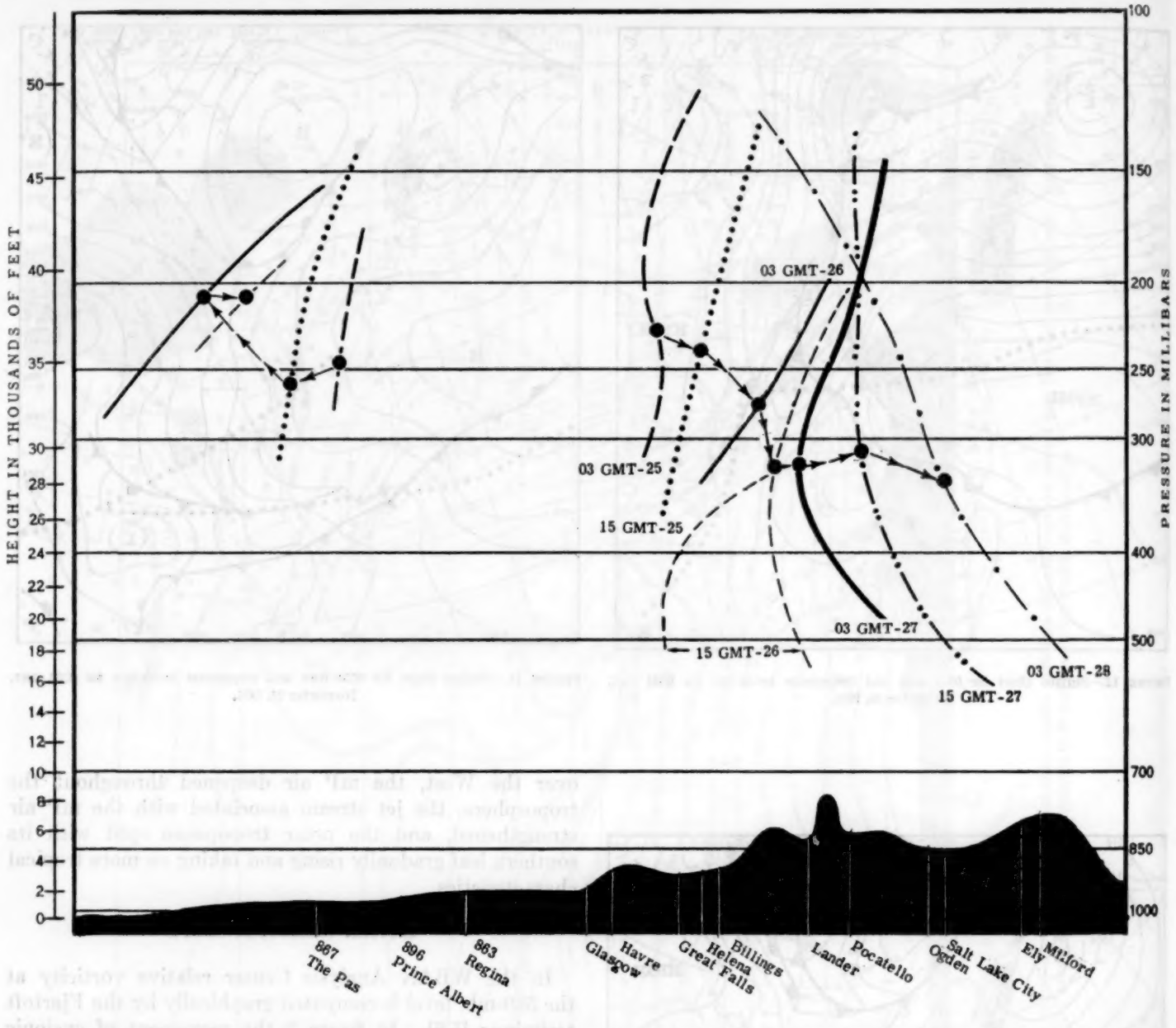

FIGURE 15.—Cross section for period November 25–28, 1954, showing slope of jet stream axis. Vertical extent of 80-knot isotach is indicated by length of axis. Large dot is jet core and arrows indicate movement of core. Note that the weak jet over Canada disappears on the 26th while the main jet over the United States increases in size and force with time. An interesting feature is that with warm ridge conditions (November 25), the axis of the jet slopes to the south with altitude while during cold trough conditions (November 28), the slope is reversed.

cold air in the troposphere the slope reversed, tilting to the north with altitude. As clearly shown by figure 15, the core of the jet moved to lower elevations as it moved southward. In this particular case, the implication is that as the vertical slope of a jet reverses itself going from a warm ridge to a cold trough, the horizontal axes of jets taken from constant pressure charts will cross somewhere near the inflection point of the upper flow.

The 1000–500-mb. thickness patterns are shown in figure 16. They show shrinkage (cooling) of over 1,000 ft. during this period for part of the northwestern United States. Thickness changes by layers for some of the stations along the cross section are tabulated in table 1. They show the cooling in the lower layers quite well for Great Falls, and Ogden, Utah, with compensation by a change (vertical motions in the upper stratosphere and/or advection of warmer or colder air into the layer) in the upper troposphere and the stratosphere. The most dramatic changes took place at Great Falls. There the thickness shrunk 1,190 ft. in the 1000–500-mb. layer and 950 ft. in the 500–300-mb. layer. This change can be accounted for by the complete cooling of the troposphere with the passage of a strong cold front. With only an 80-ft. rise at the 1000-mb. level, there must have been considerable change in thickness above 300 mb. to compensate for the strong cooling below 300 mb. With only an 880-ft. increase in thickness between the 300-mb. and 100-mb. levels, there is left a change of 1,180 ft. un-

TABLE 1.—*Changes in thickness (in tens of feet) of layers above selected stations for period 0300 GMT, November 25 to 0300 GMT, November 28, 1954. Change in height for 1000-mb. level*

Thickness layers / Stations	Churchill, Manitoba, Canada	Great Falls, Mont.	Ogden, Utah	Ely, Nev.	Las Vegas, Nev.	San Diego, Calif.
0-25 mb.			+540	+410		
25-50	+240	+1180	−140		+420	+60
50-100			+110	0		
100-200	−40	+740	+490	+220		+60
200-300	−230	+140	+290	−50	−30	−10
300-500	−30	−950	−210	−390*	+160	+20
500-1000	+120	−1190	−940		−420	−50
1000 mb.	−60	+80	−140	−200	−130	−80

*First transmission missing.

accounted for above 100 mb. An interesting feature, as shown in table 1, is the close relationship between the tendency of the 1000–500-mb. layer and that of the layer above 100 mb. In the case of Great Falls, these changes are practically identical, but with opposite sign. The same is true of Las Vegas, and San Diego, but deviates somewhat at Ogden, and Churchill. This relationship was pointed out by Showalter [7].

CONCLUSION

In the foregoing paper, the tropopause is treated as a physical surface embedded in and moving with the atmosphere. The variations in the tropopause and changes in other related meteorological parameters are noted as they move through a vertical cross section. It is apparent that the use of cross sections is necessary for a detailed analysis of the many minor tropopause leaves. Thus the current practice of tropopause analysis using only a horizontal chart, is at best a crude solution regardless of the care taken in such analysis.

ACKNOWLEDGMENTS

The authors are indebted to the staff of WBAN Analysis Center for their comments and criticisms.

REFERENCES

1. World Meteorological Organization, Commission for Aerology, Final Report, 1st Session, Toronto, Canada, August 10–September 5, 1953, *WMO No. 18, RP. 8*, 80 pp. (Decision p. 5 appendix.)

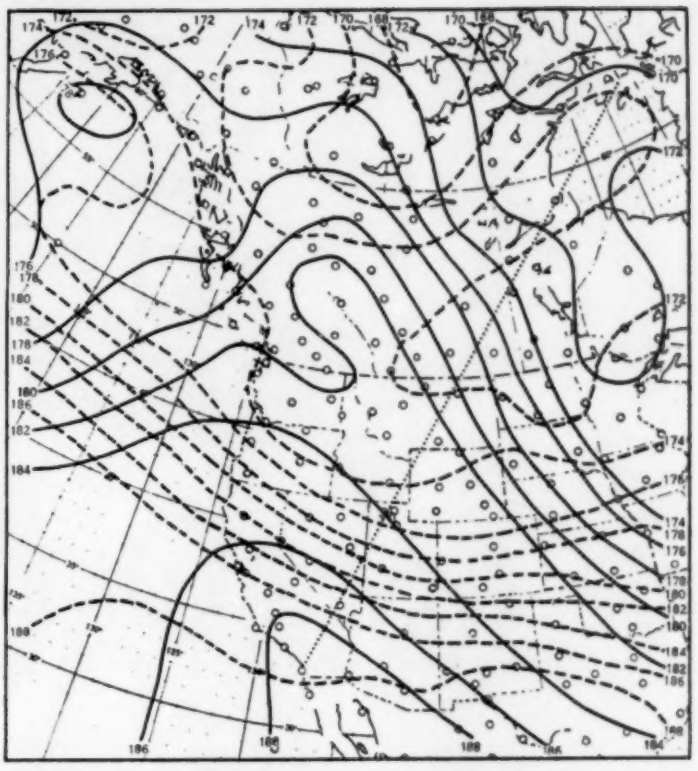

FIGURE 16.—1000–500-mb. thickness for 0300 GMT, November 25 (solid lines) and for 0300 GMT, November 28, 1954 (dashed lines). Note the strong changes in the Idaho-Montana region.

2. J. S. Sawyer, "Day-to-Day Variations in the Tropopause," Great Britain Air Ministry, *Geophysical Memoirs* No. 92, 1954, pp. 4–5.
3. E. Hovmöller, "The Trough-and-Ridge Diagram," *Tellus*, vol. 1, No. 2, May 1949, pp. 62–66.
4. Harry F. Hawkins, Jr., "The Weather and Circulation of November 1954—Including a Study of Some Major Circulation Changes," *Monthly Weather Review*, vol. 82, No. 11, Nov. 1954, pp. 335–342.
5. R. Fjørtoft, "On a Numerical Method of Integrating the Barotropic Vorticity Equation," *Tellus*, vol. 4, No. 3, Aug. 1952, pp. 179–194.
6. Alan N. Sanderson and Charles F. Thomas, "Application of the Fjørtoft Vorticity Techniques," U. S. Weather Bureau, August 1954, 8 pp. (manuscript).
7. A. K. Showalter, Notes to J. Bjerknes on Mechanism of Pressure Changes, March 11, 1954 (unpublished).

U. S. GOVERNMENT PRINTING OFFICE: 1955

Chart I. A. Average Temperature (°F.) at Surface, November 1954.

B. Departure of Average Temperature from Normal (°F.), November 1954.

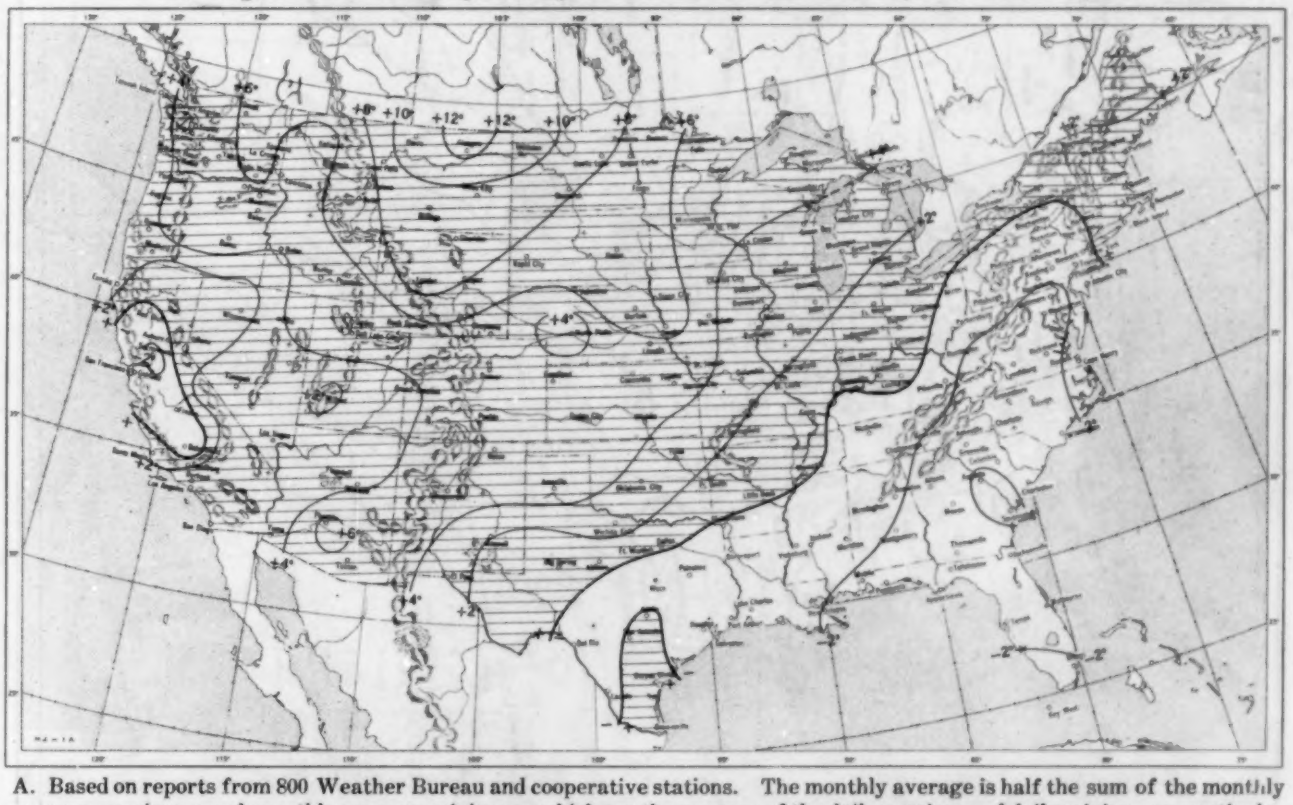

A. Based on reports from 800 Weather Bureau and cooperative stations. The monthly average is half the sum of the monthly average maximum and monthly average minimum, which are the average of the daily maxima and daily minima, respectively.

B. Normal average monthly temperatures are computed for Weather Bureau stations having at least 10 years of record.

Chart II. Total Precipitation (Inches), November 1954.

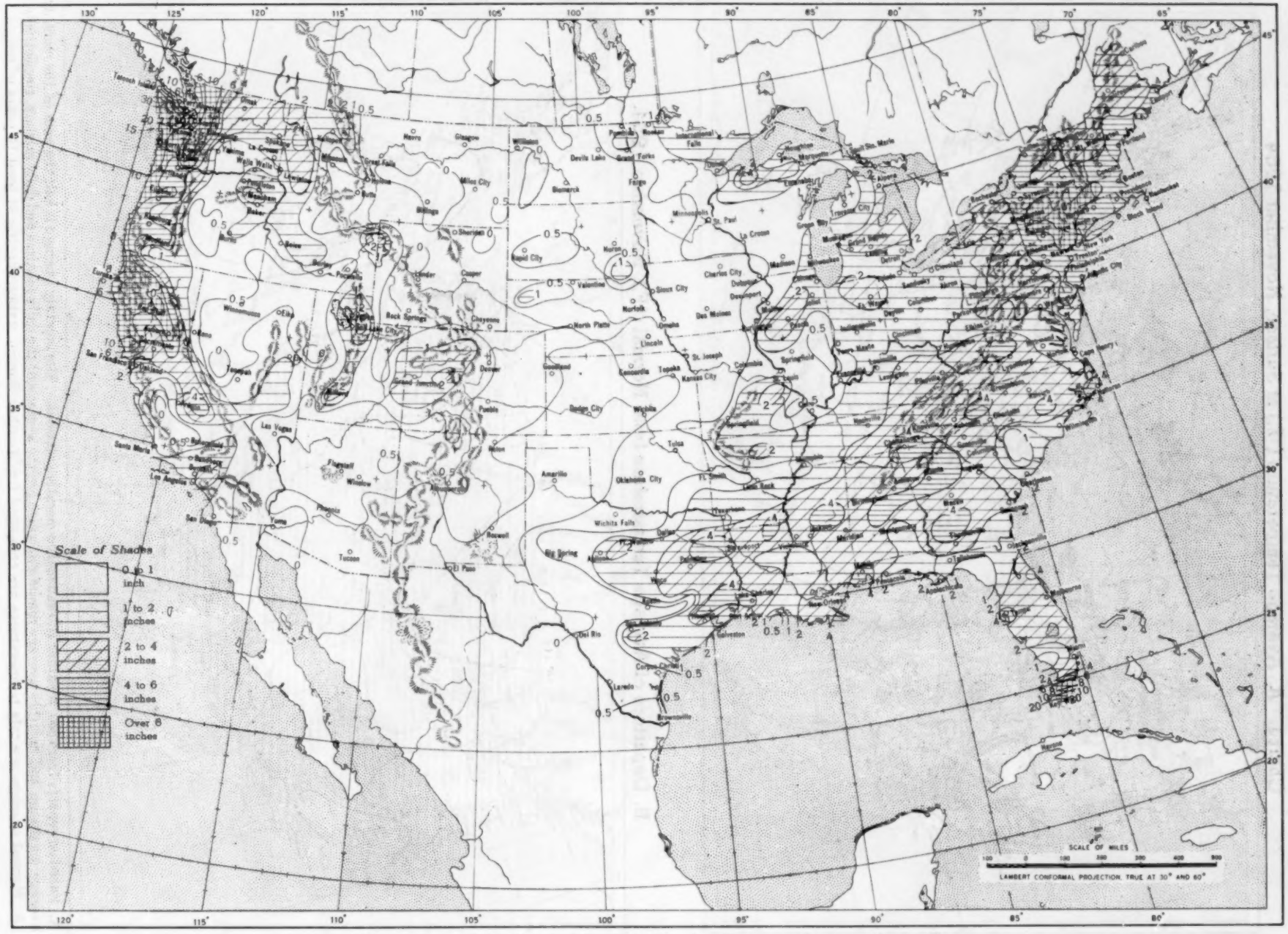
Scale of Shades
0 to 1 inch
1 to 2 inches
2 to 4 inches
4 to 6 inches
Over 6 inches
SCALE OF MILES
LAMBERT CONFORMAL PROJECTION, TRUE AT 30° AND 60°

Based on daily precipitation records at 800 Weather Bureau and cooperative stations.

Chart III. A. Departure of Precipitation from Normal (Inches), November 1954.

B. Percentage of Normal Precipitation, November 1954.

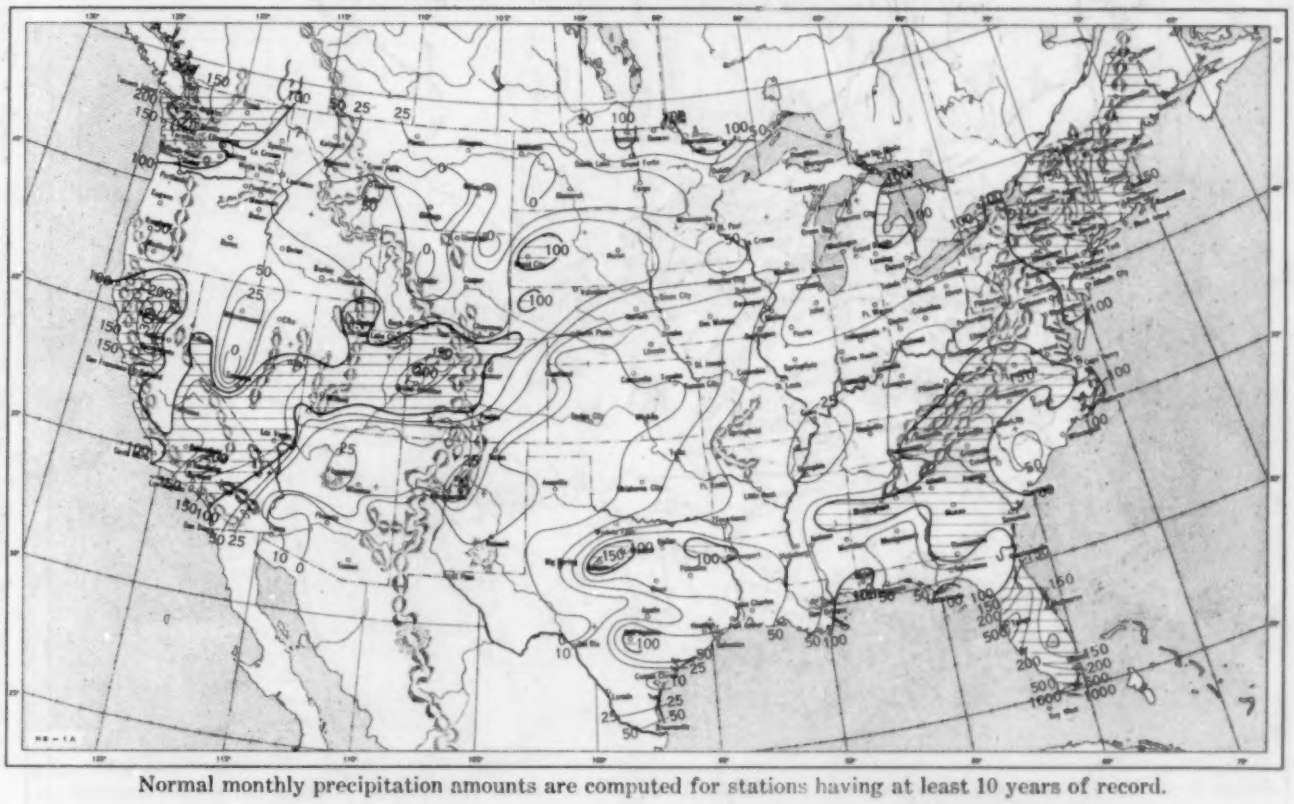

Normal monthly precipitation amounts are computed for stations having at least 10 years of record.

Chart IV. Total Snowfall (Inches), November 1954.

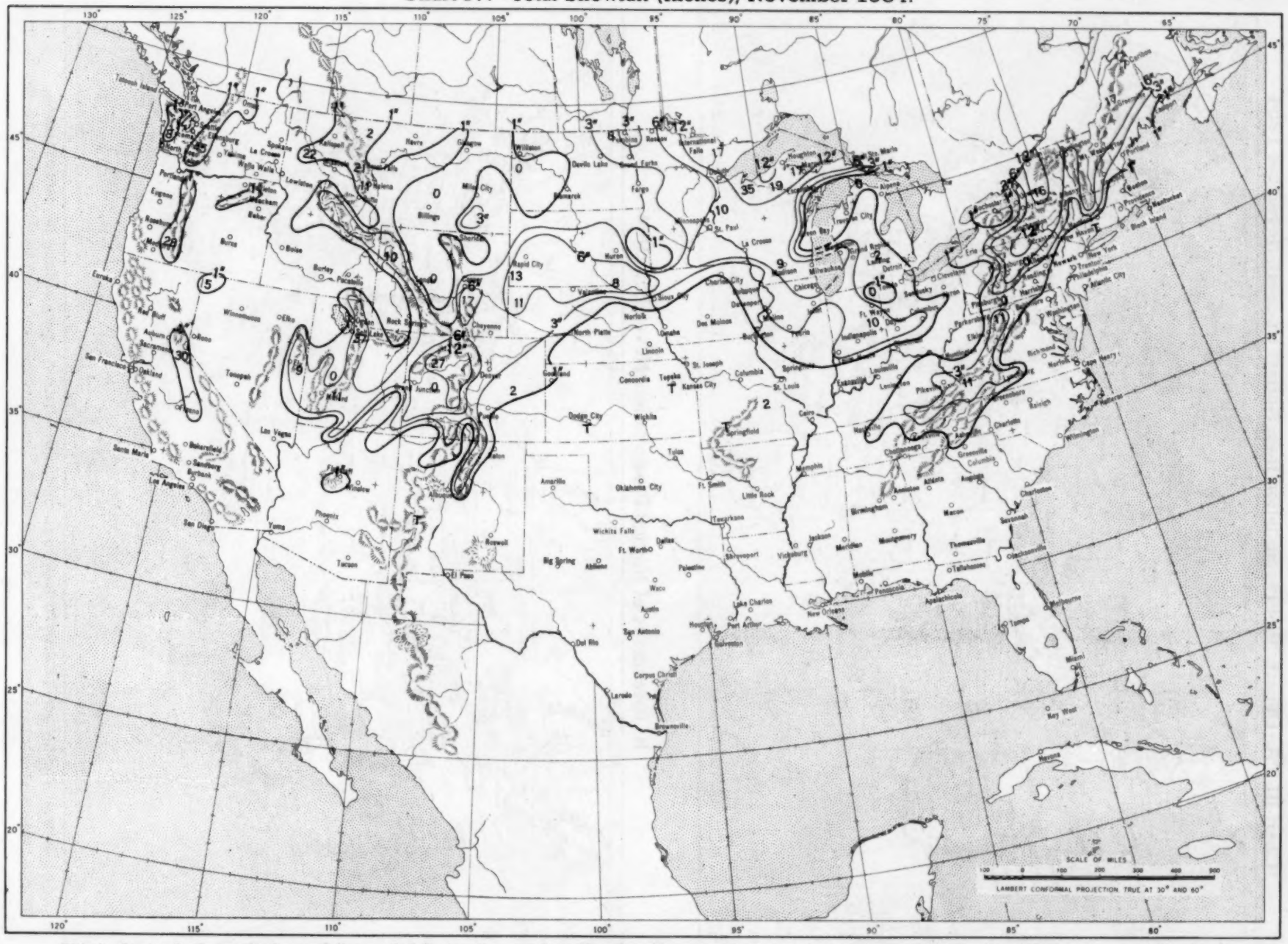

This is the total of unmelted snowfall recorded during the month at Weather Bureau and cooperative stations. This chart and Chart V are published only for the months of November through April although of course there is some snow at higher elevations, particularly in the far West, earlier and later in the year.

Chart V. A. Percentage of Normal Snowfall, November 1954.

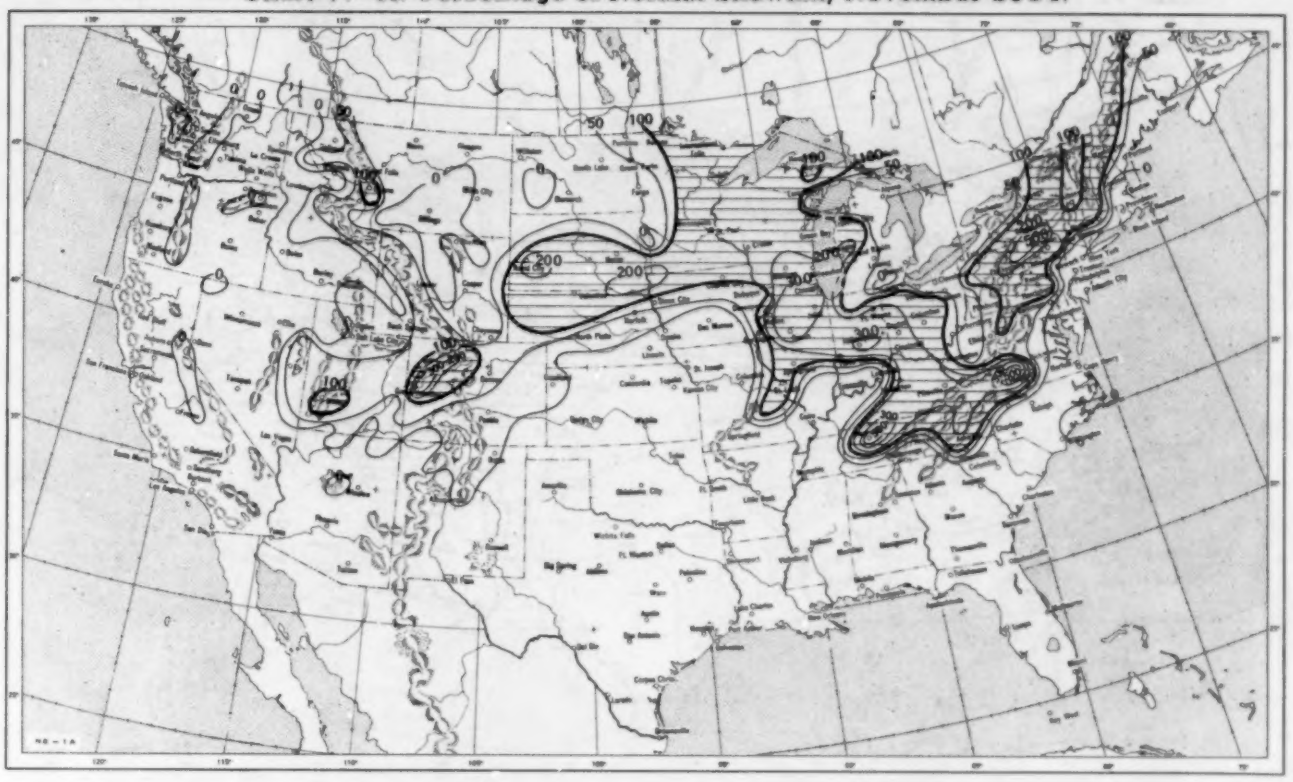

B. Depth of Snow on Ground (Inches).

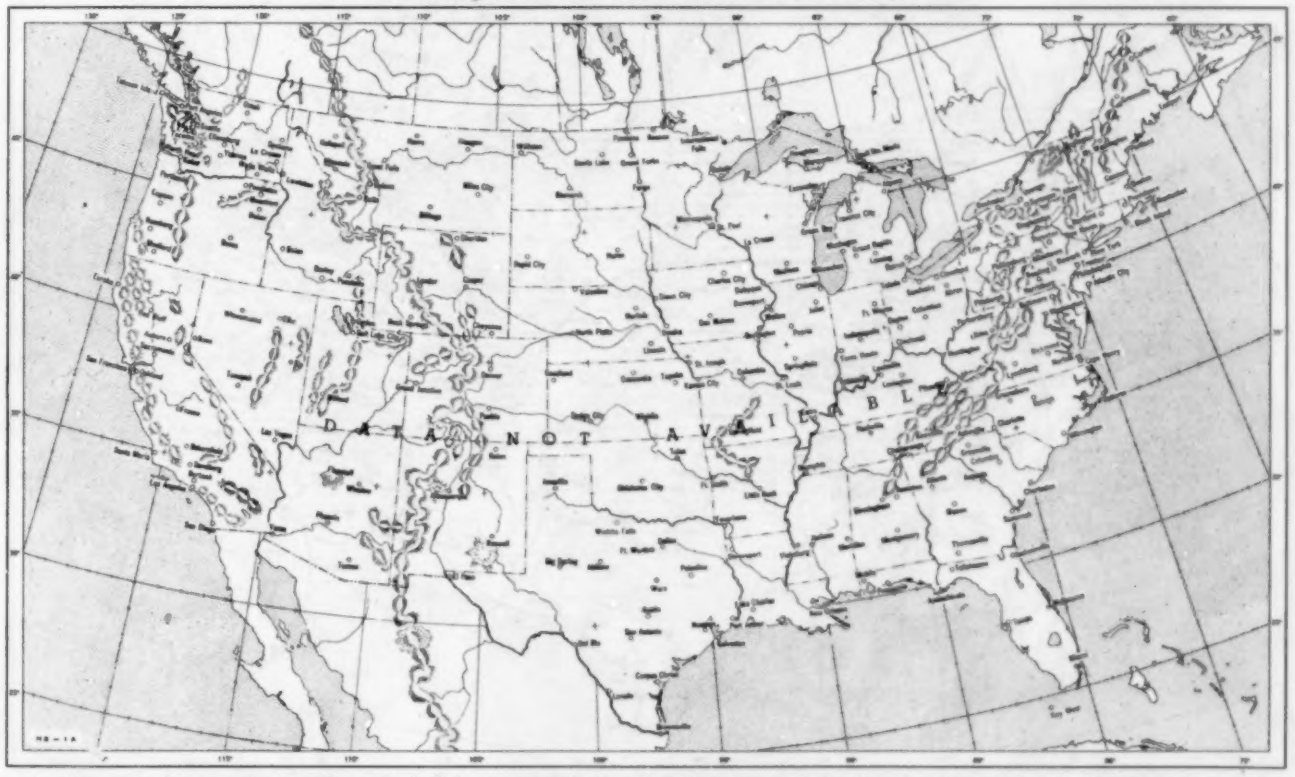

A. Amount of normal monthly snowfall is computed for Weather Bureau stations having at least 10 years of record. B. Shows depth currently on ground at 7:30 a. m. E. S. T., of the Tuesday nearest the end of the month. It is based on reports from Weather Bureau and cooperative stations. Dashed line shows greatest southern extent of snowcover during month.

Chart VI. A. Percentage of Sky Cover Between Sunrise and Sunset, November 1954.

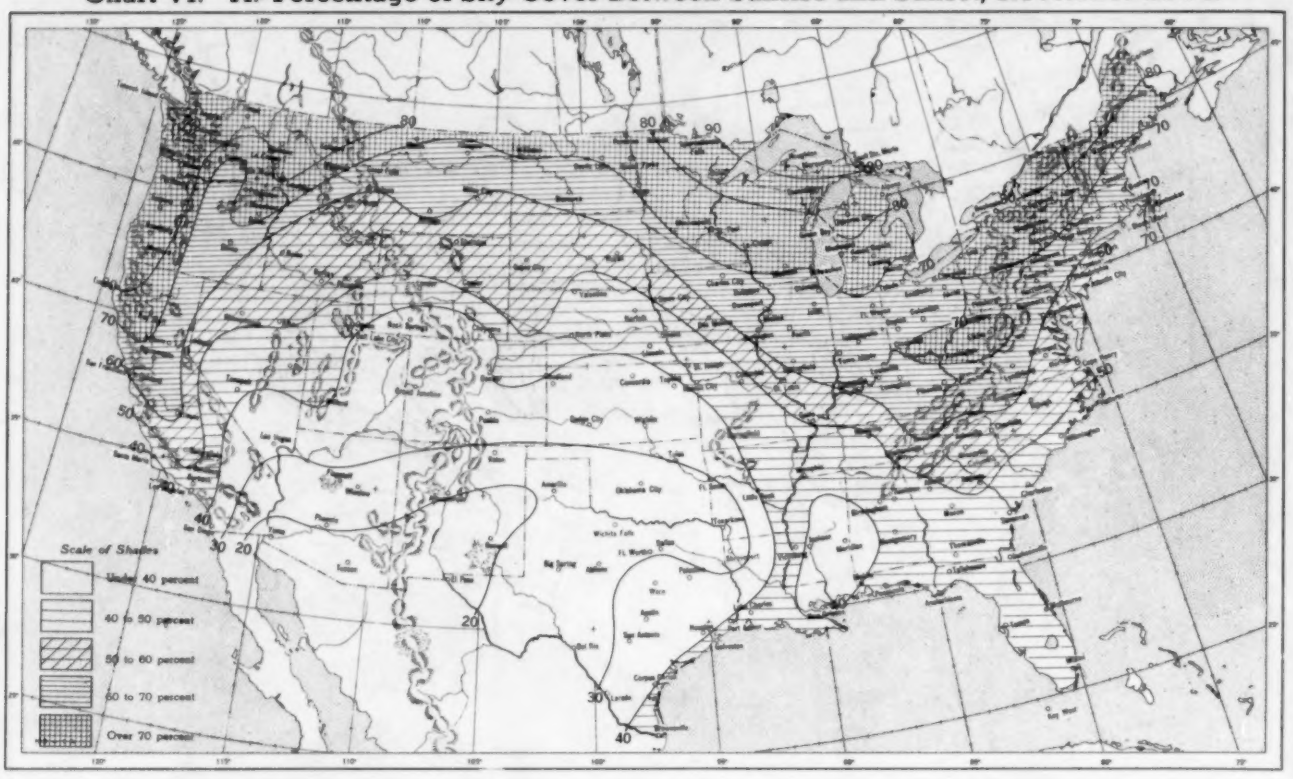

B. Percentage of Normal Sky Cover Between Sunrise and Sunset, November 1954.

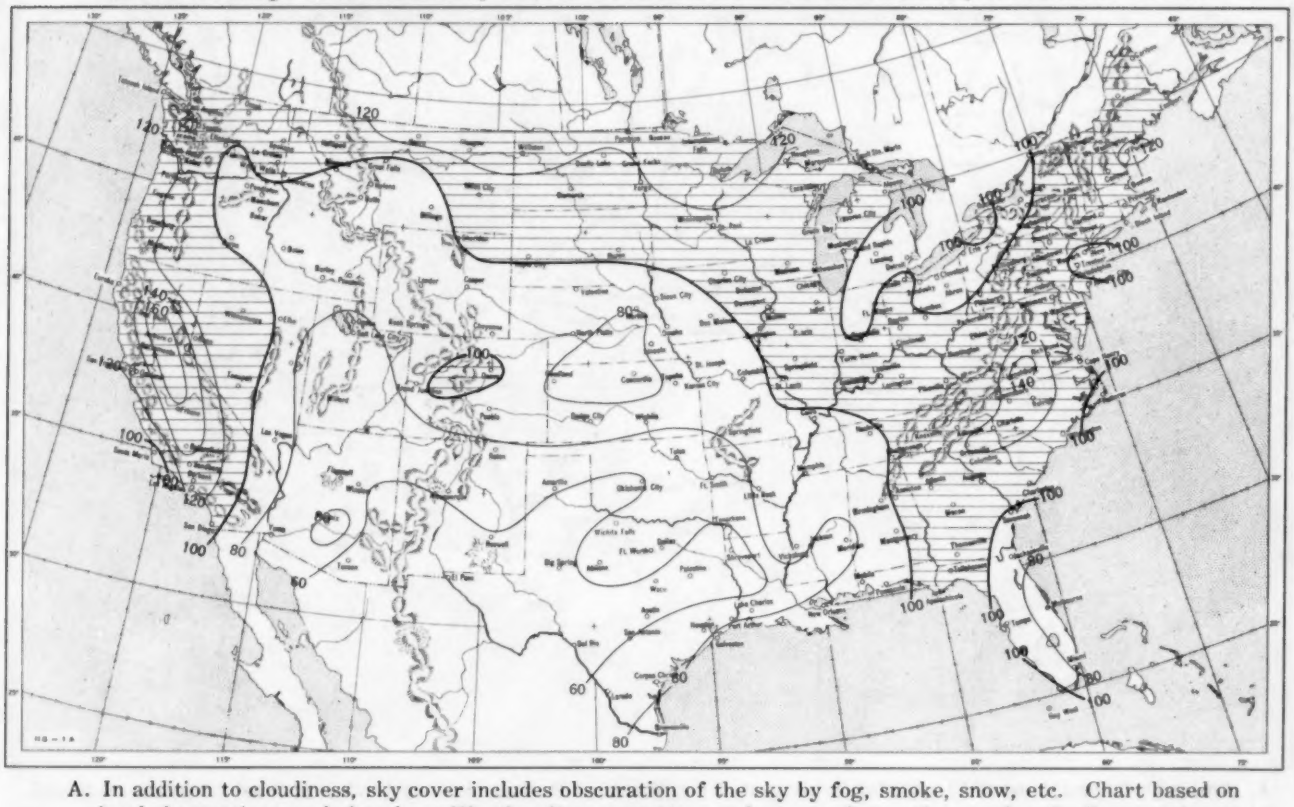

A. In addition to cloudiness, sky cover includes obscuration of the sky by fog, smoke, snow, etc. Chart based on visual observations made hourly at Weather Bureau stations and averaged over the month. B. Computations of normal amount of sky cover are made for stations having at least 10 years of record.

Chart VII. A. Percentage of Possible Sunshine, November 1954.

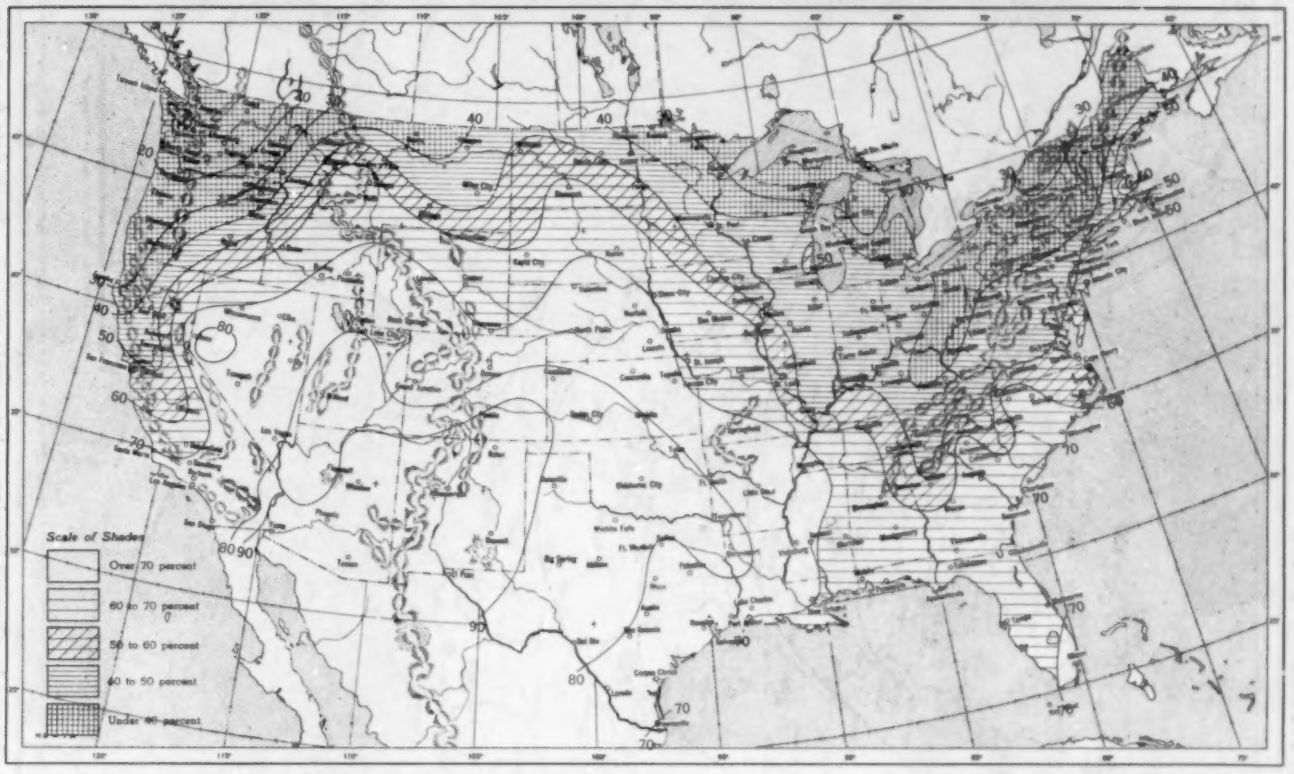

B. Percentage of Normal Sunshine, November 1954.

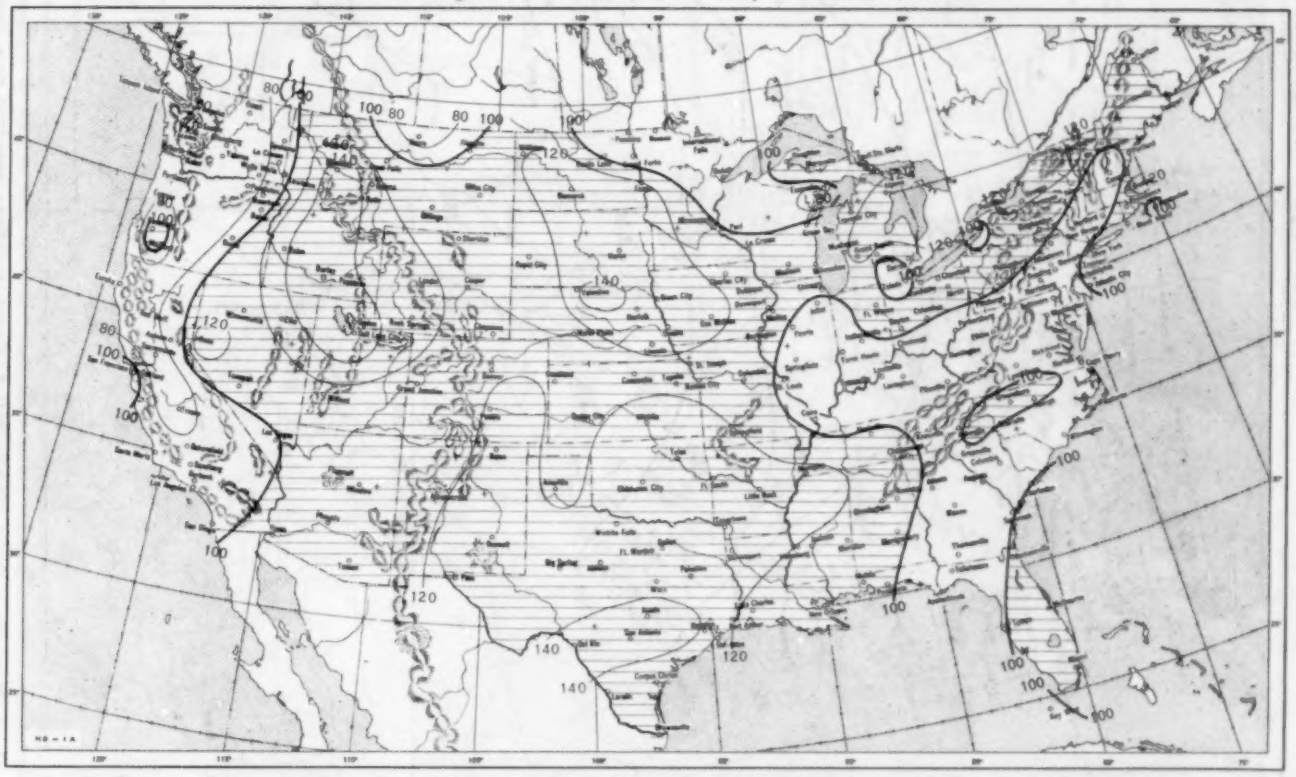

A. Computed from total number of hours of observed sunshine in relation to total number of possible hours of sunshine during month. B. Normals are computed for stations having at least 10 years of record.

Chart VIII. Average Daily Values of Solar Radiation, Direct + Diffuse, November 1954. Inset: Percentage of Normal Average Daily Solar Radiation, November 1954.

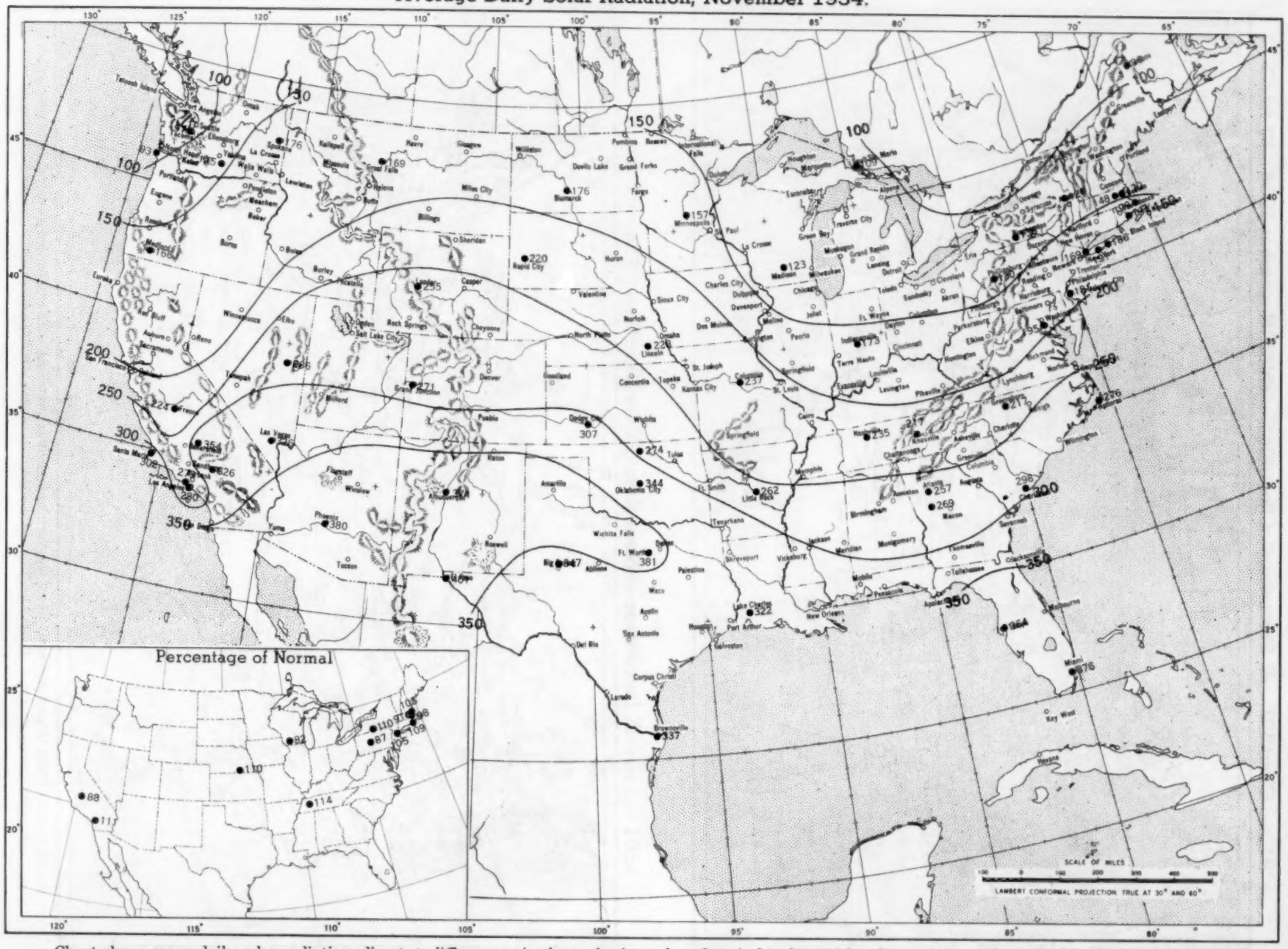

Chart shows mean daily solar radiation, direct + diffuse, received on a horizontal surface in langleys (1 langley = 1 gm. cal. cm. $^{-2}$). Basic data for isolines are shown on chart. Further estimates are obtained from supplementary data for which limits of accuracy are wider than for those data shown. Normals are computed for stations having at least 9 years of record.

Chart IX. Tracks of Centers of Anticyclones at Sea Level, November 1954.

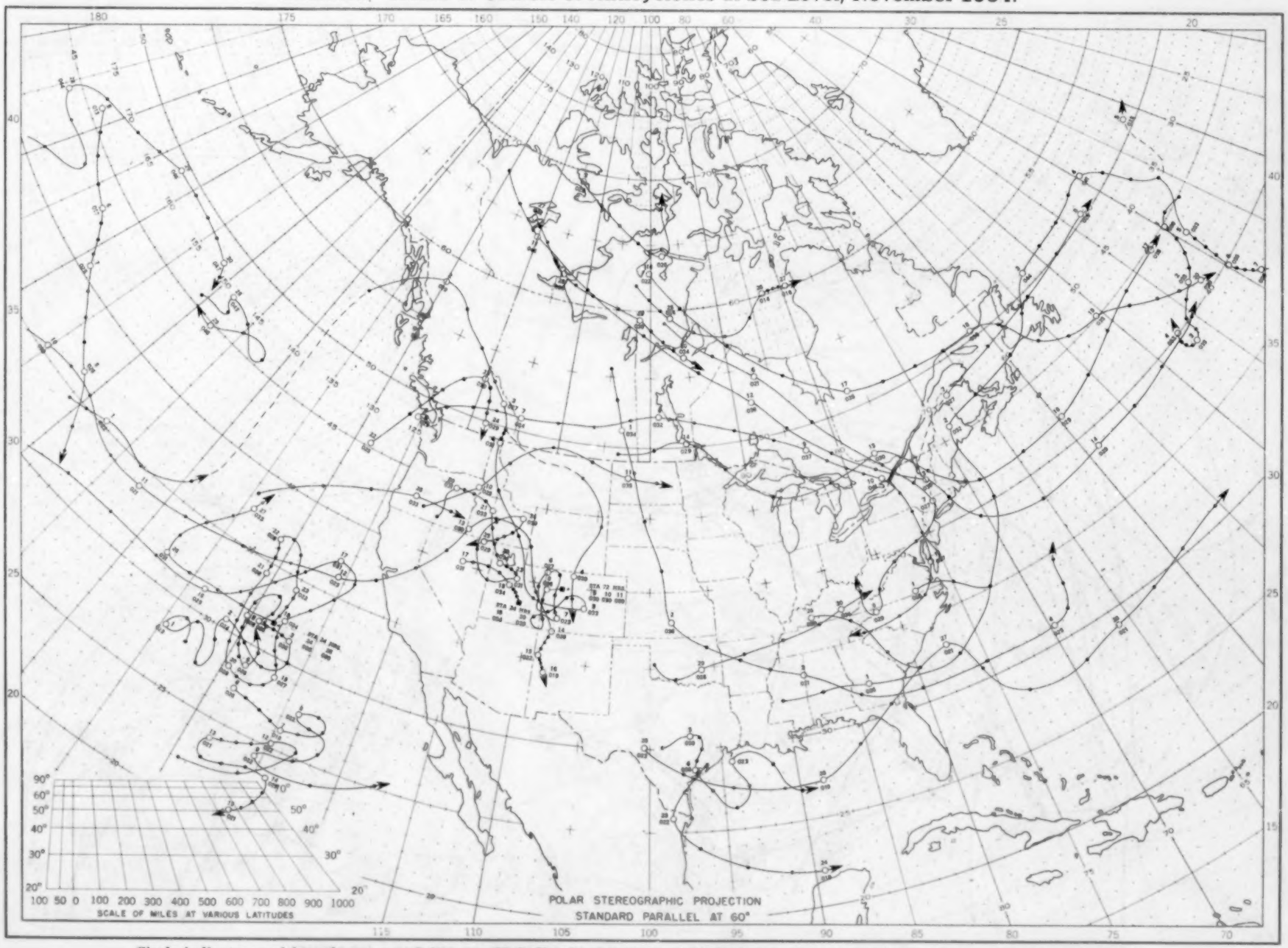

Circle indicates position of center at 7:30 a. m. E. S. T. Figure above circle indicates date, figure below, pressure to nearest millibar. Dots indicate intervening 6-hourly positions. Squares indicate position of stationary center for period shown. Dashed line in track indicates reformation at new position. Only those centers which could be identified for 24 hours or more are included.

Chart X. Tracks of Centers of Cyclones at Sea Level, November 1954.

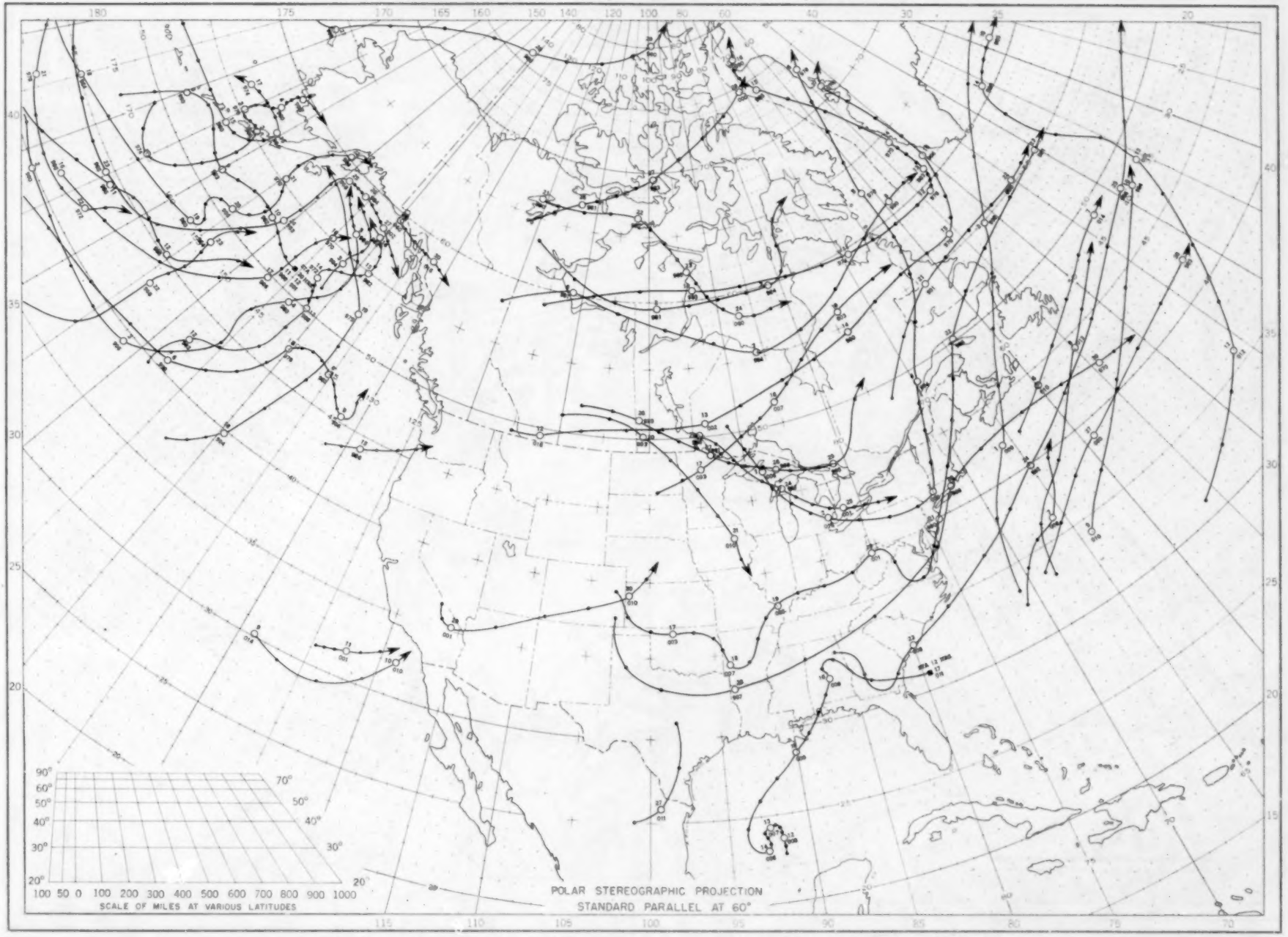
SCALE OF MILES AT VARIOUS LATITUDES
100 50 0 100 200 300 400 500 600 700 800 900 1000
POLAR STEREOGRAPHIC PROJECTION
STANDARD PARALLEL AT 60°

Circle indicates position of center at 7:30 a. m. E. S. T. See Chart IX for explanation of symbols.

Chart XI. Average Sea Level Pressure (mb.) and Surface Windroses, November 1954. Inset: Departure of Average Pressure (mb.) from Normal, November 1954.

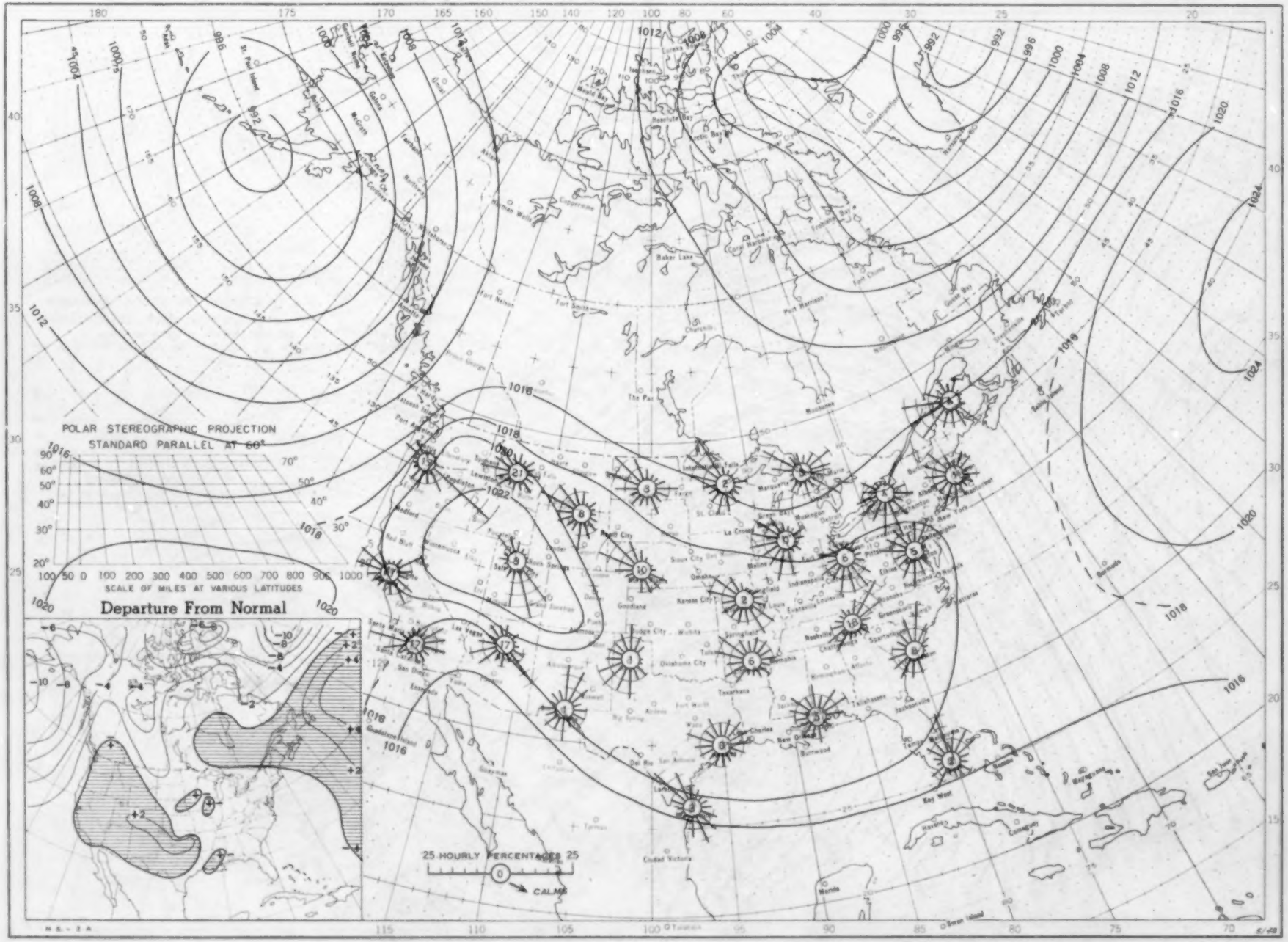

Average sea level pressures are obtained from the averages of the 7:30 a. m. and 7:30 p. m. E. S. T. readings. Windroses show percentage of time wind blew from 16 compass points or was calm during the month. Pressure normals are computed for stations having at least 10 years of record and for 10° intersections in a diamond grid based on readings from the Historical Weather Maps (1899-1939) for the 20 years of most complete data coverage prior to 1940.

Chart XII. Average Dynamic Height in Geopotential Meters (1 g.p.m. = 0.98 dynamic meters) of the 850-mb. Pressure Surface, Average Temperature in °C. at 850 mb., and Resultant Winds at 1500 Meters (m.s.l.), November 1954.

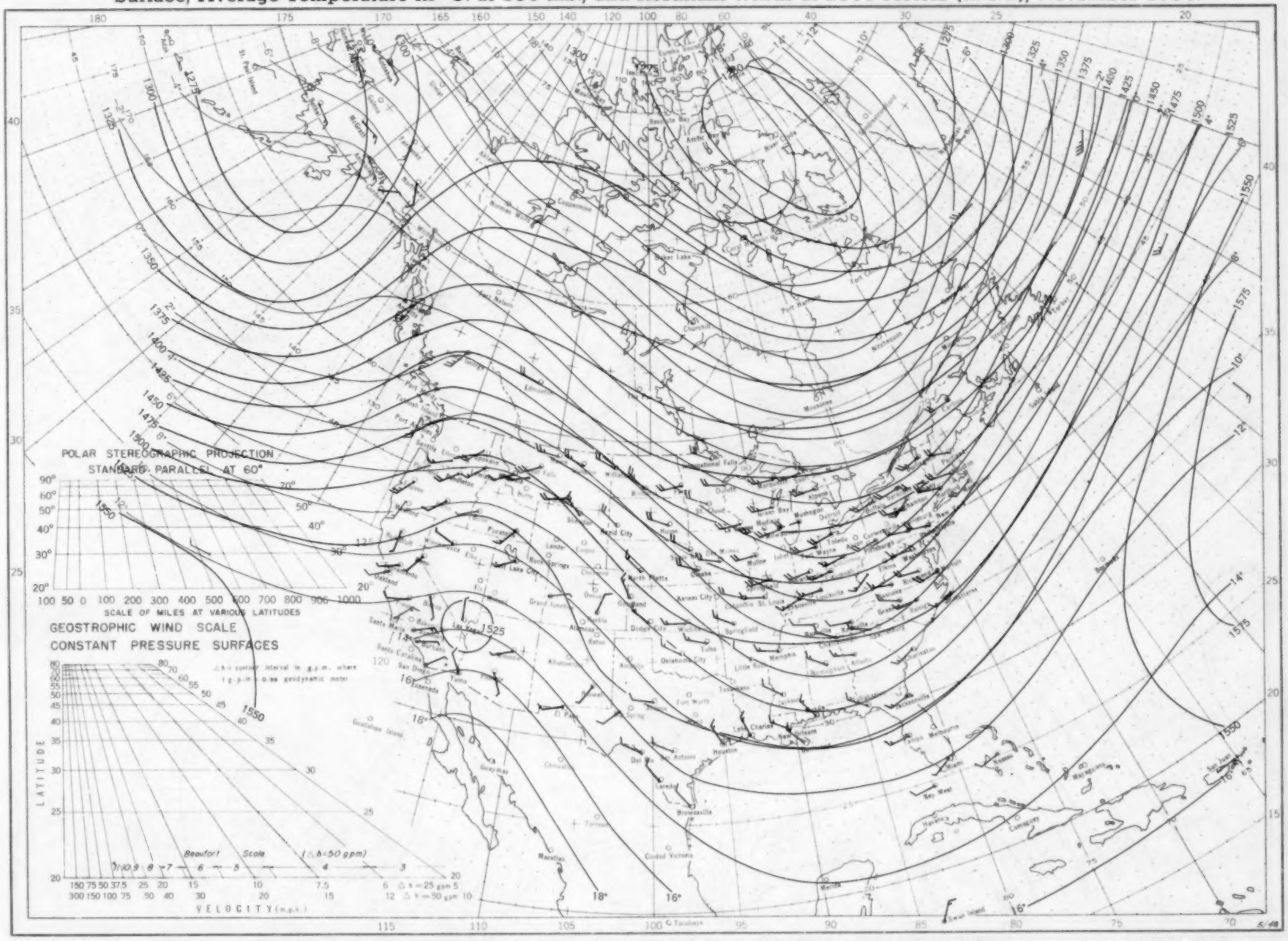

Contour lines and isotherms based on radiosonde observations at 0300 G. M. T. Winds shown in black are based on pilot balloon observations at 2100 G. M. T.; those shown in red are based on rawins taken at 0300 G. M. T. Wind barbs indicate wind speed on the Beaufort scale.

Chart XIII. Average Dynamic Height in Geopotential Meters (1 g.p.m.. = 0.98 dynamic meters) of the 700-mb. Pressure Surface, Average Temperature in °C. at 700 mb., and Resultant Winds at 3000 Meters (m.s.l.), November 1954.

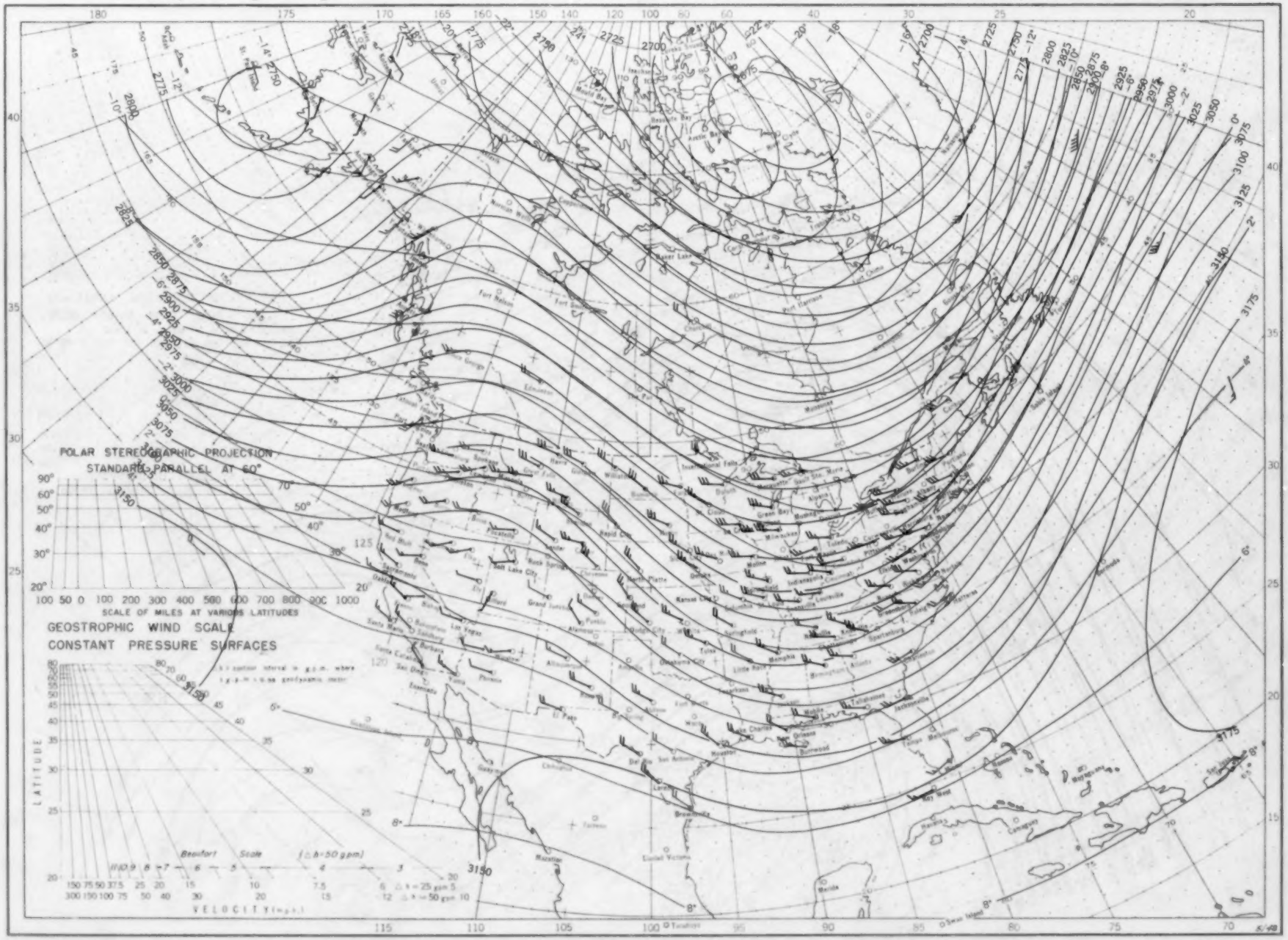

Contour lines and isotherms based on radiosonde observations at 0300 G. M. T. Winds shown in black are based on pilot balloon observations at 2100 G. M. T.; those shown in red are based on rawins taken at 0300 G. M. T. Wind barbs indicate wind speed on the Beaufort scale.

Chart XIV. Average Dynamic Height in Geopotential Meters (1 g.p.m. = 0.98 dynamic meters) of the 500-mb. Pressure Surface, Average Temperature in °C. at 500 mb., and Resultant Winds at 5000 Meters (m.s.l.), November 1954.

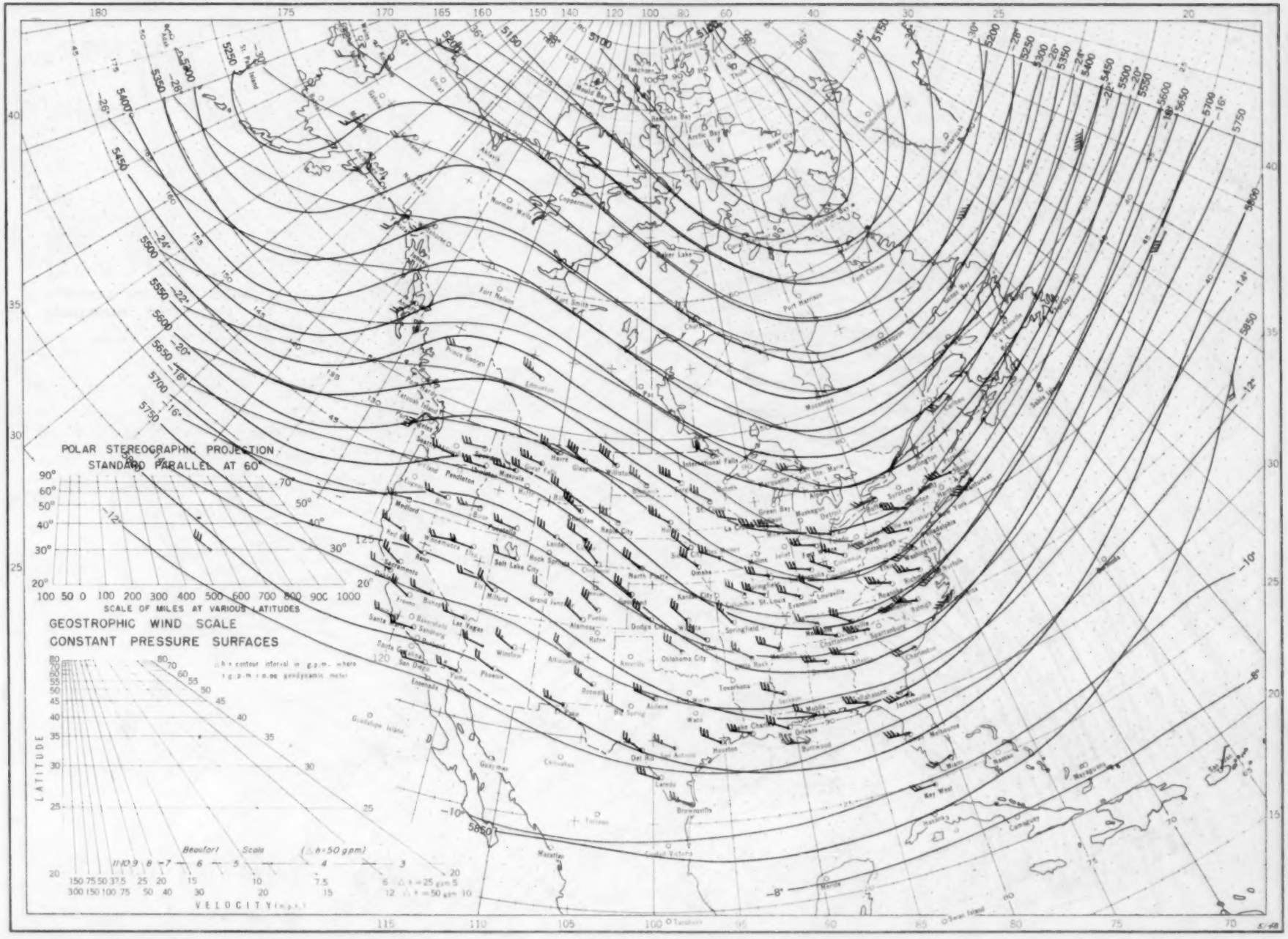

Contour lines and isotherms based on radiosonde observations at 0300 G. M. T. Winds shown in black are based on pilot balloon observations at 2100 G. M. T.; those shown in red are based on rawins at 0300 G. M. T. Wind barbs indicate wind speed on the Beaufort scale.

Chart XV. Average Dynamic Height in Geopotential Meters (1 g.p.m. = 0.98 dynamic meters) of the 300-mb. Pressure Surface, Average Temperature in °C. at 300 mb., and Resultant Winds at 10,000 Meters (m.s.l.), November 1954.

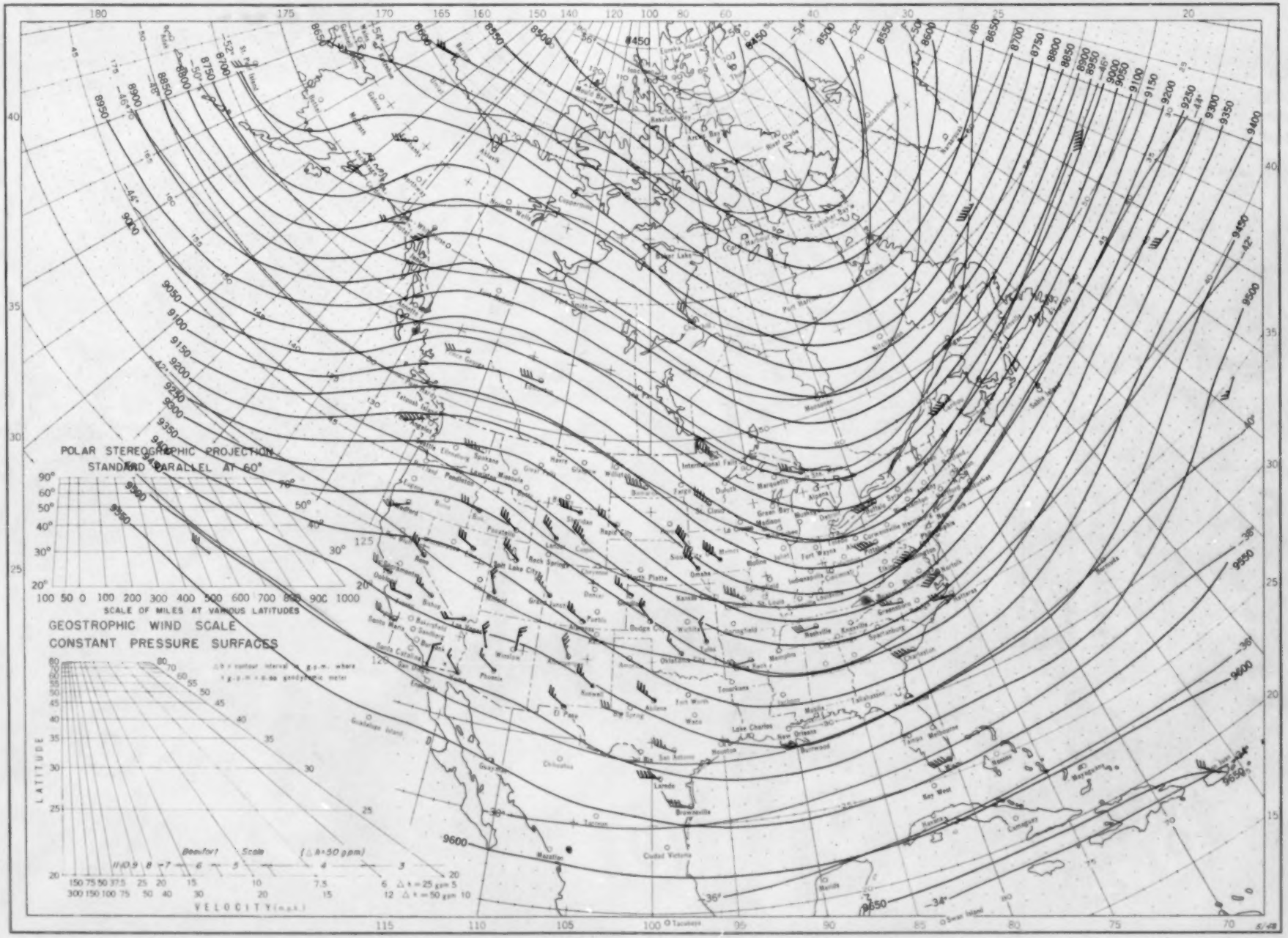

Contour lines and isotherms based on radiosonde observations at 0300 G. M. T. Winds shown in black are based on pilot balloon observations at 2100 G. M. T.; those shown in red are based on rawins at 0300 G. M. T. Wind barbs indicate wind speed on the Beaufort scale.